Groundwater isotopes in ecohydrological analysis of peatland landscapes

Samer Elshehawi

Groundwater isotopes in ecohydrological analysis of peatland Landscapes

Samer Elshehawi
PhD Thesis, 2019.

University of Groningen
The Netherlands
ISBN: 978-94-034-1310-5
ISBN (electronic version): 978-94-034-1309-9

Printed by: Ridderprint BV, the Netherlands.

The work done in this thesis was carried out at the Center for Energy and Environmental Sciences (IVEM) and the Center for Isotope Research (CIO), which are part of the Energy and Sustainability Research Insitute Groningen (ESRIG) at the University of Groningen, the Netherlands.

university of groningen

Groundwater isotopes in ecohydrological analysis of peatland landscapes

PhD Thesis

to obtain the degree of PhD at the
University of Groningen
on the authority of the
Rector Magnificus prof. E. Sterken
and in accordance with
the decision by the College of Deans.

This thesis will be defended in public on

Friday 8 February 2019 at 16.15 hours

by

Samer Enan Ali Abdelsalam Elshehawi

born on 14 September 1988
in Cairo, Egypt

Supervisors
Prof. A.P. Grootjans
Prof. J. van der Plicht

Co-supervisor
Dr. P.P. Schot

Assessment Committee
Prof. J.T.M. Elzenga
Prof. R. van Diggelen
Prof. H. Joosten

Groundwater isotopes in ecohydrological analysis of peatland landscapes

Preface

On a slightly cold and rainy October day in 2014, I visited a peatland in the Drentsche Aa brook valley. As a person who has never set foot in a peatland before, and who has done geological field work in dry areas, I had no boots or rain gear. The outcome of the day was not pleasant at all. After a few times of falling in ditches or tripping over unseen plant roots, I was cold, wet and holding grudge feelings for all peatlands of the world. My relation with peatlands was not off to a great start or to a love at the first sight to say the least. However, over the past few years my perception of peatlands has become one of admiration and respect. After people find out that my work is related to peatlands, they often ask: “uh, but are there peatlands in Egypt?”. The answer is probably no, at least in the present. As a guy who grew up in a grey city, Great Cairo, I have not had much exposure to natural landscapes, except for the vast sand dunes in the desert. It is, hence, a valid point to wonder how did an Egyptian guy gets bogged into peatland sciences. Well, the answer consists of a series of (un)fortunate events.

The first event was the beginning of the Egyptian revolution in early 2011, which overlapped with the last year of my bachelor study. While I was studying petroleum geosciences, I had little to no enthusiasm to actually pursuing a career in the oil and gas industry. The revolution was a catalyst, which led me to participating in a human rights summer school upon finishing the bachelor study. After the summer school, I was enthusiastic about pursuing a career in human rights related direction. However, I still liked to approach that from a scientific point. The logical option was to change course into environmental sciences to combine the geology background with human rights into environmental justice. While trying to find an environmental science study program, a scholarship from Erasmus Mundus landed me in the Netherlands at the end of the summer of 2013 to follow the research master program (Energy and Environmental Sciences) at the University of Groningen.

While adapting to the new education system and learning new things, a disappointment was growing by following the course shift in Egypt from a hope of a brighter future to a gloomy and violent one. This has made rethink whether or not I wanted something to do with Egyptian affairs anymore, specifically water management in Egypt. Due to the confusion, I went to meet my appointed tutor, who was appointed to me because he had something to do with water. And there he was Ab Grootjans, the “peat guy” as I remembered his lectures. After listening to my complaints and doubts about doing research about water management in Egypt, he said “you have some basic knowledge in hydrology. Right? Well, there is a project and I need a student to do some research on the groundwater age in a nature reserve in Drenthe, so think about it”. I accepted the offer.

After finishing the Drentsche Aa project, I flew to the southern hemisphere to start a new field work adventure in Maputaland in South Africa. After a 12-hour flight, Ab introduced me to his Afrikaans colleague: Piet-Louis Grundling, who was to decide our fate. Piet-Louis wasted no time. We drove over the night for another 8 hours to arrive

in the beautiful landscapes of Maputaland. After a small stop to drop our baggage. We took off to the field with Marvin, Sihle and Mohamed. Our visit was to the Vasi peatland complex, where I met the second peatland, which was quite a different experience. Unlike the wet climatic conditions in the Netherlands, the peatlands in Maputaland sustain their development, despite the net dry conditions, where evapotranspiration is estimated to twice as much as precipitation. The focus of the study was to save what is left undestroyed by the fire yet, Vasi-North, but in 2017 the fire took over it too and left it a witness of the costs of unsustainable land use practices, namely forestation here. During the same visit, I had the opportunity to visit the beautiful Matlabas mire in the Waterberg mountain areas with Piet-Louis and Althea, where we did some quick fieldwork. Afterwards I was back in Maputaland, and left trying to recover from a mean tick bite, under the care of Marvin and Caro who were kind enough to take me to the hospital. While staying in Maputaland for five weeks, Marvin was kind enough to show me the peatlands, where he was doing his research, and each one of them was unique.

By the completion of the master's degree, I had some financial help by Ab on behalf of Ecological Restoration Advice (ERA) foundation to publish our work. Henk Everts and Nico de Vries were kind enough to offer me a space in their office to work from. Besides this, I was assisting other colleagues with some ecohydrological research in the province of Drenthe in the Netherlands and in Slitere National Park in Latvia. In Latvia, I got to meet more interesting people like Mara, Olgerts, Leszek, Alma and Christ-Janis, with whom we ran around the whole park to install water pipes, flush them and take samples in just a few days. By the end of the year, we applied for the new PhD scholarship scheme to do a thesis to combine these separate projects into a research highlighting the positive role of the groundwater isotopes in ecohydrological research of peatlands. This was not going to be possible without the help of Rien, Hans and Harro.

During the PhD period, we did extra fieldwork in Vasi, Matlabas and Slitere to improve our understanding of these systems and to look into some of the questions that were still unanswered. The plans to improve the work was done with the help of Paul Schot and Martin Wassen, who were nice enough to have me as a guest at the environmental sciences research group of Utrecht University. Together, we worked to improve the manuscripts and plan and execute the fieldwork in South Africa and Latvia. Also, the last fieldwork was done in Slitere National Park with the help of a master student: Alvaro, from Utrecht University, who completed a master project on modelling the groundwater flows in Slitere.

By the end of my PhD, the cherry on top of the cake was participating in the IMCG excursion in the Netherlands. I got to meet many beautiful people, with whom you get to appreciate peatlands beauty. However, I still failed to have a peat-only-diet for more than four hours, I will look forward to doing so next time. I am thankful to everyone who I met, shared a discussion or a beer. I look forward, and hope, to continue working closely to peatlands, to learn more and more about them. After all, I hope to sing along "Bring back my boggy to me" for many years to come.

Samer Elshehawi,
December 2018

1

Introduction

Wetlands are amongst the most productive terrestrial ecosystems (Mitsch & Gosselink, 2000a). They are defined as a landscape with permanent or seasonal water table near or above the surface (Mitsch & Gosselink, 2000a; Maltby & Barker, 2009). The different types of wetlands contribute to different eco-services, e.g. biodiversity, recreational purposes, water purification, and they are increasingly important for 'cashing' carbon credits in socio-economic projects, by acting as carbon sinks and stocks (Mitsch & Gosselink, 2000b; Joosten & Clarke, 2002; Maltby & Barker, 2009). Wetlands in general are a function of climate, hydrology and vegetation interactions (Joosten & Clarke, 2002). While wetlands have different types, fifty percent of all wetlands are peatlands or mires (Joosten & Clarke, 2002). Mires are the peatlands that actively accumulate peat, at which peat is an accumulation of partially decomposed organic matter, with thickness of at least 30 cm (Joosten & Clarke, 2002).

Peatlands generally are divided into bogs, which depend primarily on rainwater, and fens that are dependent on groundwater supply (Joosten & Clarke, 2002). Fen peatlands are further divided as landscape systems depending on their hydrological systems, i.e. spring, percolating or floodplain fens (Joosten & Clarke, 2002; Grootjans *et al*., 2006). The origin the hydrological flows are conditioning factors for the ecological conditions of peatlands (Schot & Molenaar, 1993; Grootjans *et al*., 2006; Van Loon *et al*., 2009; Gilvear & Bradley, 2009; Grootjans & Van Diggelen, 2009).

Peatlands develop by accumulating peat through open water (lake) terrestrialisation, via paludifying over the mineral soil directly or through a mixture of both processes (Heathwaite *et al*., 1993; Joosten & Clarke, 2002). The peat development can be related to climatic factors, e.g. increase in precipitation rates, sea level rise or regression or to regional/local hydrogeologic factors (See Dommain *et al*., 2011; Dekker *et al*., 2015). In most of these cases especially in fen peatlands, there is an associated groundwater system development which can allow peat accumulation under a water table elevation that is at or close to the surface (Joosten & Clarke, 2002).

The groundwater systems sustaining a peatland are often spatially and temporally larger than the peatlands boundaries (Van Diggelen, 2006). Different examples of groundwater systems that give rise to different base-rich, i.e. rich in calcium and basic ions, fen peatland landscapes were discussed concisely by Grootjans *et al*., (2006). Also, the local, sub-regional and regional groundwater systems can co-exist in a single

basin or catchment, with the local system associated with high topographic changes in the immediate surrounding, while the regional system is associated with the gentle relief of a larger part of the catchment (Toth, 1963). Several studies have looked at the groundwater systems on the landscape to understand the hydrological systems conditioning a given peatland or wetland (See Engelen et al., 1992; Schot & Molenaar, 1992; Stuyfzand, 1993). Also, the process by which groundwater flow discharges and flows within peatlands are determining for their vegetation gradient (Grootjans *et al*., 1993; Van Loon *et al*., 2009).

In the essence of restoring wetlands, the mechanisms that sustain the wetland on a landscape level should be understood to create a management plan appropriate for the wetland ecosystem and its restoration target (Van Andel & Grootjans, 2006). Dutch scientists have developed different aspects of ecohydrological approaches that investigates the hydrological system related to a given ecosystem (Wassen & Grootjans, 1996). Grootjans & Van Diggelen, (2009) and Grootjans & Jansen, (2012) further defined an ecohydrological approach that is a quick and dirty scan scientific analysis, i.e. time and cost efficient, of the hydrological conditions in a wetland and its surroundings. The approach aims at identifying the processes by which different groundwater flows that sustain a peatlands functionality and vegetation. It uses multidisciplinary approaches that measure the physical and chemical parameters, e.g. temperature profiles, water table depth, ion composition, of the groundwater in and around a wetland system and the peat characteristics e.g. macro-fossils and radiocarbon dating. These methods can be synthesised to develop a conceptual model of the conditioning hydrological systems. Such a model can further be used for prospective management and restoration plans (Grootjans & Van Diggelen, 2009; Grootjans & Jansen, 2012).

Environmental isotopes, especially of C, O and H, are widely used in hydrogeological research (Clark & Aravena, 2005; Mook, 2006). Generally, environmental isotopes in such approaches has been limited, and mainly to the ratios of the stable oxygen and deuterium isotopes: $\delta^{18}O$ and $\delta^{2}H$. For instance, $\delta^{18}O$ and chloride ions were used as tracers along with groundwater simulation to identify changes in regional groundwater flows in one of the Dutch wetland landscapes (Schot & Molenaar, 1992). Further, $\delta^{18}O/\delta^{2}H$ were used in an ecohydrological scheme to understand the conditions that allowed Mfabeni peatlands to persist over 40,000 years in a landscape with a water budget deficit, i.e. evaporation exceeding precipitation, on the northeast coast of South Africa (Grundling, 2014a). Also, $\delta^{18}O/\delta^{2}H$ were used to identify the zones which are dependent on groundwater supply to the vegetation in a, predominantly, bog landscape (Isokangas *et al*., 2017).

Meanwhile, carbon isotopes in ecohydrology have been limited to peat radiocarbon dating (Klimkowska *et al*., 2010) and the shifts in $\delta^{13}C$ to investigate past climatic conditions (Norström *et al*., 2009). The use of radiocarbon dating of water has been difficult due to several reasons. The first reason was that the available technology at the time required large amounts of water per sample, up to 20 litres. The second reason is the uncertainty due to the geochemical interaction effect on the actual ^{14}C content in a sample (Mook, 2006). While several models have been developed to correct for the dilution effects caused by these geochemical effects and

hence radiocarbon can be used with caution (Geyh, 2000; Mook, 2006; Han *et al*., 2012; Faurescu *et al*., 2015), It still remains problematic to obtain accurate groundwater ages.

THESIS OUTLINE

The focus here is to integrate the commonly used methods, e.g. groundwater table depth and pressure, peat temperature profiles, water ionic composition, and peat radiocarbon dating, with the C, H and O rare isotopes. The methods are used over the course of four peatland case studies. The first three chapters show a review of south African peatlands development (Chapter 2) to establish the conditions allowing peatlands initiation and development. Further, we look into conceptualizing the ecohydrological flows in two of the peatland systems in South Africa. The first one, Vasi Peatland Complex, is a degraded system in Maputaland Coastal Plain, due to the intensive land use in its surrounding (Chapter 3). The second system, Matlabas, is part of a Marakele National Park, which is located in a mountainous inland area. The Matlabas mire is nearly pristine at some parts of the landscape with some areas showing some degraded states and some eroding channels are present (Chapter 4). Further in chapter 5, the focus is on identifying groundwater flows in the Drentsche Aa Brook Valley Landscape to test different hypotheses on the water origins influencing the restoration targets. The last case study looks into the groundwater flow origins sustaining different peatland types in Slitere National Park in Latvia, which is home to many endangered species on the European and global level. The chapters list and their research questions are:

- Chapter 2: South African peatlands: review of Late Pleistocene-Holocene developments using radiocarbon.
    - what are the spatiotemporal conditions favourable for peat accumulation in South Africa and how this relates to their current distribution?
- Chapter 3: Ecohydrological assessment of the Vasi peatland complex in South Africa indicates degradation driven by changes in land use.
    - (i) what is the possible interaction between local- and regional groundwater systems in the Maputaland and the origin of the groundwater supply to the Vasi peatland complex? (ii) what are the hydrological flow directions and the possible hydrological link among the different basins in the complex? and (iii) is the degradation of the Vasi peatlands related to external land use management practices?
- Chapter 4: Anthropogenic disturbances of natural ecohydrological processes in the Matlabas mountain mire, South Africa.
    - (i) how did the Matlabas peatland develop over time in relation to the principal water flows? and (ii) how do the recent changes in land use affect the mire?

- Chapter 5: Natural isotopes identify origin of groundwater flows influencing wetland vegetation in the Drentsche Aa brook valley, the Netherlands.
    - What are the origins of groundwater flows to the fen peatlands, based on hypotheses from different ecohydrological and groundwater simulation studies?
- Chapter 6: Natural isotopes illustrate groundwater origins and control over the landscape and biodiversity in Slitere National Park.
    - What are the groundwater systems conditioning the mires in Slitere National Park?

Aim

The aim of the thesis is to test and highlight the added value of the C, H and O rare isotopes inclusion in the ecohydrological approaches is tested in different peatland landscape systems. The research question is: How does the integration of the C, H and O rare isotopes in an ecohydrological approach, in a time- and cost-effective manner, provide a better understanding of the hydrological processes conditioning a peatland?

2

South African peatlands: review of Late Pleistocene-Holocene developments using radiocarbon dating*

South Africa has a limited number of peatlands and most of them are relatively small compared to those in cooler temperate regions in the northern hemisphere. We gathered 40 basal peat samples representative of South Africa's peatlands to explore peatlands development during the Late Pleistocene and Holocene. Depth profiles of nine of them were also investigated using radiocarbon dating, which yielded information on past environmental changes affecting South African peatlands. The data showed three peaks in the frequency of peatland initiation, which are consistent with available climatic and sea level fluctuation data: one after the Last Glacial Maximum (LGM) and two during the Mid to Late Holocene. Inland peatlands in mountain valleys showed optimal growing conditions during the glacial-interglacial transition, continuing until the Early-Holocene. This is due to the switch to the wet and warm interglacial climate. In contrast, coastal peatlands showed optimal initiation conditions over two phases during the Holocene, which is consistent with sea level rise peaks that led to optimal moist conditions occurring ca. 6,000–3,000 and 1,000 years ago. Sea level rise reduced groundwater drainage, which led to a rise in the primary groundwater table. However, data from some of the coastal peatlands indicate independence from the sea level fluctuation, and that they are rather controlled by climatic conditions and their local hydrogeomorphic setting, e.g. perched groundwater aquifers. Some peatland complexes show a pattern of phased initiation with peat initiation consistent with altitude difference, which could be due to a positive feedback of blocking caused by peat accumulation in lower reaches, reducing groundwater drainage to the sea.

* This chapter is accepted as: Elshehawi, S., Grundling, P.L., Gabriel, M., Grootjans, P., van der Plicht., J. (in press) South African peatlands: Review of Late Pleistocene- Holocene developments using radiocarbon dating. *Mires and Peat.*

INTRODUCTION

Peatlands are important for climate regulation due to their role as carbon sinks (Graham, 1991). Acting as archives for palaeoclimatic research, peatlands can allow us to reconstruct past climates extending back to the Late Pleistocene (Lowe & Walker, 1984; Kalnina *et al*., 2014). Peatlands form by the accumulation of partly decomposed plant remains (peat), and are defined as having a peat thickness of at least 30 cm and over 30 % dry mass by volume of organic matter (Joosten & Clarke, 2002). While most peatlands are located in the temperate zones of the northern hemisphere, some exist in the southern hemisphere (Mitsch & Gosselink, 2000a; Joosten & Clarke, 2002; Yu *et al*., 2010). In South Africa, peatlands cover less than 0.5% of the area of the country (Marneweck *et al*., 2001; Joosten & Clarke, 2002). An overview of the distribution and types of peatlands in South Africa has been given by Grundling *et al.* (1998) and Grundling & Grobler (2005). They found that the coastal plain of Maputaland, which is a part of KwaZulu-Natal province, contains about 60% of South Africa's peatlands (Figure 1).

Meadows (1988) assessed the beginning (initiation) and subsequent growth of peatlands in South Africa by radiocarbon dating the basal peat of 26 peatlands. The histogram of the peat initiation data spans the Late Pleistocene and Holocene, with increased frequency of initiation during the Holocene. The peatland initiation frequency was related to the glacial-interglacial transition and to the rainfall increase that took place during the Holocene (Meadows, 1988; Chase & Meadows, 2007). However, this study did not include peatlands from Maputaland, some of which were sampled in later investigations (e.g. Grundling *et al*., 1998; Grundling *et al.,* 2000; Finch & Hill, 2008; Baker *et al.,* 2014). Also, the southwestern coast with its year-round rainfall zone hosts some peatlands, for example, Kromme and Vankervelsvlei (Irving & Meadows, 1997; Chase & Meadows, 2007). Some studies on South African coastal peatlands have suggested a possible link between sea level and accumulation rates of coastal peatlands in Maputaland (Grundling, 2004; Gabriel *et al*., 2017a).

In this paper, we update and expand on the existing literature on Late Quaternary peat accumulation in South Africa and analyse peatland development from the Late Pleistocene to the Late Holocene. For instance, we update the peatland initiation frequency by incorporating the coastal peatlands from Maputaland and other peatlands which were dated later than 1988. Further, we investigate seven peat profiles to infer the changes in the conditions favouring peat accumulation. Age-depth radiocarbon calibration models enable the assessment of peat-accumulation rates (Blaauw & Christen 2005, 2011). Accumulation rates can be deduced and used to understand climatic changes over the time scale studied (Meadows, 1988; Blaauw & Christen, 2005; Piotrowska *et al*., 2011). Increasing (or decreasing) peat accumulation rates are functions of climate, vegetation and hydrology (Joosten & Clarke, 2002). For example, moist colder conditions are expected to result in higher peat initiation frequency and accumulation rates (Meadows, 1988). We aim to identify past spatiotemporal patterns in peat initiation and conditions favourable for peat accumulation in South Africa and how this relates to their current distribution.

Peatlands in South Africa

South Africa is a predominantly semi-arid country. The climate in South Africa varies from relatively humid on the eastern coast to relatively dry on the western coast. The higher mountains and plateaus, mainly in the central parts, are also relatively humid. The average rainfall in South Africa ranges between 600-1100 mm yr^{-1} (Chase & Meadows, 2007). The southwestern part of South Africa has two rainfall zones: a winter rainfall zone (WRZ) and a year-round rainfall zone (YRZ), while the rest of South Africa is a summer rainfall zone (SRZ) (Gasse, 2000; Chase & Meadows, 2007). Maputaland, in the summer rainfall zone, is the most humid region of South Africa, as the precipitation ranges between 600 and 1100 mm yr^{-1} in the west and east, respectively (Grundling, 2014a). South African peatlands are mainly minerotrophic (fens), with primary dependence on groundwater supply (Grundling & Grobler, 2005). The negative balance between rainfall and total evaporation makes it likely that peatlands in South Africa originate from continuous groundwater flow (e.g. Grundling *et al.,* 2015). Nevertheless, the present distribution of peatlands in South Africa reflects the rainfall distribution of the country (e.g. Grundling, 2014b).

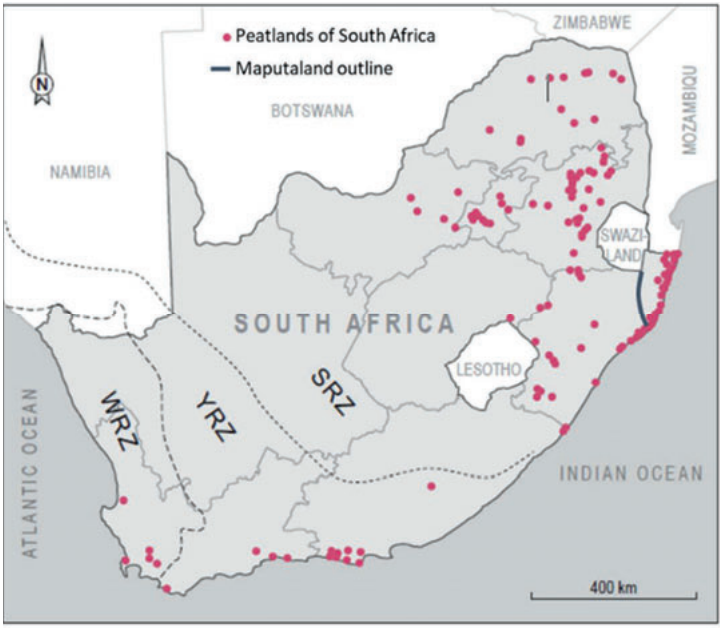

Figure 1. Peatland distribution in South Africa, SRZ: summer rainfall zone, YRZ: year-round rainfall zone and WRZ: winter rainfall zone (Adapted from Grundling *et al.,* 2017).

Mfabeni mire, a coastal mire in Maputaland, is the oldest known mire in South Africa, dating back to more than 43,000 years ago (Finch & Hill, 2008; Baker *et al*., 2014; Grundling, 2014b). Generally in Maputaland, accumulation rates derived from radiocarbon dating of peat layers are about 1-2 mm yr^{-1} (e.g. Thamm, 1996; Baker *et*

al., 2014). Further, Wonderkrater is in the interior and dates back to about 35,000 years ago (Scott *et al*., 2003; McCarthy *et al*., 2010). In Wonderkrater, increased accumulation took place about 7,500 about years ago (Meadows, 1988), with accumulation rates increasing from ca. 0.06-0.1 mm yr^{-1} during the Late Pleistocene to 0.2-0.38 mm yr^{-1} during the Holocene mm yr^{-1} (McCarthy *et al.,* 2010).

MATERIALS AND METHODS

Sampling and laboratory analysis

Peat cores were taken from seven study areas during this investigation. The study areas cover two of the rainfall zones: the summer and the year-round rainfall zones. They are distributed over different landscape types including coastal and inland areas (Figure 2). The cores were taken from the central parts of the peatlands, which also have the deepest peat accumulation at each area. Core sites were chosen after a quick investigation of the peat depths, using a Russian corer, in longitudinal transects through the study areas. Table 1 lists the site names, locality, current land use, landscape and vegetation, and closest town. Age-depth models of peat profiles were produced for seven study areas in this investigation, supplemented with two areas that were studied by Baker *et al*. (2014) and Scott *et al*. (2003), and calibrated using "BACON" (Blaauw & Christen, 2011).

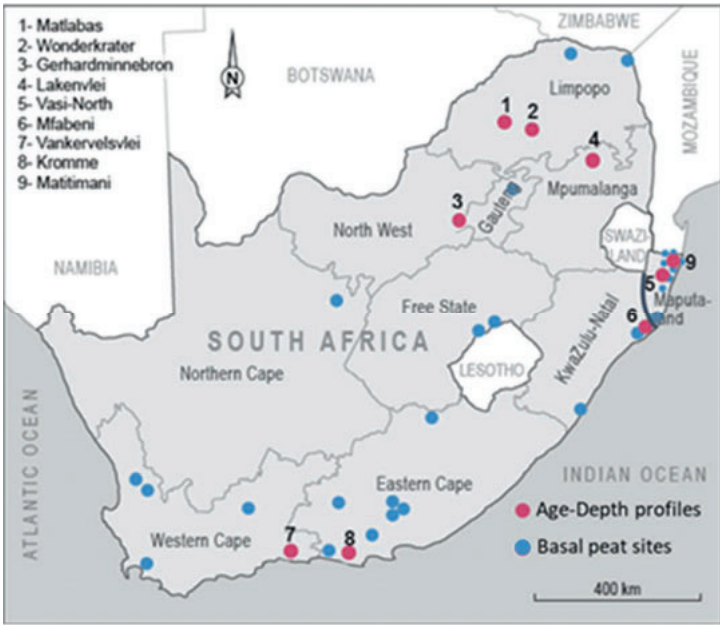

Figure 2. Red dots: Study areas where age-depth models have been constructed for the peat profiles (numbered, red dots). Seven of these areas were studied as part of this research, and two (Mfabeni and

Wonderkrater) were taken from previous studies. These last two were updated with the SHCAL13 curve. Blue dots: study areas where basal peat samples were analysed.

Table 1. Description of the study areas where peat cores were taken. SRZ: summer rainfall zone, YRZ: year-round rainfall zone.

No.	Site	(coastal / interior)	Land use	Landscape / vegetation	Closest Town	Rainfall zone
1	Vasi-North	Coastal	Conservation / tourism	Interdune valley / reeds sedge	Emanguzi	SRZ
2	Vankervelsvlei	Coastal	Forestry	Interdune valley / sphagnum	Sedgefield	YRZ
3	Kromme	Coastal	Agriculture/ water supply	Palmiet	Kareedouw	YRZ
4	Lakenvlei	Highveld (interior)	Tourism	Headwater and valley bottom / reed and sedge	Dullstroom	SRZ
5	Matlabas	Mountain (interior	Tourism	High altitude and steep slopes / grass and reeds	Thabazimbi (in Marakele National Park)	SRZ
6	Gerhardminnebron	Interior	Agriculture/ mining	Karst/ reeds sedge	Potchefstroom	SRZ
7	Matitimani	Coastal	Conservation/ tourism	Valley bottom / swamp forest	Pretoria	SRZ

The peat sampling was conducted using a Russian D-corer with 50-cm sections (De Vleeschouwer *et al*., 2010). Samples for radiocarbon dating were taken as 1-cm sections from the cores. All samples were sealed in plastic bags and sent to the Centre for Isotope Research (CIO) laboratory at the University of Groningen, the Netherlands. The samples were chemically treated using the standard AAA (Alkali-Acid-Alkali) method (Piotrowska *et al*., 2011). Then the purified datable fraction was combusted into CO_2 gas using an Elemental Analyser coupled to an Isotope Ratio Mass Spectrometer (IsoCube/IsoPrime). IRMS measures the stable $^{13}C/^{12}C$ isotope ratio.

For radiocarbon analysis, a part of the CO_2 was routed to a cryogenic trap to collect the samples for further processing. The CO_2 was transformed into graphite powder by the reaction $CO_2 + 2H_2 \rightarrow 2H_2O + C$ at a temperature of 600°C using Fe powder as a catalyst (Aerts *et al.,* 2001). Next, the graphite was pressed into target holders for the ion source of the Accelerator Mass Spectrometer (AMS). The Groningen AMS system is based on a 2.5 MV tandetron accelerator (van der Plicht *et al*., 2000). It measures the $^{14}C/^{12}C$ ratios of the graphite. From these numbers, the conventional radiocarbon age was determined.

Basal peat histogram

To update the histogram of Meadows (1988), we combined the 15 basal dates from that paper with 13 basal dates from Maputaland (Figure 2; Grundling *et al*., 1998; Grundling *et al.,* 2000; Gabriel *et al.,* 2017a), 2 from Kruger National Park (Gillson & Duffin, 2007), 1 from Wonderkrater (Scott *et al*., 2003) and 9 from this study. Table 2 lists the 40 basal radiocarbon dates of all these peatlands.

Table 2. The 40 basal peat samples for radiocarbon dating of peatland initiation. Calibrated ranges were calculated using OxCal program's SHCal13 curve for zone 1-2. We used 1-sigma with statistical accuracy of 68.2%. **: Lab nr. was not found in the source study. The elevation data are approximated above the mean sea level (m a.m.s.l.).

No.	Lab nr.	Name	Elevation	^{14}C	Error	Max.	Min.	Reference
			m (a.m.s.l.)	(BP)	(%)	(calBP)		
1	Pta-7150	Mfabeni	5	45100	4900		>	Grundling *et al.*, 1998
2	Pta-7555	Mhlanga	15	35600	1300	42770	37435	Grundling *et al.*, 2000
3	Pta-2050	Wonderkrater	1100	34400	1900	41991	33570	Scott *et al.,* 2003
4	Pta-4523	Driehoek	900	14600	290	18455	16975	Meadows, 1988
5	GrN-4011	Aliwal North	1550	12600	110	15210	14255	Meadows, 1988
6	Pta-3845	Cornelia, Clarens	1900	12600	100	15195	14280	Meadows, 1988
7	Pta-4207	Dunedin	1400	12500	160	15190	14070	Meadows, 1988
8	Pta-4318	Salisbury	1400	11800	120	13835	13310	Meadows, 1988
9	63604	Gerhardminnebron	1400	11680	60	13560	13455	This paper
10	GrN-4586	Cape Hangklip	100	11140	65	13090	12790	Meadows, 1988
11	Pta-3682	Craigrossie, Clarens	1900	10600	100	12705	12080	Meadows, 1988
12	63458	Matlabas	1800	9755	50	11220	11095	This paper
13	Pta-7572	Trafalgar Mpenjati	10	9730	100	11255	10725	Grundling *et al.*, 2000
14	Pta-4522	Sneeuberg	1000	9460	70	9540	9265	Meadows, 1988
15	63598	Lakenvlei	1850	8295	45	9415	9255	This paper
16	63247	Vasi-North	50	7760	45	8545	8435	This paper
17	63612	Vankervelsvlei	30	7640	40	7670	7610	This paper
18	Pta-7566	Trafalgar: Lot 187	15	5870	70	6795	6445	Grundling *et al.,* 2000
19	Pta-1388	Scot	700	5070	60	5910	5625	Meadows, 1988
20	13333	Matitimani	10	5465	25	6305	6175	This paper
21	Pta-5256	Nhlangu	20	4840	100	5740	5310	Grundling *et al.,* 1998
22	Pta-7083	KuKalwe	5	4640	60	5570	5045	Grundling *et al.*, 1998
23	Pta-4335	Ellerslie	1400	4200	60	4840	4525	Meadows, 1988
24	Pta-7074	Muzi	40	4200	50	4835	4530	Grundling *et al.,* 1998
25	Pta-6370	KwaMboma	25	4120	60	4820	4425	Grundling *et al.*, 1998
26	UW-169	Loerie	300	4010	70	4790	4155	Meadows, 1988
27	Pta-3868	Deelpan	1200	3890	90	4515	3985	Meadows, 1988
28	63238	Vasi Pan	55	3660	35	3980	3870	This paper
29	Pta-4342	Compassberg	1300	3590	70	4075	3640	Meadows, 1988
30	63678	Kromme	460	3415	35	3700	3610	This paper
31	**	Malahlapanga	400	4940	100	5840	5480	Gillson & Duffin, 2007
32	Pta-2683	Norga	200	2980	80	3340	2870	Meadows, 1988
33	Pta-7087	Velindlovu	20	2820	45	2995	2770	Grundling *et al.*, 1998
34	63616	Colbyn	1330	2360	30	2380	2340	This paper
35	Pta-6752	Majiji	70	2140	70	2310	1925	Grundling *et al.,* 1998
36	**	Mfayeni	350	1365	35	1295	1185	Gillson & Duffin, 2007
37	Pta-5253	Mgobezeleni	10	1100	40	1065	905	Grundling *et al.*, 1998
38	12588	KwaMazambane	20	997	80	922	860	Gabriel *et al.,* 2017a
39	Pta-6363	Mseleni	15	770	50	740	560	Grundling *et al.,* 1998
40	Pta-4531	Nuweveldberg	1800	760	50	735	560	Meadows, 1988

The basal radiocarbon dates were calibrated using the "OxCal" software, which uses a Bayesian statistical framework for age modelling (Bronk Ramsey, 2009). The calibration was carried out with the southern hemisphere calibration curve, namely SHCAL13 for zone 1–2 (Hogg *et al.,* 2013). Some samples were affected by the post-

bomb period (after 1960) and were reported in percent modern carbon (pMC) instead of BP. These were dated using the bomb-matching calibration curve for the southern hemisphere (Hua *et al*., 2013).

RESULTS

Frequency of peatland initiation

Peatland initiation frequency of the 40 South African peatlands over a period of 50,000 years was plotted in Figure 3. It shows four peaks, at 15,000, 10,000, 6,000 (up to 3,000) and 1,000 calBP. Less than 10% of the radiocarbon dated peatlands were initiated in the period ca. 50,000–21,000 calBP, 30% during 21,000–11,000 calBP and 17% in the period ca. 11,000–6,000 calBP. The majority of the peatlands (> 40%) were initiated after ca. 6,000 calBP, and 75% of these were coastal peatlands. The peak for interior mountain peatlands occurred during the time interval of 21,000–11,000 calBP. The largest number of total peatland initiations occurred during the period after 6,000 calBP.

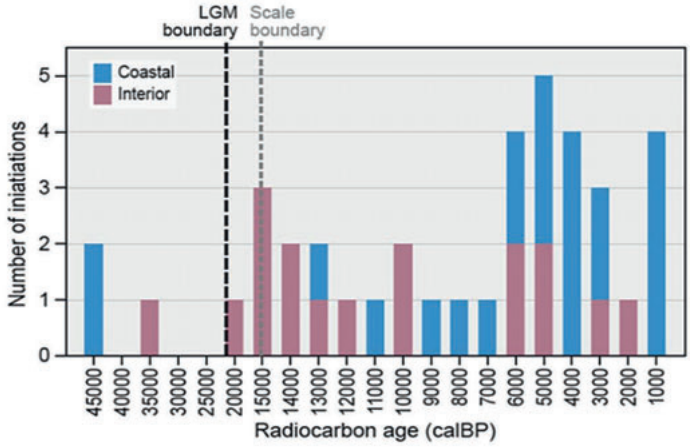

Figure 3. Histogram of interior (17) and coastal (23) peatland initiation based on 40 basal radiocarbon dates in South Africa over a period of ca. 45 000 calBP years. LGM = Last Glacial Maximum.

Time-space series

Time-space series were constructed to show the spatial distribution of peatland basal dates in South Africa. The series consists of four time-space maps showing the basal radiocarbon dates of 40 peatlands within time intervals: 50,000–21,000, 21,000–11,000, 9,000–6,000, 6,000 calBP–recent (Figure 4).

Age-depth models

Figure 5 shows peat accumulation rates of nine peatlands, each of which had different scales and segments with different slopes, which show the change in accumulation rates. The age-depth model for Mfabeni had seven segments with an almost vertical

line (periods of high accumulation), except after 20,000 calBP until 10,000 calBP. The slope for Wonderkrater was almost steady, except for the last few thousands of years where the curve changed from a more vertical to a slightly more horizontal slope (peat accumulation slowed down). The Gerhardminnebron peatland commenced during the Late Pleistocene and showed a steady slope of accumulation. Vasi-North and Lakenvlei both commenced around 8,000 calBP, but Lakenvlei had a more horizontal segment (lower peat accumulation) with accelerated accumulation rates around 4,000 calBP.

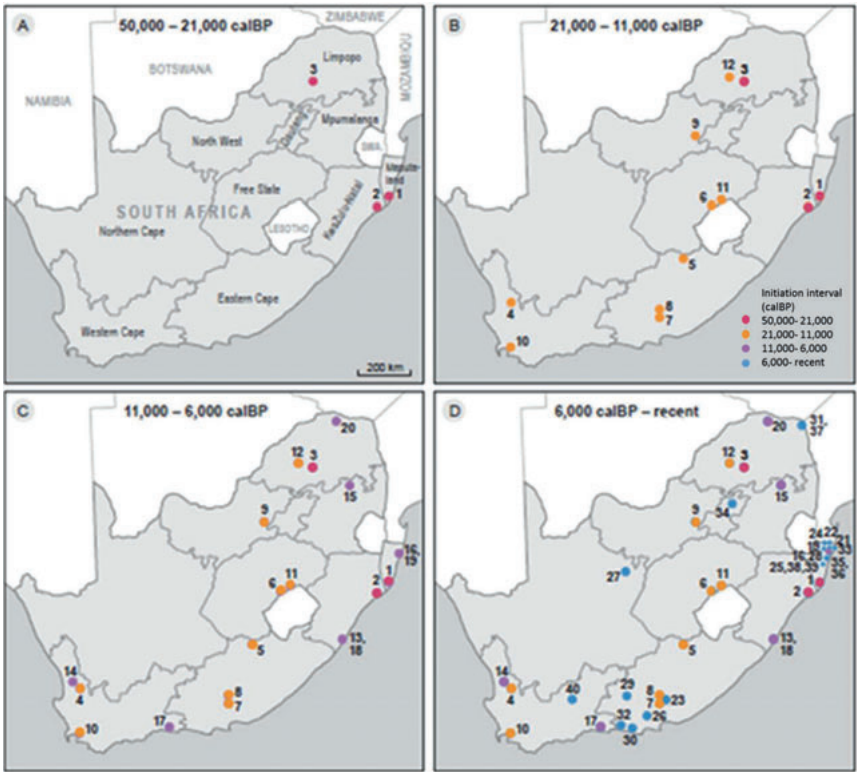

Figure 2. Time-series maps of peatland initiation based on radiocarbon dating in South Africa. Four time intervals are given, showing the basal radiocarbon dates of 40 peatlands: 50,000–21.000, 21,000–11,000, 11,000–6,000, 6,000 calBP–recent. 1—Mfabeni, 2—Mhlanga, 3—Wonderkrater, 4—Driehoek, 5—Aliwal North, 6—Cornelia, Clarens, 7—Dunedin, 8—Salisbury, 9—Gerhardminnebron, 10—Cape Hangklip, 11—Craigrossie, Clarens, 12—Matlabas, 13—Trafalgar Mpenjati, 14—Sneeuberg, 15—Lakenvlei, 16—Vasi-North 17—Vankervelsvlei, 18—Trafalgar: Lot 187, 19—Matitimani, 20—Scot, 21—Nhlangu, 22—KuKalwe, 23—Ellerslie, 24—Muzi, 25—KwaMboma, 26—Loerie, 27—Deelpan, 28—Vasi Pan, 29—Compassberg, 30—Kromme, 31—Malahlapanga, 32—Norga, 33—Velindlovu, 34—Colbyn, 35—Majiji, 36—Mgobezeleni, 37—KwaMazambane, 38—Mfayeni, 39—Mseleni, 40—Nuweveldberg.

Vankervelsvlei, Matlabas and Matitimani were initiated around 7,000–6,000 calBP. Vankervelsvlei had steady rates of peat accumulation while Matlabas and Matitimani went through different phases, but they all had slower rates between 5,000–3,000

calBP. Kromme was the last peatland to be initiated and had the highest accumulation rate of the nine sites, especially during the first 1,000 years of development.

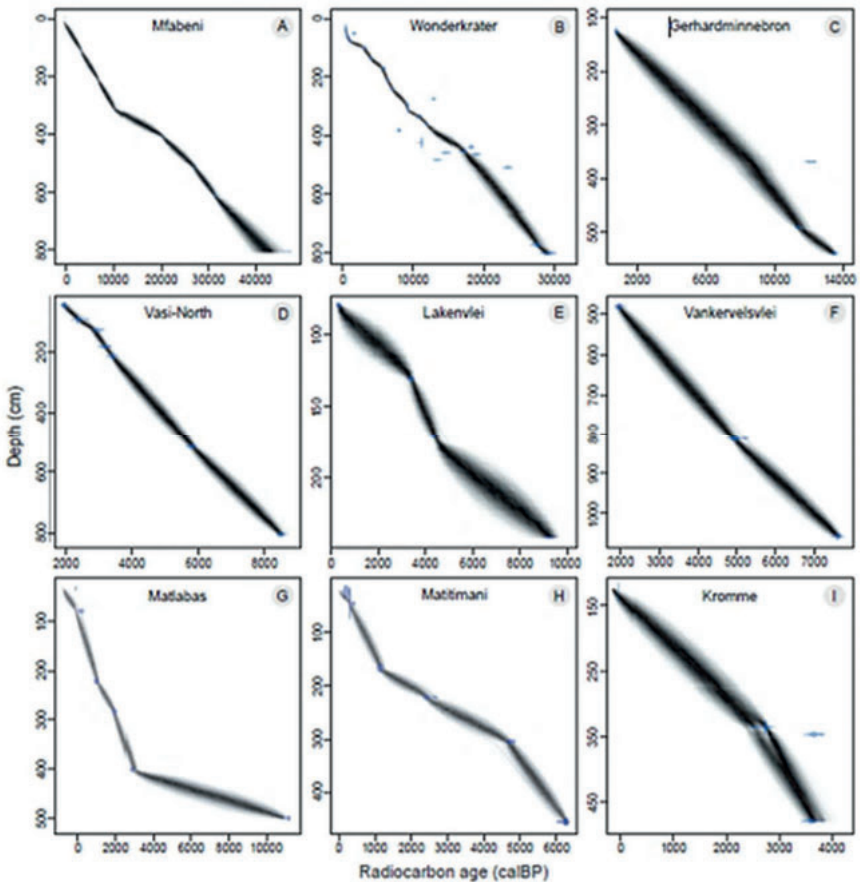

Figure 3. Age-depth models of nine peatlands in South Africa. The blue ranges represent the calibrated sample age ranges while the black shadows represent the calibrated range of each point interpolated between the sampled ages (calBP cm-1). calBP—radiocarbon calibrated calendar age, A (Adapted from Baker *et al.,* 2014), B (Adapted from Scott *et al.,* 2003), C to I (data collected during this study).

DISCUSSION

50 000–11 000 calBP

During the Late Pleistocene, the cold and dry conditions of the glacial period were not favorable for peat formation on a global scale (Bell & Walker, 1992; Yu *et al*., 2010). However, some areas in the southern hemisphere developed peatlands in marginal conditions. Tropical peatlands in Southeast Asia, for instance, were initiated earlier during this period than ones in the northern hemisphere (Yu *et al*., 2010). We also

found that in South Africa, around twelve peatlands initiated their development during the Late Pleistocene and that this period had two distinct periods of peatland initiation. The first period, prior to the LGM, included the smallest portion of peatland initiation. It included the initiation of only three peatlands: Mfabeni and Mhlanga (both in the south of the coastal plain of Maputaland) and Wonderkrater, which is an interior mountain spring peatland, of which Mfabeni is the oldest one. The second period, which occurred post LGM during the glacial-interglacial transition, included the initiation of nine peatlands, seven of which are interior peatlands. The glacial-interglacial transition peak for the South African interior peatland initiation is similar to the pattern of montane peatlands in Southeast Asia, whose initiation peaked around 17,000–13,000 years ago (Page *et al*., 2004; Yu *et al.,* 2010).

The accumulation rates during the glacial-interglacial transition period, ca. between 21,000 to 11,000, was generally lower than both the earlier glacial and the later interglacial periods. For instance, both the Mfabeni and Wonderkrater peatlands showed higher accumulation rates prior to LGM, after which the rates decreased by ~50%. The lower accumulation rates in this period could infer that the transition period was warmer, yet with dry conditions not favouring peat accumulation. However, it is noted that in Mfabeni, the accumulation rates appeared to mirror fluctuations in sea level (Ramsay, 1995; Ramsay & Cooper, 2002; Grundling, 2004; Grundling *et al*., 2013b). The accumulation rates at Gerhardminnebron and Matlabas during the Late Pleistocene were also low, indicating that despite the initiation of peatlands in the glacial-interglacial period, the conditions were not optimal until the Holocene.

Holocene

Early Holocene (11 000–6000 calBP)

Peatland initiation frequency during the Early Holocene was relatively low after LGM. Except for two interior peatlands that initiated, developing during the period 10,000–9,000 calBP, almost all the peatlands that developed during the Early Holocene were situated along the coast. This was due to post glacial climatic changes in Southern Africa, which resulted in a dry and warm climate (Truc *et al.,* 2013) with an accompanying rise in sea level starting around 9,000 calBP (Ramsay, 1995; Gasse, 2000; Ramsay & Cooper, 2002; Grundling, 2004). Only from 6,000 calBP onwards did the number of peatland initiations increase. In the inland regions, this delay may have been caused by the successive replenishment of groundwater. In the coastal regions, however, the rising of sea level to the present levels for the first time around 7,000–6,000 calBP might have been the primary driver of higher water-tables (Ramsay & Cooper, 2002; Grundling, 2004; Gabriel *et al.,* 2017a). Other studies linked a rise in sea water levels to an increase in peatland initiation frequency during the Holocene (Yu *et al.,* 2010; Dekker *et al.,* 2015). However, some peatlands seem not to be related to sea level rise, but to be a reflection of local hydrogeomorphic conditions. For instance, Vasi-North (altitude of 45 to 55 m a.m.s.l.) initiated shortly after 9,000 calBP, in contrast to Matitimani peatland (which is at an altitude of only 10 m a.m.s.l) which

initiated peat accumulation ca. 7,000 calBP (Grundling *et al.,* 2013b; Gabriel *et al.,* 2017a). Furthermore, within the Vasi peatland complex, Vasi Pan, which is in the same peatland complex as Vasi-North but at a higher altitude of 64 m a.m.s.l, initiated its peat accumulation ca. 4,000 calBP following the infilling of the lower area first. The dependency of the peat accumulation on the altitude within the Vasi peatland complex (Vasi-North and Vasi Pan), and independently from the primary aquifer in Maputaland, indicates the possible existence of a perched aquifer systems that allowed peat initiation independently from the sea level fluctuation (Elshehawi *et al*.; see Chapter 4). The perched aquifers might have formed due to formation of iron-rich impervious layers (Botha & Porat, 2007; Porat & Botha 2008).

Further, accumulation rates in the older peatlands, such as Mfabeni, Wonderkrater and Gerhardminnebron, showed increased accumulation rates during the Early Holocene, up to 0.34 and 0.35 mm yr^{-1}, respectively. Matlabas in the Waterberg Mountains kept the same accumulation rate, but this was partly due to the presence of intercalating mineral sediments, which indicate high energy flows eroding the peat. The younger peatlands (e.g. Vasi-North and Lakenvlei) had accumulation rates of 1 and 0.25 mm yr^{-1}, respectively, during this period. Vasi-North started as an open lake with gyttja deposits, which constitutes about 4 m of the total organic layer in this peatland. These different accumulation rates are not only a function of climatic conditions, but also their localized geomorphic conditions and initiation and development process. For instance, Matlabas initiation took place via paludification directly over the mineral soil, due to seasonal inputs of flood water, which came in the form of high energy water flows during the wet seasons. The deposition of clay sediments by these flows decreased the permeability and allowed peat accumulation initiation. These energy flows were not stable over time which possibly led to loss of peat accumulations from early stages until the mire stabilized. Matlabas and Lakenvlei show the resemblance of the slow early accumulation rates, due to being headwaters peatlands with fluctuating energy flows. This is in contrast to peatlands initiating via terrestrialisation in low energy environments.

Mid to Late Holocene (6000 calBP– present)

Peatland initiation reached a maximum during the Mid Holocene with a total of 15 peatlands initiating during this period. Two thirds of them were coastal peatlands, mainly in Maputaland and in the year-round rainfall zone, and the other one third were interior mountain peatlands. The northern part of Maputaland had the largest share of the peatland initiations. Later in the Holocene around 2,000 calBP, peatland initiation decreased before increasing again in the last millennium. Ramsay (1995) reported a steady rise in the sea level along the eastern coast of South Africa during the Holocene (Ramsay, 1995). Gabriel *et al*. (2017a), studying macrofossils in the Matitimani peatland, also referred to sea level rise as a main driver for the initiation of coastal peatlands in Maputaland. Emphasizing the connection between peatland formation and sea level, they attributed a decline in seeds of aquatic plant species, which indicates drier hydrological conditions, to a drop in sea level from the Holocene high stand. It is likely that sea level rise also played this role in South African

peatlands, especially the coastal ones. Peatlands of the Everglades in Florida showed a similar response to a rise in sea level, which reduced the drainage of the groundwater basin (i.e. loss of water to the sea) prompting peatland initiation (Dekker *et al.,* 2015). This rise in initiation is similar in timing (during the Mid to Late Holocene) to that observed by Dommain *et al*. (2011) in some of the Indonesian inland peatland areas. However, the Indonesian coastal peatlands followed a different pattern, in which sea level fall allowed peat accumulation on the newly emergent land (Dommain *et al.*, 2011).

Besides the sea level rise, a period of high precipitation 6,800–3,600 calBP was indicated in a pollen record from Lake Eteza in southern Maputaland, which also coincided with the period of coastal peatland initiations. The higher rainfall in the coastal area of KwaZulu-Natal was caused by a strengthened southward shift of the warm Aghulas Current (Neumann *et al*., 2010). The increase in rainfall attributed to the Aghulas Current might have contributed to the peatland initiation and development, especially in the perched groundwater systems, e.g. Vasi-North. Also, the development of peatlands could create a blocking effect in the lower areas, owing to the lower permeability of peat, which could lower the drainage from the groundwater system in the upper areas, e.g. KwaMazambane and Vasi Pan (Gabriel *et al.,* 2017a). Dekker *et al.* 2015 attributed peatland development to a combined increase in rainfall, sea level rise and local hydrogeomorphic settings, e.g. the perched groundwater aquifers or the blocking effects (Dekker *et al.,* 2015). The Mid Holocene phases could be attributed to sea level rise and combinations of the three effects. In order to verify the amplitude of these effects in each area, detailed scale studies that assess the relation of the peatland hydrology to the landscape's primary aquifers might be needed.

Further, the accumulation rates of peat in Maputaland were estimated to be about 1-2 mm yr^{-1}, deduced from pollen dating (Thamm *et al.,* 1996). We found that accumulation rates during the Late Holocene were among the highest reported in South Africa. In Maputaland, the Mfabeni peatland had an accumulation rate of 0.3 mm yr^{-1} (Baker *et al*., 2014), while Vasi-North shifted from gyttja (open lake deposits) to peat or gyttja-peat accumulations (Elshehawi *et al.;* see Chapter 4) with an average accumulation rate of 1.5 mm yr^{-1}. Vasi-North and Vasi Pan recorded the highest accumulation rates in our study, yet both have radiocarbon ages of >2,000 calBP in the topsoil, due to a disturbance which led to peat erosion. Interior peatlands also had increased accumulation rates during this period when compared with the Early-Holocene. Wonderkrater had an accumulation rate of 0.22 to 0.38 mm yr^{-1} (McCarthy *et al*., 2010), while accumulation rates for Matlabas and Lakenvlei increased to almost 1 and 0.5 mm yr^{-1}, respectively. However, Lakenvlei shifted to a lower accumulation rate during the Late Holocene. Vankervelsvlei and Kromme in the year-round rainfall zone showed an accumulation rate of 1 mm yr^{-1} close to these observed in Maputaland. Kromme had a slower rate afterwards (~2.5K calBP) of almost 0.8 mm yr^{-1}. We note that Vankervelsvlei was dated at 2000 calBP at a depth of 5 m, which indicates it had a high accumulation rate of 2.5 mm yr^{-1} during the Late Holocene. On average, the accumulation rates seemed to be higher in the Mid to Late Holocene,

which possibly is related to the wetter climatic conditions, which is one of the drivers favouring peat accumulation.

CONCLUSION

Peatland initiation patterns in South Africa are consistent with the evidence for climate and sea-level fluctuations, which appear to have played a primary role in peatland initiation and development, with a possible secondary role for local hydrogeomorphic settings, over the Late Pleistocene to Holocene. There were three periods of optimal conditions for peatland initiation, one of which was right after the LGM and the other two were during the Mid to Late Holocene. The formation of interior peatlands dominated the optimal period after LGM (ca. 18,000 to 15,000 calBP) owing to climatic shifts to warm and wet conditions during the glacial-interglacial transition. The coastal peatlands had maximum humid conditions in two periods from ca. 6000 to 3000 calBP and during the last millennium owing primarily to sea level rise and possibly to a mixture of the increased rainfall in the Mid Holocene and the effect of the local hydrogeomorphic settings. Average accumulation rates ranged from 0.07 to 2.19 mm yr^{-1}, with the coastal peatlands having higher average accumulation rates than the interior ones. The average accumulation rates were higher during the Mid to Late Holocene for all of the peatlands in this study.

ACKNOWLEDGEMENT

We would like to thank the following parties for their contribution. WRC for their funding under project K5/2346. Ecological Restoration Advice Foundation (ERA) for their funding. SANPARKS for supporting the research at Malahlapanga (Kruger) and Matlabas (Marakele) with Cathy Greaver, Marius Snyders, Nick Zambatis, Stephen Midzi, and Steven Khoza for logistical and research support. Mariusz Gałka from Poznań University for sharing his data. PG Bison for permission to access Vankervelsvlei. Finally, we thank co-workers in the field: Althea Grundling, Baps Snijdewind, Antoinette Bootsma, Mafunyane Rossouw, Anton Linstrom, Lulu Pretorius, Nancy Job, Steve Mitchell and Brenton Mabuza. Also, we thank Dick Visser for preparing the figures.

APPENDIX

Appendix 1. Calculated accumulation rates of peatlands with ^{14}C dating of their profiles.

Name	Segment	^{14}C dating (calBP)		Time difference (yr)	Depth (cm)		Accumulation Rate (mm yr^{-1})
		From	to		From	to	
Mfabeni	1	43000	33000	10000	800	620	0.18
	2	33000	27000	6000	620	530	0.15
	3	27000	20000	7000	530	405	0.18
	4	20000	10000	10000	405	340	0.07
	5	10000	0	10000	340	0	0.34
Wonderkrater	1	35600	17000	18600	800	440	0.19
	2	17000	9000	8000	440	350	0.11
	3	9000	7000	2000	350	280	0.35
	4	7000	6000	1000	280	160	1.20
	5	6000	3750	2250	160	100	0.27
	6	3750	1500	2250	100	80	0.09
	7	1500	0	1500	80	0	0.53
Gerhardminnebron	1	13500	11400	2100	540	500	0.19
	2	11400	880	10520	500	120	0.36
Vasi-North	1	8490	5830	2660	805	516	1.09
	2	5830	3410	2420	516	214	1.25
	3	3410	3200	210	214	182	1.52
	4	3200	2890	310	182	128	1.74
	5	2890	2735	155	128	94	2.19
	6	2735	1965	770	94	47	0.61
Lakenvlei	1	9300	4100	5200	240	180	0.12
	2	4100	3500	600	180	130	0.83
	3	3500	350	3150	130	30	0.32
Vankervelsvlei	1	7640	4800	2840	1060	800	0.92
	2	4800	1800	3000	800	490	1.03
Matlabas	1	11160	2800	8360	500	400	0.12
	2	2800	1900	900	400	285	1.28
	3	1900	1400	500	285	230	1.10
	4	1400	-50	1450	230	35	1.34
Matitimani	1	6100	4800	1300	450	300	1.15
	2	4800	1000	3800	300	170	0.34
	3	1000	300	700	170	40	1.86
	4	300	0	300	40	10	1.00
Kromme	1	3500	2500	1000	450	340	1.10
	2	2500	0	2500	350	130	0.88

3

Ecohydrological assessment of the Vasi peatland complex in South Africa indicates degradation driven by changes in land use*

The Vasi peatland complex is situated in the northeast of South Africa. It is an unprotected area surrounded by pine- (Pinus sp.) and blue gum (Eucalyptus sp.) plantations. There is little known about the conditioning factors for the area's development and degradation causes. In order to understand the ecohydrological system of this peatland complex, water tables, ion composition of surface and groundwater, and natural isotopes of oxygen, hydrogen and carbon were measured. Macro-fossils and radiocarbon dating of the peat layer were also used to describe the historical environmental conditions. We found that the accumulation in Vasi peatlands started during the Early Holocene and was initiated via terrestrialisation of inter-dune lakes. The peat radiocarbon dating data indicate positive feedback effects of blockage, during which infilling of Vasi-North with gyttja raised the water table in the basins of Vasi Pan, which are positioned at a higher elevation. The Vasi peatland complex is primarily dependent on a perched water table due to presence of iron-rich deposits in the surrounding sand dunes (KwaMbonambi Formation). The basins of Vasi peatland complex appear to be hydrologically connected in which some basins show indications of cascading through-flow systems. Despite some indications of natural peat fires in the macro-fossil analysis, continuous accumulation appears to have lasted under a persistent water table for thousands of years. We conclude that the observed signs of degradation are not due to natural causes, but to changes in land use, i.e. surrounding plantations, which have induced a drawdown in groundwater tables.

* This chapter is submitted as: Elshehawi, S., Gabriel, M., Pretorius, L., Bukhosini, S., Butler, M., van der Plicht, J., Grundling, P.L., Grootjans, A. (in review) Ecohydrological Assessment of the Vasi peatland complex in South Africa indicates degradation driven by changes in land use.

INTRODUCTION

Peatlands are quite abundant in the northern hemisphere, but they are relatively rare in the southern hemisphere and even more so in its sub-tropical regions, e.g. South Africa (Joosten & Clarke, 2002). In South Africa, around 60% of the peatlands are situated along the coastline of Maputaland in northern KwaZulu-Natal province (Grundling *et al.,* 1998; Grundling & Grobler, 2005). Peatlands in Maputaland range from peat swamp forests in valleys that drain upland areas or link inter-dune drainage lines to coastal lakes (Grundling *et al*., 2000) to sedge-dominated fens in inter-dune depressions (Grundling & Grobler, 2005). Most of these systems started accumulating peat during the Holocene (Thamm *et al*., 1996; Grundling *et al*., 1998), but some date back to the Late-Pleistocene (Grundling & Grobler, 2005; Grundling *et al*., 2013b; Baker *et al*., 2014).

Peatlands in Maputaland primarily depend on groundwater supply (e.g. Grundling *et al.,* 2013a; Kelbe *et al*., 2016). Groundwater supply to the peatlands provide them with anoxic soil conditions and prevents rapid mineralisation of the peat (Mitsch & Gosselink, 2000a). Disturbance of the natural hydrological processes poses a threat to peatlands, e.g. by groundwater abstraction, afforestation, and eutrophication of water flows through intensive agricultural use (Maltby & Barker, 2009).

During the last decade drops in groundwater tables have been observed in large parts of Maputaland, ranging from the Muzi swamp in Tembe Elephant Park (Grundling, 2014a) in the west to the Manguzi area in the east and Lake Sibaya in the south (Weitz & Demilie, 2014). The Vasi peatland complex in eastern Maputaland is surrounded by expanding pine (*Pinus* sp.) and blue gum (*Eucalyptus* sp.) plantations (Figure 1a). According to local residents (pers. comm. S. Bukhosini 2014) the water table in the Vasi peatlands has been dropping steadily during the past 20 years, and regular peat fires were observed. Grundling & Blackmore (1998) reported severe burning of the peat in 1996 and suggested that fire risk might be reduced by removing relatively small sections of the tree plantations, which should have positive knock-on effects on water tables. However, they warned that this might not be sufficient in the long run as the period 1997-1998 had been characterised by high rainfall (Grundling & Blackmore, 1998). More recently, peat fires have started again in the Vasi peatland complex, leading to an increased loss of peat and destruction of the sedge-dominated vegetation (Figures 1b and c).

Currently, the hydrological system of the Vasi peatland complex is not well understood. Grundling *et al*. (2013a), and Kelbe *et al*. (2016), studied the relation between the water table depth and the spatial distribution and temporal behaviour of the wetlands in the northern Maputaland coastal plain. They concluded that the occurrence and development of wetlands was greatly influenced by topography on both local and sub-regional levels. The studies further suggested that the permanent wetlands, which contained rather thick peats were influenced by a high and steady regional water table. Meanwhile temporary wetlands are most likely disconnected from the regional water table. However, such systems could be important in providing water to wetlands at lower elevations via cascading (e.g. Stuyfzand, 1993). Hence, the

interaction between local and regional hydrological systems could be important to sustain peatlands, such as the ones in the Vasi peatland complex (Grundling *et al.,* 2013a; Kelbe *et al.,* 2016).

Bate *et al*. (2016), also studied the impact of pine and blue gum plantations on the hydrology in the Mgobezeleni catchment area near the town of Mbazwana, using a hydrological model (MODFLOW). They concluded that groundwater tables have dropped within and beyond the areas where the plantations were established. They also calculated a significant drawdown of the water table due to the dry climate cycle but also, more importantly, to the groundwater interception and evapotranspiration rate of the commercial plantations. The model results revealed that between 2004 and 2014, these combined effects had induced a cone of depression in water tables of up to 7-9 meters in the central parts of the plantations.

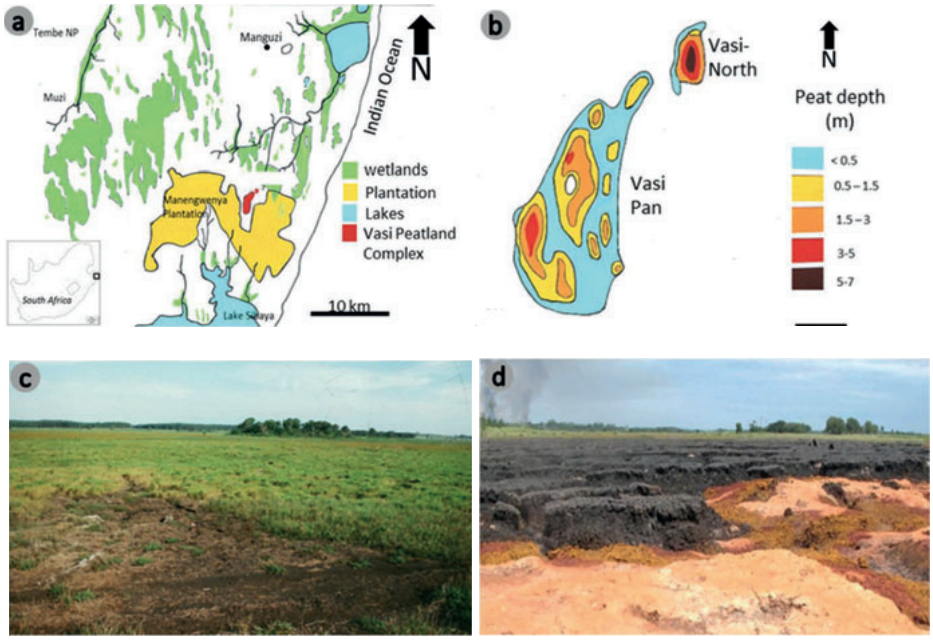

Figure 1. (a) Location of the study area: Vasi peatland complex (red), north of Lake Sibaya in KwaZulu-Natal, South Africa. The Vasi peatland complex is surrounded by the Manzengwenya plantations (yellow). (b) Peat depths in the Vasi Peatland Complex (source: Grundling & Blackmore, 1998). (c) A photograph of one of the basins in Vasi Pan taken in 1998, with the vegetation cover still intact. (d) A photograph of the same basin on March, 2014. The vegetation cover has disappeared, 30–40cm of the peat has turned into ashes with widened fissures in between and some areas point to old spring sites, which can be identified by the orange/brown colour indicating iron deposits.

In the present study, we aim to gain a better understanding of the past and present hydrological conditions of the Vasi peatland complex. More specifically, we want to know whether the peatlands are fed by local hydrological systems or whether the groundwater supply involves larger regional hydrological systems. For insight into

the origin of water flows, we used stable isotope ratios of hydrogen and oxygen (δ^2H and $\delta^{18}O$) (Schot & Van der Waal, 1992; Gat, 1996; Clark & Aravena, 2005). If the Vasi peatlands are indeed influenced by regional groundwater with long residence times, we would expect to find groundwater with lower radiocarbon values (^{14}C) than groundwater from local hydrological systems, due to their longer flow line and hence residence times (Mook, 2006). In addition, if the present levels of severe peat degradation do not result from the expanding pine and blue gum plantations but rather from the re-occurring dry climate cycles, we would expect loss of peat in the past and also considerable discontinuities during periods of peat accumulation in the past. Hence, an ecohydrological system approach was used (Grootjans & Van Diggelen, 2009), in which we intergrated macro-fossil and stratigraphic research of past peat development with results of hydrological research on present hydrological conditions. We described and dated peat profiles, measured water tables, and analysed ion composition, isotopic signatures and also analysed ^{14}C contents of the ground and surface water in the Vasi complex and wider surroundings.

The specific objectives are to 1) investigate the possible interaction between local- and regional groundwater systems in the Maputaland and the origin of the groundwater supply to the Vasi peatland complex, 2) identify the hydrological flow directions and the possible hydrological link among the different basins in the complex, and 3) verify whether the degradation of the Vasi peatlands is related to external land use management practices.

METHODS

Study area

The Vasi peatland complex (27°11'12.31" S, 32°42'40.00" E) is located in the northern part of the Maputaland coastal plain (MCP), 10 km inland from the Indian Ocean coastline at a height of about 50-60 m above mean sea level (a.m.s.l., Grundling, 2014a). The Vasi peatland complex consist of several peatlands with varying peat depths (Figure 2). Most peat deposits are situated in the area known as Vasi Pan. North of Vasi Pan lies a smaller peatland: Vasi-North, where the thickest peat layer is 5-7 meters. Both areas are surrounded by the Manzengwenya State Plantation, which was established in the 1960s (Thamm *et al.,* 1996). Vasi Pan consists of three distinct basins separated by small sandy ridges running south to north. Vasi-North is separated from Vasi Pan by a sandy ridge with a width of 300 m. The total area of Vasi Pan is about 210 ha, while Vasi-North is only 12 ha (Grundling & Blackmore, 1998; Grundling *et al*., 2016). The Vasi peatlands have been used for livestock grazing by the inhabitants of the nearby village of Mvelabusha, and subsistence gardens were maintained on the Vasi-North peatland in the past.

The average annual rainfall in Maputaland increases from 700 mm/year in the Lebombo Mountains in the west to around 1100 mm/year in the east (Grundling *et al.,* 2013a). The summer wet season lasts from November to March (Grundling *et al.,* 2013a). The catchment of the Vasi peatland complex receives up to 750-800 mm of

rain per year and has a significant precipitation deficit, as the maximum potential evapotranspiration for this area is about 2200 mm/year (Mucina & Rutherford, 2006). The primary aquifer in Maputaland Coastal Plain consists of the Uloa, KwaMbonambi, Kosi Bay and Sibaya Formations, from bottom to top. They overlie an aquiclude formation consisting of claystones and siltstones (Zululand Group), which is considered the base of the primary aquifer (Kelbe *et al.,* 2016). The Uloa Formation consists of karst rocks with intercalated mudstones. It is, however, overlain by an impervious layer (Port Durnford Formation) and Lignite in the east side of the plain, which separates it from the primary aquifer in this area (Botha *et al.,* 2013; Kelbe *et al.,* 2016). The Kosi Bay Formation is exposed to the surface at the Muzi swamp in the west (Figure 1a), while it is overlain by the KwaMbonambi Formation to the east close to Vasi Peatland Complex (Figure 1a) (Porat & Botha, 2008). The Kosi Bay Formation, which consists of sandy silts, and the dune profile, extensively covers the Maputaland Coastal Plain. Further, the Kosi Bay Formation may contain interspaced clayey (Lignite) and iron-rich soil layers (red sands), which can create perched local groundwater aquifers (Botha & Porat, 2007). The KwaMbonambi Formation consists of reworked sand dunes which cover mostly the eastern parts of the Maputaland Coastal Plain, starting from the surroundings of the Vasi Peatland Complex. Important features of the study area are sandy parabolic ridges (Sibaya Formation) along the coast (Botha & Porat, 2007). These ridges stretch along the south-north direction (Botha *et al.,* 2003) forming an upland area between the Pongola River valley in the west, which drains northwards parallel to the Lebombo Mountain and the numerous coastal lakes in the east (Bruton & Cooper, 1980). However, they are not of importance to the current scope of the Vasi Peatland Complex.

Origin of groundwater flows

Study layout

The study layout is divided into two frames. The first frame is an extensive analysis of groundwater quality, i.e. measurement of ^{14}C, $\delta^{13}C$, $\delta^{2}H$ and $\delta^{18}O$ isotopic contents and ion composition in water samples, of different wet landscapes over the Maputaland Coastal Plain (Figure 2a). The second frame includes internal observation of groundwater within the Vasi Peatland Complex catchment (Figure 2b). The extensive (larger scale) campaign took place over a period of one week from the 18th to the 25th of October, 2017. This layout was aimed at investigating the relation between the groundwater system in Vasi Peatland Complex and the other primary or regional groundwater system in the Maputaland Coastal Plain. Hence during this campaign, eighteen samples were collected from (i) areas to the west of Vasi Peatland Complex (e.g. Muzi system, which is partly in Tembe Elephant Park, community wells 1 to 3), (ii) areas from the north of Maputaland Coastal Plain (e.g. Manguzi forest, Subsistence Farming, Matitimani and KwaMbazambane peatlands and Gezisa river), and (iii) areas within, and in the surrounding of, the Vasi Peatland Complex (e.g. community wells 4 to 6 and Siyadla river). The samples taken from this campaign were analysed for their ^{14}C, $\delta^{13}C$, $\delta^{2}H$ and $\delta^{18}O$ isotopic contents and ion composition (See

Laboratory analysis).

The focus during the first campaign was to understand the flow origins (discharge and recharge areas) and directions within the Vasi peatland complex area. The second campaign, which took place in the period from January to April, 2015, was focused on the Vasi-North basin supplemented with single points connecting to Vasi Pan (Figure 2b). The low density of observation points within Vasi Pan is due to the frequent fires occurring there. Also, the water table in Vasi Pan is lower at the dune areas, which would be costly to drill deeper holes. This campaign included measuring water table depth and hydraulic head, and sampling water to analyse δ^2H and $\delta^{18}O$ isotopic content, once taken in March and once in April after a 5-mm rainfall event, and ion composition (Figure 2b). This campaign observation points consisted of eight points in the Vasi peatland complex, with each point including tubes (a total of 17) in the peat and sand layers (See next section). The observation points were aligned in two west-east transects in Vasi-North (VNA and VNB), which is the same direction as of the regional groundwater flow direction in Maputaland Coastal Plain, and 3 separate points in Vasi Pan. Four community wells nearby were included, hence a total of 21 samples. A second round was added to the first campaign, during which water was sampled for a repeated δ^2H and $\delta^{18}O$ analysis after a rainfall event of 5 mm that took place in April, 2015. Four other piezometers were added in Vasi-North: three tubes making transect VNC and a shallow piezometer in the peat layer at transect VNA (VNA4P1). Despite the increased number of tubes, the total number of the samples in this campaign was 18 because some tubes fell dry. Additionally, a rain sample was also collected in April, 2015 from a rain gauge at location CW6 (Figure 2a). The sampling points and their tube types, depth and diameters and the sediment medium are listed in Appendix 1.

Groundwater tubes installation and sampling

The holes for the tubes (wells and piezometers) were drilled using a hand auger in the sand layers (diameter: Ø = 50-mm), and a Russian peat corer in the peat layers (Ø = 60-mm). The wells were made out of polyvinyl chloride (PVC) tubes (Ø = 50 mm) perforated along their entire lengths, while the piezometers had diameters of 20 and 40 mm (due to limited availability at the local stores) and a 20-cm screen at the bottom. All the groundwater tubes were flushed using a hand pump before sampling, which was done one to four days after the flushing. In some cases, flushing the groundwater tubes was not possible, especially for the community wells. In such cases, ^{14}C samples were not taken, e.g. CW5 in 2017. Water samples were collected using 100-ml PVC bottles for ion composition analyses, 30-ml dark glass bottles for stable isotopes analysis and 500-ml dark glass bottles for carbon isotope analysis. They were all filled to the brim, with no field filtering or measurements. They were filtered within one to two weeks after sampling in the laboratory, and then stored in a refrigerator at 4ºC.

Water table depth and hydraulic pressure

To assess current water flows in the Vasi peatland complex's basins, water table depth

and the hydraulic heads were measured. Water table depths were monitored on a weekly basis for 2 months (March and April 2015) using wells. The hydraulic heads in the peat and in the basal mineral soil were measured using piezometers. The surface elevation was surveyed at each sampling point, as well as selected points of topography, e.g. a ridge top, by a private firm (FJ Loock Land Surveyors) using a differential GPS linked to a base station.

Figure 2. (a) Sampling points in northern Maputaland (MCP) during 2017 from (i) river samples: RSi— Siyadla river, RGe— Gezisa river, (ii) peatlands: PMu— Muzi, PSF— Subsistence farming, VP— Vasi Pan, VN— Vasi North, PMg: Manguzi forest spring, PKw—KwaMbonambe, PMat— Matitimani, and (iii) community wells (CW). (b) groundwater tube nests (wells and piezometers) measured and sampled in 2015 in Vasi Pan and Vasi-North. The white dots indicate the locations of the cores for 14C dating and stratigraphy description.

Laboratory analysis

Ion composition analyses

Samples for ion composition analyses for both two campaigns were sent to the laboratory of the Institute for Soil, Water and Climate in Pretoria, South Africa. They were filtered and pH was measured. Water ion compositions (HCO_3, Cl, SO_4, Ca, Na, Mg, K, SiO_2, Fe, PO_4 and NH_4) were analysed in the laboratory using ICP-MS (Bos & Fredeen, 1989). The ion composition of the water is used to indicate the groundwater origin and flow directions. The samples are first grouped using principal component analysis (see below) to correlate and cluster similar water types, and tracers are then used to identify groundwater flow directions. The samples ion composition was checked for ion balance (Appelo & Postma, 2005). Chloride and sulphates were used as tracers to identify internal water flows within Vasi-North basin, where chloride was used to determine flow directions, while sulphates were indicators of anoxic discharge zones (Appelo & Postma, 2005).

In order to identify groundwater from different water sources, 13 ions and nutrients (excluding the PO_4 ion because it was not included in the second round in 2017) were analysed using principal component analysis (PCA) (Jackson, 1991). The PCA is used to correlate water samples with similar ion compositions, which allows to identify similar water types. The "Factoextra" package was used, which is a "R" package intended for multivariate statistical analyses, including PCA (Kassambara, 2017). The PCA outcome was visualized as a plot of 13 variable loadings (ion type and magnitude contribution to the principal components) and variation in sample distribution variation based on the first two principal components.

^{2}H and ^{18}O stable isotopes

The stable isotope ratios of hydrogen and oxygen ($\delta^{2}H$ and $\delta^{18}O$) can be used to get more insight into the origin of water flows. This is done by plotting the samples data with the global meteoric water line (GMWL: $\delta^{2}H = 8\ \delta^{18}O + 10$), which indicates evaporation processes, the samples would be along slope of 4 to 5 instead of 8, along a flow line (Schot & Van der Waal, 1992; Gat, 1996; Clark & Aravena, 2005). Isotopic compositions are expressed in ratios (R) of rare to abundant species. For example, for the stable isotopes of the element carbon this ratio is defined as the following:

$$^{13}R\ [CO_2] = [^{13}CO_2]/\ [^{12}CO_2]$$

Changes in isotopic ratios are denoted in δ-values, which represent deviation from a reference material:

$$\delta = ((R_{measured} - R_{reference})/\ R_{reference}) - 1$$

The δ-values are expressed in permil (‰). The reference materials used here are the Vienna convention standards: Pee Dee Belemnite (V-PDB) for the ^{13}C ratio, and the Standard Mean Ocean Water (V-SMOW) for the ^{2}H and ^{18}O ratios (Clark & Aravena, 2005; Mook, 2006). The isotope ratios ($\delta^{2}H$ and $\delta^{18}O$), from the first campaign, were measured by isotope ratio mass spectrometry (IRMS) at the Centre for Water Resources Research at the University of KwaZulu-Natal. Samples from the second campaign were analysed by IRMS at the Environmental Isotope Laboratory at

the iThemba LABS in South Africa.

Radiocarbon dating of water

Water samples for carbon isotope analysis were collected from 14 locations (Figure 3a). The samples were analysed at Centre for Isotope Research (CIO) at the University of Groningen in the Netherlands. The dissolved inorganic carbon (DIC) was captured via the samples' CO_2 gas and pressed into graphite. After this, activity of the graphite sheets was counted using the accelerator mass spectrometer (AMS) facility. The results were given in percent modern carbon (pMC) relative to a reference material, with the present defined as year 1950: $^{14}C_{sample} = (^{14}C_{measured} / {}^{14}C_{reference})$ pMC (Mook, 2006). Hence, a sample from a water flow that had infiltrated around 1950 would have ^{14}C =100 pMC, while an earlier infiltrating sample would be less than 100 pMC. The $\delta^{13}C$ content of the samples was measured using IRMS and was reported as permil (‰). The $\delta^{13}C$ are used to exclude the ^{14}C values affected by chemical processes (Han *et al*., 2012). The samples with $\delta^{13}C$ values outside the range from -11 to -14 ‰ could be affected by geochemical processes masking the ^{14}C values. For instance, the samples with $\delta^{13}C$ values that are more depleted, close to -25 ‰, could have diluted ^{14}C values, due to release of dead organic material (Mook, 2006; Han *et al*., 2012).

Stratigraphy and ^{14}C dating

Stratigraphy description

To investigate the stratigraphy of the Vasi-North substrates (at Core VN, See Figure 3b), a series of soil profile cores were taken using a Russian peat corer with a chamber length of 50 cm, with continuous cores in one hole, up to a total depth of about 8 m. The vertical extent of each horizon identified between the upper peat layer and the basal mineral layer was recorded. The substrates from each section were described for colour, type of peat and decomposition degree (Von Post Scale: H1-H10; Von Post, 1922) and macro-fossils following the reference scheme for South African peatland substrates proposed by Gabriel *et al.,* (2017b). In this way, we described soil profiles along a transect (VNA1 to VNA4), extracting peat material about every 20 cm.

Radiocarbon dating: Chronology and accumulation rates

For ^{14}C dating of the organic matter, soil samples were collected from two locations, Vasi-North (Core VN) and Vasi Pan (Core VP) (Figure 2b). The samples were taken from the cores at 1-cm sections directly above stratigraphic boundaries. The first core (VN) consisted of seven samples, while core VP consisted of four samples. All the samples were described in the field. The samples were then sealed in plastic bags and sent to the CIO, University of Groningen. They were treated using alkali-acid-alkali (AAA) to remove the contaminants that might affect sample age and to isolate the organic datable fraction. This fraction was combusted to CO_2, which in turn was reduced to graphite (Aerts *et al.,* 2001). In the graphite, the $^{14}C/^{12}C$ ratio was measured by AMS (van der Plicht *et al.,* 2000). The radiocarbon dates were calculated according to the

convention, i.e. using the oxalic acid reference, correction for isotopic fractionation using the $\delta^{13}C$ value of the sample and using the conventional half-life (Mook & van der Plicht, 1999).

In general, conventional ^{14}C age is reported in Before Present (BP). However, radiocarbon dates reported in BP, need to be calibrated to historical (calendar) ages (cal BP). In this case, we used SHCal13, which is the most recent curve recommended for the calibration of southern hemisphere samples (Reimer *et al.,* 2013). However, for modern samples influenced by the bomb peak (nuclear tests around 1950), other curves were constructed using the calibration for regional zones 1–2 valid for the southern hemisphere (Hua *et al*., 2013). For calculating calibrations, we used OxCal software (Bronk Ramsey, 2009). This program yields calibrated age ranges that are not symmetric or Gaussian, because of fluctuations in the calibration curve. The 1σ (68.2% probability) intervals were applied. Furthermore, to estimate the accumulation rates of each layer, we divided each layer's thickness by the difference in median calibrated ^{14}C age between the bottom and top boundaries.

RESULTS

Origin of groundwater flow

Water table depth and hydraulic head

The measured surface elevations and water table depths along the main transect across Vasi Pan and Vasi-North are shown in Figure 3. The average elevations of these basin surfaces decreased from around 56 m a.m.s.l. at Vasi Pan to 54 m at Vasi-North. The bordering sand ridges ranged in width from 150 m to 300 m and reach a height of about 3–5 m above the surface of the basins (58 to 60 m a.m.s.l.), with the widest ridge separating Vasi Pan from Vasi-North. The water table depth also decreased along the transect from Vasi Pan to Vasi-North, following the elevation gradient of the basin surfaces.

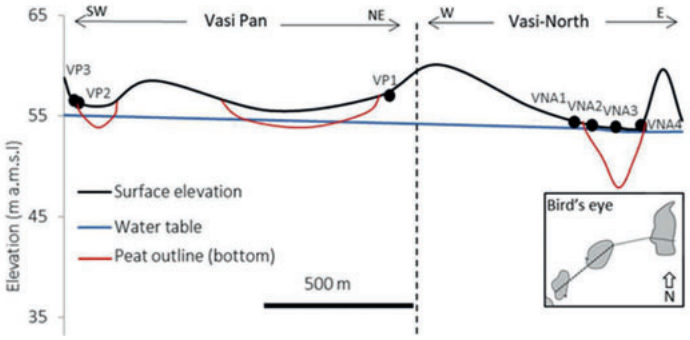

Figure 3. Topographic relief (black line) and water table depth (blue line) along a transect extending through Vasi Pan (0–1200 m, SW to NE direction) and Vasi-North (1200–2000 m, W-E direction); water table depth was measured on 24-03-2015.

At Vasi-North, the hydraulic head of the water table in the mineral soil in the western side was higher than the one in the peat layer by 0.05 m. However, in the eastern side the hydraulic head of the water table in mineral layer was lower than that of the peat layer by about 0.21 m. This indicates that there is an upward flow of groundwater at the western side of the pan and a downward flow at the eastern side (Figure 4).

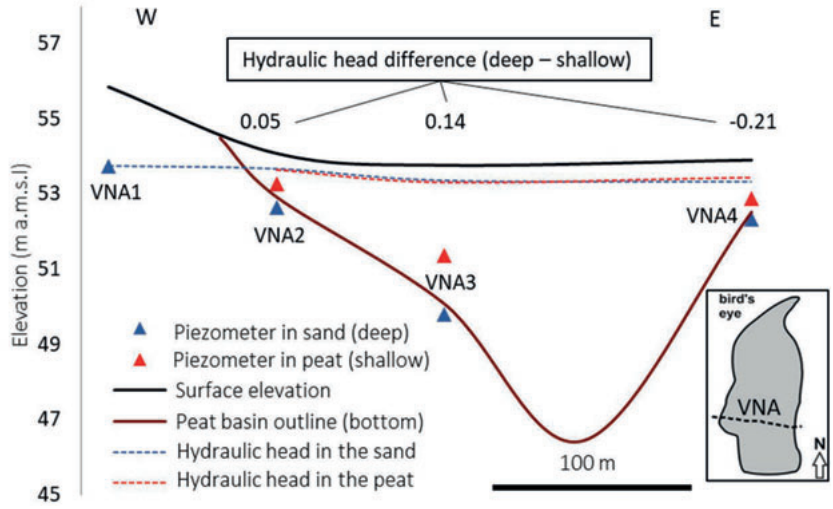

Figure 4. Hydraulic heads of the water table in the organic layer (blue dashed line) and the mineral layer (red dashed line) along transect A, west to east direction, in Vasi-North.

Ion compositions and tracers

PCA results of the water's ion composition are shown in Figure 5. These results are expressed in a plot of the first two principal components (PC1 and PC2). PC1 explained 40.5% of the variation, while PC2 explained 22.2% (Figure 5a). The PCA results were divided into two figures to ease interpretation: (a) the ion variables and their contribution to PC1 and PC2, and (b) the correlations of samples to PC1 and PC2. The contribution of ion concentration to the principal components are expressed in both arrow length and colour. The direction of the arrows indicates the qualitative relationship between ion content and the principal components. For example, SO_4 and Fe ions are directly proportional to PC1 and inversely proportional to PC2, which means samples with higher SO_4 and Fe ions content are likely to be found in the quadrant with positive values for PC1 and negative ones for PC2.

The PCA indicated four groups with respect to ion composition. Group A, located in the negative quadrant of Figure 5b, has the most samples. Characterised by generally low ion content, group A contains the rainwater sample taken in 2017, along with all the samples from the community wells except for CW1 and CW2, the Siyadla river samples, some of the Vasi Pan samples, and samples from the southwestern parts of Vasi-North (samples 5 and 7). Group B contains samples directly proportional

to PC1, with higher SO_4, NH_4, Mg, Na and Cl content. Most of the samples in group B originate from the middle and eastern parts of Vasi-North. They showed especially high SO_4 content (except for 8, 10 and 26), with the highest values in sample 16 from VNB3 (west of Vasi-North). Group C, with higher HCO_3, SiO_2 and PO_4, contains samples 27 and 37, which are from two peatlands in the northern part of MCP (the spring in Manguzi forest and KwaMazambane).

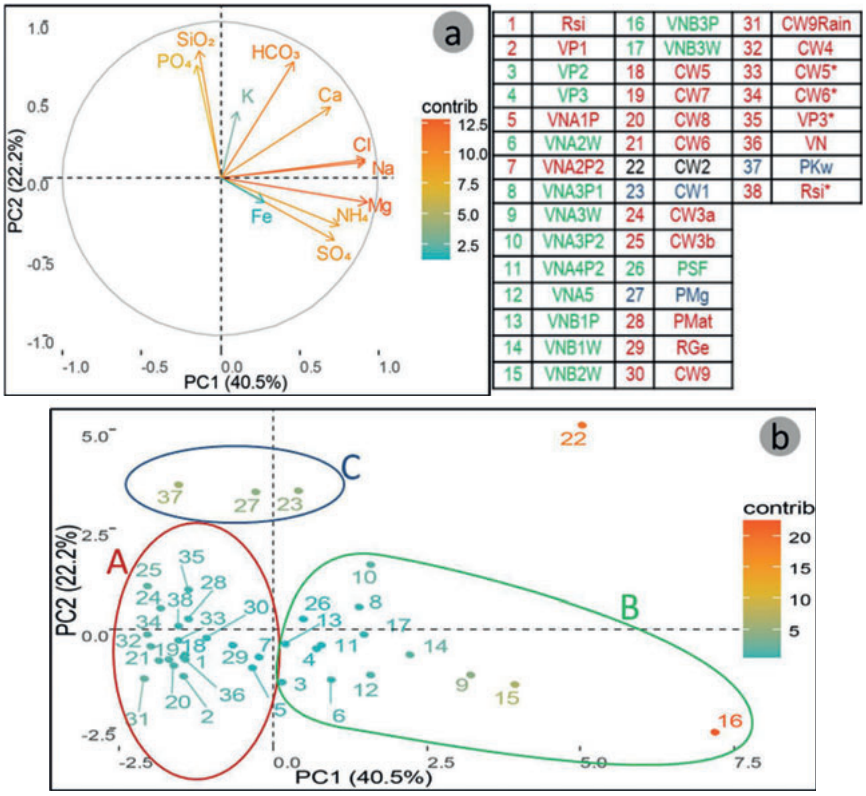

Figure 5. PCA of water ion composition based on the first two principal components (PC1 and PC2): (a) The contribution of variables (ions) to the first two PCs, where the arrow length indicates the magnitude and arrow direction indicates which PC axis received the greatest contribution. (b) The distribution of the samples along PC1 and PC2, where the axis units express the magnitude of variation along the principal component.

For a closer look at the spatial distribution of ion composition in the groundwater, Figures 6a and b show the W–E spanning transect A in Vasi-North, with profiles of chloride and sulphates concentrations in the groundwater. These ion gradients show a trend of increasing towards the east, but the highest concentrations were found in the central part of the basin. The sulphate ion gradient shows a possible anoxic pocket at VNA3 at 4-m depth.

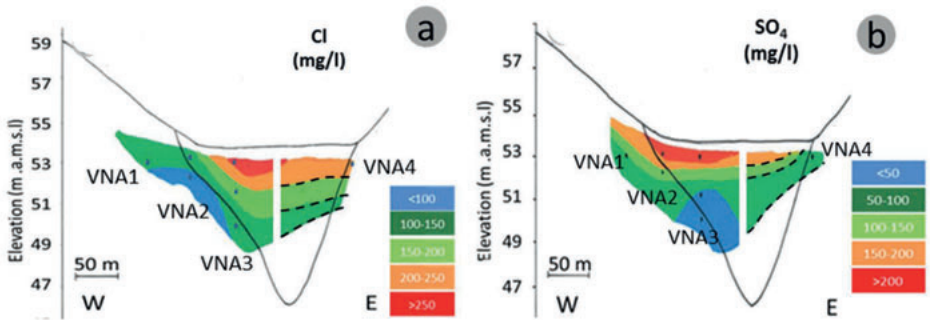

Figure 6. Distribution of the groundwater solute tracers along transect A in Vasi-North: (a) chloride and (b) sulphate. The data to the right from the white bar are interpolated lines stretching the data in the western side to the single point at VNA4.

$\delta^{18}O$ and $\delta^{2}H$ stable isotopes

The stable isotopes results were generated by plotting the samples with the global meteoric water line (GMWL): (i) the larger-scale second field campaign with the samples covering MCP (Figure 7); and (ii) the first field campaign, in the Vasi area, which included two rounds of sampling: before and after a 5-mm rainfall event (Figure 8a and b, respectively). Figure 7 shows that most samples from the regional groundwater (community wells and river water) and the rainwater from October 2017 had isotopic values with $\delta^{18}O$ values > -2 ‰. Muzi system and the community wells nearby it in Tembe Elephant Park are the only one with isotopic content that shifts below the GMWL. Figure 8a shows that most of the water samples have different isotopic values in the second sampling round, except for the samples from community well, with $\delta^{18}O$ values < -2 ‰ (CW6, 7 and 8).

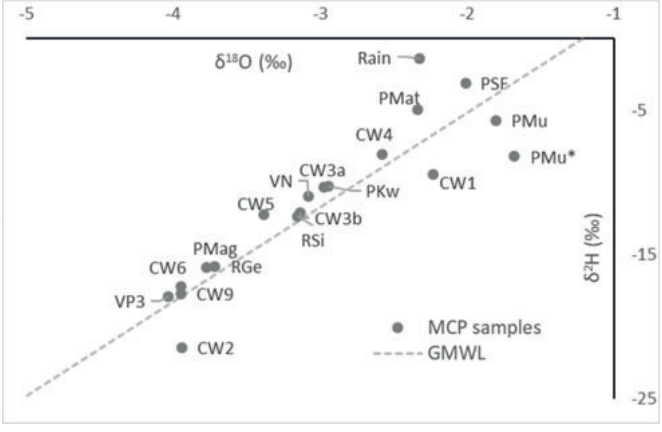

Figure 8. Stable isotopes content in water samples from the second campaign covering the northern part of the Maputaland Coastal Plain.

The samples from the sand layer in the western parts of Vasi-North (A1P, A2P2 and B1P) were also shown to have isotopic content similar to the community wells. Sample A5, which was taken from the basin east from Vasi-North, also had similar values close to these points. Most of the peat water samples had $\delta^{18}O$ values > -2 ‰ (e.g. A2W, A3W, A3P1, B1W and B3W). Some samples (e.g. B3P, B1W, CW5) had values indicating evaporation processes, i.e. below GMWL.

After the rainfall event (Figure 8b), all of the samples had isotopic values that shifted above the GMWL, except for sample A4P2 (west of Vasi-North). Despite this, the samples with $\delta^{18}O$ values > -2 ‰ remained more or less the same. It appears the local meteoric water line (LMWL) would plot well above the GMWL with a deuterium excess of close to -15 ‰.

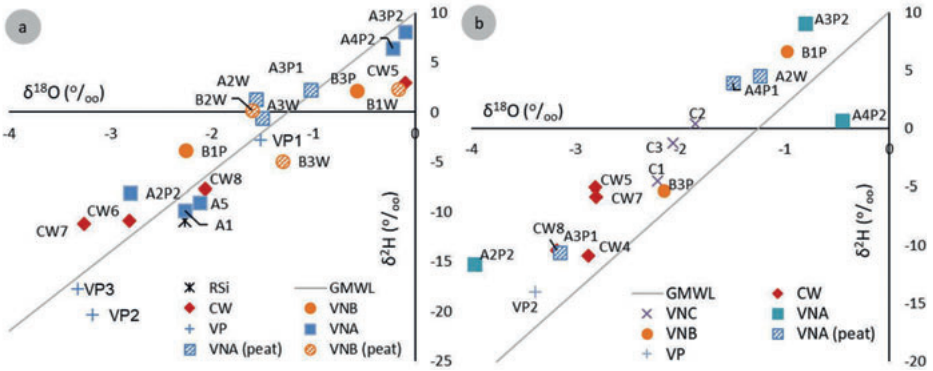

Figure 9. (a) Isotopic compositions of the water samples from the Vasi Peatland Complex in March 2015. (b) Isotopic compositions of the water samples taken in April 2015 after a 5mm rain event. VNC transect was measured only in April.

Groundwater ^{14}C dating

Table 1 lists the results of the carbon isotope analysis. Most of the samples appeared to be within the range of current infiltration or infiltration during the past 60 years (post 1950, higher or close to 100 pMC). The lowest ^{14}C results were observed near the Muzi system (PMu, CW1 and CW2). Some samples from the peatlands indicated a shift to enrichment of dead organic matter, which is indicated by lower $\delta^{13}C$ values (e.g. VN, VP3, PMat, RGe). This was also the case in the community wells near the Vasi peatland complex (e.g. CW4, CW6).

Chronological development

Stratigraphy

Figure 9 shows Vasi-North's stratigraphic profile, with the lowest 5-6 meters filled with organic gyttja. On the eastern side of the transect, a gradual change from organic gyttja to peat-gyttja and sedge peat was found. Peat-gyttja, which is a mix of sedge peat and gyttja, is very prominent in South African inter-dune depression peatlands

(Gabriel *et al*., 2017b). In the western part, however, a peat-gyttja horizon occurred in the sedge peat. Furthermore, the first 5-6 m from the bottom in the west part consisted of gyttja, in which only a few vegetative residues of plants were found; amongst them were stem bases of *Cladium mariscus* subsp. *jamaicense,* which grows in shallow water. Above the gyttja layer, from 182-128 cm, well-preserved radicell peat (H4-H6) was found containing remnants of rhizomes of *Cladium mariscus* subsp. *jamaicense* and seeds of *Eleocharis dulcis*. The substrate from 128-94 cm was found to be composed of peat-gyttja. At 94 cm, there was again a shift to radicell peat and a decline of gyttja. The topsoil of the whole peatland consisted of amorphous peat, with soil aggregates and cracks mostly found in the first 10-20 cm.

Table 1. ^{14}C dating of 14 groundwater samples in the northern part of the Maputaland Coastal Plain.

No	Code	Lab No (GrM)	^{14}C uncorrected (pMC)	±	δ^{13}C (‰; IRMS)	±
1	Pmu	11527	75.71	0.15	-12.71	0.15
2	CW2	11528	71.71	0.15	-12.63	0.15
3	CW1	11529	51.2	0.12	-9.51	0.15
4	CW3a	11530	102.48	0.31	-13.26	0.15
5	CW3b	11532	98.12	0.18	-8.49	0.15
6	PSF	11534	107.3	0.19	-12.45	0.15
7	PMag	11535	98.06	0.18	-11.20	0.15
8	PMat	11537	97.89	0.18	-16.30	0.15
9	RGe	11538	100.57	0.19	-19.35	0.15
10	CW9	11539	108.36	0.19	-19.73	0.15
11	CW6	11540	108.75	0.19	-17.13	0.15
12	CW4	11542	115.91	0.20	-17.84	0.15
13	VA3	11544	87.52	0.17	-19.53	0.15
14	VN	11545	99.56	0.18	-20.09	0.15

^{14}C dating, accumulation rates and ^{13}C shifts

Table 2 lists the results of the stratigraphic layers ^{14}C dating and calculations for accumulation rate. The start of organic accumulation in the Vasi peatland complex was dated to 8490 cal BP, starting with the gyttja layer in the Vasi-North basin. In Vasi Pan, gyttja accumulation started around 3660 cal BP. The periods of gyttja accumulation were characterised by relatively low accumulation rates (0.4-0.6 mm/year). In contrast, fibrous sedge peat started to accumulate in Vasi Pan by 2885 cal BP, when lower lying Vasi-North was still accumulating peat-gyttja. The average accumulation rate for the peat was around 1.5 mm/yr with a maximum of 4 mm/yr observed during the period from 2900 to 2700 cal BP in Vasi Pan. The δ^{13}C values indicate that most of these peat samples consisted of C3 plants, which have average values of -24‰ (O'Leary 1981). Only a few had the signatures of C4 or mixed C3/C4 plant types, with values between -10 and -20‰.

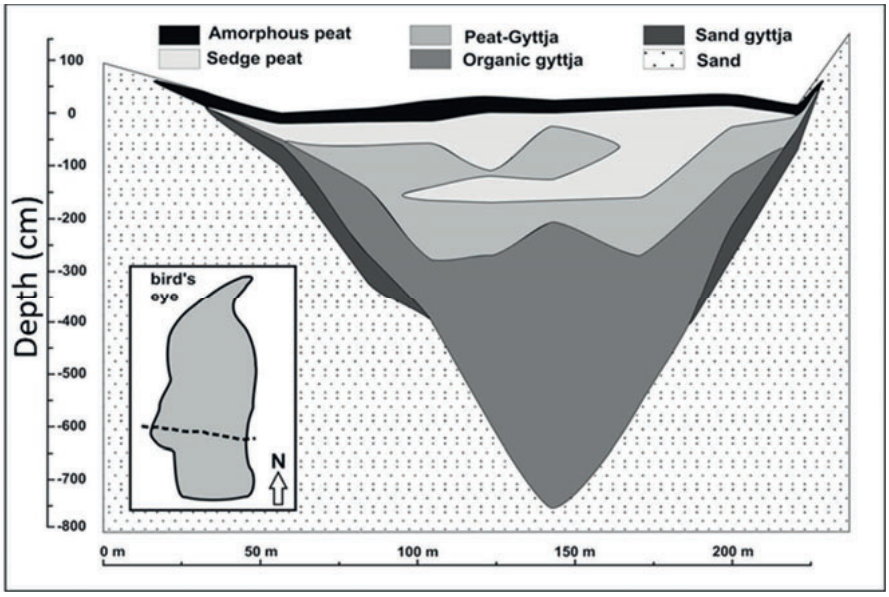

Figure 10. Detailed stratigraphy of the substrates in Vasi-North. The small inset (left) shows the transect position in the peatland.

Table 2. List of the measured radiocarbon dates in BP for the peat samples, the $\delta^{13}C$ values, and the calibrated date range (in cal BP, calendar years relative to 1950 AD). The ^{14}C values were rounded to the nearest value of 0 or 5 cal BP. Accumulation rates were calculated using the difference in age per difference in depth.

Site	Depth (m)	Depth (m - a.m.s.l.)	Lab nr. (GrA)	Sample description (degree of decomposition; Von Post scale)	^{14}C (BP)	Calibrated age range (calBP,1σ)	$\delta^{13}C$ (‰)	Accumulation Rate (mm yr^{-1})
Vasi-North	0.47	53.32	63234	Amorphous peat (H10)	2045 ±30	1930-2000	-16.65	1.15
	0.94	52.85	63236	Radicell peat (<H5)	2385 ±30	2325-2425	-20.72	0.63
	1.28	52.51	63237	Peat-gyttja	2890 ±35	2880-3005	-24.14	1.75
	1.82	51.97	63238	Radicell peat	3050 ±35	3080-3325	-26.17	1.51
	2.14	51.65	63239	Gyttja	3230 ±35	3375-3450	-23.57	1.25
	5.16	48.63	63240	Gyttja with high water content	5105 ±40	5750-5890	-19.83	1.09
	8.05	45.74	63241	Gyttja bottom (underlain by sand)	7760 ±45	8435-8545	-17.76	--
Vasi Pan	0.4	56.68	63242	Amorphous peat (H10)	2420 ±30	2345-2455	-19.77	0.48
	0.65	56.43	63243	fibrous peat (H3)	2745 ±30	2765-2845	-20.27	4.39
	1.01	56.07	63264	gyttja	2820 ±35	2795-2930	-25.11	0.39
	1.42	55.66	63247	Gyttja bottom (underlain by sand)	3660 ±35	3870-3980	-22.32	--

DISCUSSION

Groundwater flow systems

Radiocarbon dating indicates that the groundwater flows in Vasi peatland complex and its surrounding dunes are recent. It is also the case for most of the groundwater flows discharging to the other wetlands in northern Maputaland coastal plain. Most of the radiocarbon data has values near 100 pMC, which is due to the bomb peak in 1950 (Mook, 2006). The source of these flows is likely to be either from the KwaMbonambi Formation or the Kosi Bay Formation and also likely to be limited to localized catchments (Weitz & Demlie, 2014; Kelbe *et al.,* 2016). Only groundwater in the Muzi system is relatively old (up to a few hundred years old). Whereas this system seems to be under the influence of groundwater discharging from the Uloa Formation (Weitz & Demlie, 2014), which was also evident in the water's ion composition (>1000 mg/l). The ion composition of the groundwater discharging at Vasi peatland complex indicates consistent similarity with groundwater feeding other peatlands in the north-eastern part of the Maputaland coastal plain (Bate *et al.,* 2016). Similarly, the groundwater stable isotopes content at the western sides of the basin to the ones observed on the regional scale of the Maputaland Coastal Plain, except for the groundwater in the Muzi system.

The difference in the groundwater source in the upstream area, i.e. Muzi system, from the ones in the middle, i.e. Vasi Peatland Complex and the downstream, i.e. Matitimani and KwaMbazambane peatlands, could be due to formation of nested local to intermediate groundwater systems in the Kosi Bay and KwaMbonambi Formations on top of the regional system in the Uloa Formation. Some of these local systems could be perched local systems due to the existence of the iron-rich sand deposits at lower depths (Botha & Porat, 2007; Kelbe *et al*., 2016). Toth (1963) has shown that such local systems could also be nested within a gently sloping regional aquifer, which is the case in the Maputaland Coastal Plain. Kelbe *et al*. (2016) has indicated that such layering of groundwater systems could be existing, but it was one of the limitations within their constructed groundwater model, and would require more information.

An important finding is that the initiation of gyttja accumulation in Vasi Peatland Complex, ca 9000 calBP, is earlier than the peak in peat initiation in the other peatlands in Maputaland. For instance, Grundling (2004), has indicated that the peatland initiation peak in the Maputaland Coastal Plain coincides with the sea level rise peak ca. 4000 years ago. Also, the peat initiation in Matitimani is quite younger (ca. 6000 calBP; see Gabriel *et al.,* 2017a) than that of the Vasi Peatland Complex. This is an indication that the Vasi Peatland Complex is independent from the groundwater systems supplying the other peatlands in the lower areas in Maputaland Coastal Plain. It indicates the more likely hypothesis taking place is the one that the Vasi Peatland Complex is supplied by a perched aquifer within the KwaMbonambi Formation. It would also mean that we can separate the local to intermediate system of Kosi Bay and KwaMbonambi Formations into intermediate and local ones, respectively.

Vasi Peatland Complex

Notably within the Vasi Peatland Complex, the water table depth showed a gradient that was independent of the topographic heights (dune ridges). However, it followed the height gradient of the surface of the peat basins, the water table depth gradient increased from Vasi Pan to Vasi-North. This is an indication of a possible cascading system where the groundwater flows from one basin to the next in the elevation gradient. Such systems were also observed in other peatland systems, e.g. Mfabeni mire (Grundling, 2014b), and a small mire near the High Tatra Mountains in Slovakia (Grootjans *et al.,* 2006). The concept was introduced by Stuyfzand (1993), whose conceptual model suggested a discharge of groundwater (inflow) on one side of the slack and recharge (outflow) of the water on the other side of the slack (Stuyfzand, 1993). Furthermore, the hydraulic head data in Vasi-North indicate the groundwater discharge to the southwestern edges of the basin at VNA2 and VNA3.

It is noted that under the long dry conditions, the change in the chemical composition of the discharging groundwater is possibly related to the processes occurring in the upper/surface peat basins itself, e.g. oxidation and evaporation (Naucke *et al*., 1993), which then cascades from one basin to the next. By synthesizing the data from the water table depths and tracer data, it seems that the Vasi peatland complex functions as an inter-dune cascading system, with through-flow systems within the basins. Figure 10 shows a conceptual model of the groundwater discharge zones in Vasi-North, the through-flow directions and the hypothetical connection to the Vasi Pan basins.

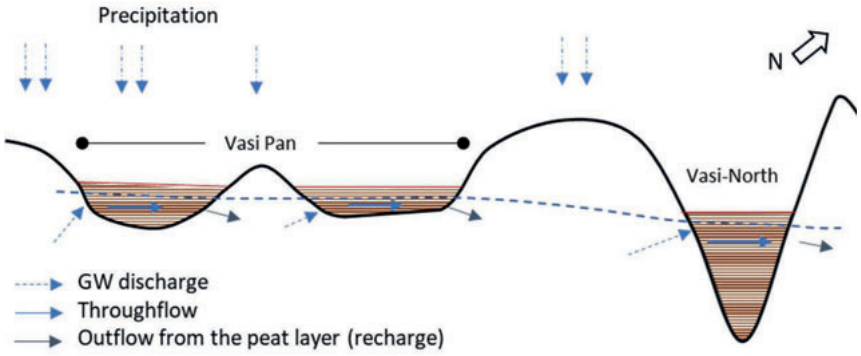

Figure 10. Conceptual model of the hydrological system of Vasi Peatland Complex. Dashed blue lines (a) represent discharge of groundwater (inflow), light blue lines (b) indicate a hypothetical through-flow within the peatland, and dark blue lines (c) represent recharge from the peat (outflow) into the adjacent dune at the opposite side of the wetland.

Past hydrological conditions

The peatlands in the Vasi peatland complex are a typical example of terrestrialising peatlands (Heathwaite *et al*., 1993). Vasi-North, the lowest lying basin in the complex, developed as an open-lake system accumulating gyttja during the Early-Holocene, around 8850 cal BP. The persistent, millennia-long, accumulation of organic matter

seems to have dominated most of Vasi-North's developmental pathway. The timeline of gyttja layer initiation in the basins of the complex indicate that Vasi-North's infilling might have provided a positive feedback mechanism initiating peat accumulation in the Vasi Pan basins. The lower permeability of gyttja and peat layers acted as obstructions, raising the water table in the higher parts of the complex, i.e. Vasi Pan. Similar observations have been made for the nearby Mfabeni peatland by Grundling *et al.* (2013b), and Matitimani (Gabriel *et al*., 2017a). In turn, this also explains why the Vasi-North basin became degraded last in the sequence, after those in Vasi Pan, indicating that degradation spread from one basin to the other in an inverse timeline to that of initiation consistent with the lower altitude of the basins.

While the Vasi peatland complex might be in a separate watershed from other peatlands in the Maputaland coastal plain, the climatic conditions over the last millennia seem to be similar or at least with no large variations. The average accumulation rate for the peat (mean around 1.5 mm/yr with a maximum of 4 mm/yr for the period from 2900 to 2700 cal BP) is consistent with estimations by older studies on peat dating in Maputaland with values no higher than 2.5 mm (Thamm *et al*., 1996; Page *et al.,* 2004; Baker *et al*. 2014).

Synthesis and reflection on degradation cause

Despite the existing groundwater discharge to Vasi-North during the wet season, the water table has been dropping steadily during the study period from January 2014 up to the end of the wet season in April 2015. Specifically, the groundwater table dropped to more than 50 cm below the surface on the eastern side of Vasi-North. Most of the wells (<1 m deep) within the peat layer were dry by April 2015. Meanwhile, the water table depth at Vasi Pan dropped to more than 1.5 m below the surface of the peat layer (at VP2), while VP1 was dry.

Furthermore, the top layers in the Vasi peatland complex are highly degraded (See table 2). The radiocarbon ages of the bottom of the amorphous peat layers at Vasi Pan and Vasi-North were about 2390 and 1965 cal BP respectively, indicating that most of the accumulations younger than ca 2000 years has disappeared due to peat oxidation, burning and wind erosion. Moreover, the macro-fossil analysis of the two peat profiles indicated the impact of wet and dry periods (Gabriel *et al.*, 2017a). For instances, indications of the occurrence of dry conditions causing natural fire incidents were also found in some nearby peatlands, represented by microcharcoal fossils (Gabriel *et al.,* 2017). However, the degradation profile did not indicate the occurrence of long persisting dry periods leading to high degradation levels in the lower layers such as observed for the top one. Also, no evidence was also found for loss of peat in the past by intensive fires and considerable discontinuations in peat ages from the initiation time at 8850 until the most recent date at 1950 cal BP. Lastly, the order in which the degradation, i.e. the higher Vasi Pan degrading first followed by Vasi-North, is taking place is indicating the gradual, yet persistent groundwater table lowering.

Hence, the persistent lowering of the groundwater table does not seem to have been a natural characteristic of the Vasi peatland complex under past hydrological conditions. It could be similar to the situation in the Mbazwana catchment, south of

the Vasi peatland complex, where simulations of the water table draw appeared to be affected more by evapotranspiration of plantations and woodlots rather than natural grasslands (See Bate *et al.,* 2016). Also, Grundling & Blackmore (1998), reported on the quick recovery of the water table in 1998 after the plantations were cleared away from inside the Vasi-North basin. Therefore, we could confirm that effect of the plantations on the drawdown in the groundwater table is more likely to be the dominant driver than natural climate cycles.

CONCLUSIONS

The inclusion of the natural isotopes has provided an opportunity to classify the groundwater systems supplying the peatlands both in Vasi Peatland Complex and the other areas in Maputaland. However, the focus of this study was Vasi Peatland Complex, it is noted that the radiocarbon dating of groundwater has given the opportunity to differentiate between local and regional groundwater systems. This was one of the limitations of the hydrological modelling of the groundwater table depth, which can be overcome using such an approach.

The development of the Vasi peatland complex might have been driven by feedback mechanisms consisting of the following: (i) a rise in a perched water table in the KwaMbonambi Formation that allowed for (ii) accumulation of organic matter which led (see also below) to (iii) a higher water table in the neighbouring basins and (iv) creating a cascading system. Also, while the Vasi peatland complex is a separate hydrological entity, its basins cannot be considered as separate hydrological entities. The basins of the Vasi peatland complex, therefore, appear to be hydrologically connected.

The extreme degradation of the Vasi peatlands and the persistent lowering of the water table. These cannot be looked upon as a system dependent on isolated internal hydrological conditions, but rather as a reflection of wider issues in external landscape management. This leads to possible losses of ecosystem services provided by the Vasi peatland complex, e.g. CO_2 sequestration. The vulnerability of Vasi-North can also negatively affect the local economic and subsistence activities on the longer term (e.g. grazing, gardening). Following the suggestions that Grundling & Blackmore (1998) expressed almost 20 years ago, we also emphasize the need for a proper water management plan that regulates and restricts further continuation of present forestry practises, since continuation of these practises will only lead to a further drop in water tables in the peatlands, exposing them again to peat fires.

It is also clear that the groundwater flows are likely to be intercepted by the plantations, which was proven in other study areas south of the Vasi peatland complex, has resulted in a drawdown in the water table. Therefore, the Vasi peatland complex basins are receiving less ground water flow and are consequently desiccating to the point where extensive peat fires occur. Restoration efforts should therefore not only be restricted to dealing with desiccated peat, ash layers and salt encrusted surface layers as well as revegetation. The catchments of these peatlands need to be managed and in particular the removal of plantations from recharge zones and

adjacent to peatlands where groundwater flows are intercepted by tree roots. Furthermore, the impact of in- situ peatland cultivation should be mitigated by controlling draining, thereby minimising desiccation and establishment of alternative crops suitable to grow outside peatlands.

FURTHER RESEARCH

The possible drawdown cone resulting from the plantation area needs to be quantified in order to plan a rationalised buffer zone that protects the peatland groundwater supply. Also, the response of peatlands to withdrawal of plantation areas and recovery of the water table should be investigated. Furthermore, the best options in restoring severely desiccated, burned and unvegetated peatlands with salt-encrusted surface layers should be studied in more detail.

ACKNOWLEDGEMENT

We would like to acknowledge the Water Research Commission of South Africa for the partial funding of this study (WRC Report No. 2346/1/17). We thank the foundation Ecological Restoration Advice (ERA), The Netherlands, for their help in funding the project. We also thank the Isibusiso Esihle Science Discovery Centre, Nqobile Zungu, Nhlanhla Masinga and Camelia Toader for their assistance with the field visits and campaigns. Further, we thank Esther Chang for the language revisions.

APPENDIX

Appendix 1. Overview of the observation tubes, their types, diameters, and depths and the sediment medium.

No.	Campaign	Code	Depth (m)	Sediment type	Type
1	2015	S	0	--	River water
2	2015	VP 1	2.9	Sand	Piezometer
3	2015	VP 2	2.1	Sand	Piezometer
4	2015	VP 3	3.9	Sand	Piezometer
5	2015	VNB 1p	1.3	Sand	Piezometer
6	2015	VNB1w	0.8	Peat	Well
7	2015	VNB 2w	0.95	Peat	Well
8	2015	VNB3p	2.2	Sand	Piezometer
9	2015	VNB3w	1	Peat	Well
10	2015/2017	CW5	--	--	Manzengwenya Plantations well
11	2015	CW7	--	--	Community well
12	2015	CW8	--	--	Community well
13	2015/2017	CW6	--	--	Community well
14	2015	VNA1	2.1	Sand	Piezometer
15	2015	VNA 2w	0.8	Peat	Well
16	2015	VNA 2p	1.5	Sand	Piezometer
17	2015	VNA 3p1	2.4	Peat	Piezometer
18	2015	VNA 3w	1.25	Peat	Well
19	2015	VNA 3p2	4	Sand	Piezometer
20	2015	VNA 4P2	1.6	Sand	Piezometer
21	2015	VNA4P1	1.12	Peat	Piezometer
22	2015	VNA 5	1.5	Sand	Piezometer
23	2015	VNC 1	1.9	Sand	Piezometer
24	2015	VNC 2	1.6	Sand	Piezometer
25	2015	VNC 3	1.65	Sand	Piezometer
26	2017	Pmu	1.8	Sand	Piezometer
27	2017	CW2	>10	Sand	Community well
28	2017	CW1	>10	Sand	Community well
29	2017	CW3a	0.2	Sand	Community well
30	2017	CW3b	>10	Sand	Community well
31	2017	PSF	0.2	Sand	Piezometer
32	2017	PMg	1.5	Sand	Piezometer
33	2017	Pmat	1.5	Sand	Piezometer
34	2017	RGe	0	--	River water
35	2017	CW9	46	Sand	Community well
36	2017	Rain	Rain	--	Rain gauge
37	2017	CW4	>10	Sand	Community well
38	2017	VN	3.5	Sand	Well
39	2017	PKw	1	Sand	Well

Appendix 2. Ion composition analyses of the water samples from the Vasi peatland complex in 2015. All the macro ions are reported in mg/l.

No.	Code	pH	NO_3	Cl	SO_4	PO_4	HCO_3	Na	K	Ca	Mg	Fe	NH_4	SiO_2	TDS
1	S	6.39	0	67	2	0.00	43	32	3	9	7	0.74	0.05	10	162
2	VP1	5.8	0.14	19	15	0.02	47	9	5	9	4	7.44	2.31	2	109
3	VP2	4.01	1.31	33	171	0.00	5	33	3	33	9	11.40	6.07	13	289
4	VP3	4.98	1.99	137	151	0.00	12	88	10	39	15	0.47	0.93	11	455
5	VNB1P	5.84	1.29	84	120	1.34	65	64	4	27	20	1.65	0.12	5	386
6	VNB1W	5.95	0.38	194	209	0.05	56	130	22	26	33	1.37	1.90	3	670
7	VNB2W	5.41	3.81	321	190	0.47	54	185	5	22	37	1.00	26.57	3	819
8	VNB3P	5.15	0.87	354	407	0.00	43	225	4	37	62	3.51	44.53	4	1134
9	VNB3W	5.71	0	201	5	0.00	127	82	4	30	14	3.17	27.09	14	464
10	CW51	6.56	0.27	125	10	0.00	52	63	5	18	9	0.00	0.09	9	282
11	CW6	4.81	1.87	48	10	0.43	7	22	2	6	4	0.04	0.03	10	101
12	CW7	4.71	2.02	51	5	0.00	37	20	2	8	7	0.00	0.03	6	132
13	CW8	5.31	2.17	63	5	0.41	11	27	2	7	5	0.00	0.04	9	122
14	VNA1	5.6	0.32	113	34	0.06	26	49	5	16	14	4.53	3.14	7	257
15	VNA2W	5.7	1.09	140	136	0.00	40	96	6	21	19	7.78	1.57	3	458
16	VNA2P	5.94	0.18	50	89	0.00	71	31	5	30	15	3.02	1.45	6	291
17	VNA3P1	5.94	1.15	184	1	0.00	163	89	6	34	15	8.49	15.74	21	494
18	VNA3W	5.53	2.48	297	149	0.00	71	177	4	22	34	2.78	15.08	4	757
19	VNA3P2	6.2	0.66	126	1	0.00	245	55	6	58	10	14.17	18.18	33	501
20	VNA4P2	5.73	1.22	197	41	0.00	55	102	5	16	11	1.66	18.18	19	429
21	VNA5	5.54	1.26	180	143	0.00	43	109	5	26	18	3.11	15.28	7	525

Appendix 3. Ion composition analyses of the water samples from the Maputaland coastal plain in October 2017. All the macro ions are reported in mg/l.

No	Code	pH	Cl	NH_4	SO_4	PO_4	HCO_3	Ca	Mg	Na	K	Br	Fe	SiO_2	TDS
1	Pmu	7.68	684	0.42	1826	18.01	655	260	131	725	54	3.37	0.53	51	4029
2	CW2	8.26	441	0.41	52	1.86	386	89	28	268	10	4.55	<0.01	45	1085
3	CW1	8.23	90	0.26	2	1.99	298	65	15	29	6	1.58	<0.01	35	359
4	CW3a	6.94	25	0.21	26	1.6	30	6	5	29	11	0.37	0.28	24	118
5	CW3b	7.2	35	0.25	0	1.22	41	4	5	27	3	0.61	<0.01	44	97
6	PSF	7.22	201	1.47	36	0.22	61	10	18	133	5	2.63	0.59	26	441
7	Pmag	7.58	123	0.04	8	4.24	123	17	13	72	53	0.58	0.03	19	353
8	Pmat	6.58	79	0.00	4	0.48	29	10	6	51	6	0.38	0.52	27	171
9	RGe	6.27	79	0.18	7	0.31	9	5	5	48	8	0.64	0.14	18	156
10	CW9	6.23	131	2.44	3	0.85	9	3	8	62	5	0.89	<0.01	18	228
11	Rain	6.92	12	0.89	4	0.09	20	7	2	9	1	0.42	<0.01	1	47
12	CW4	6.31	48	0.23	3	0.3	9	3	3	29	2	0.41	<0.01	20	92
13	CW5	5.21	97	0.20	7	0.62	5	4	7	43	2	0.41	<0.01	10	165
14	CW6	6.27	42	0.03	6	0.4	11	3	2	29	1	0.28	0.19	28	90
15	VP3	3.2	53	0.68	131	3.61	0	8	6	37	5	0.18	1.19	34	247
16	VN	7.01	26	0.06	48	0.16	34	7	10	29	3	0.19	<0.01	12	140
17	PKw	6.9	70	0.02	18	6.15	98	10	8	53	7	0.32	0.49	52	219
18	Rsi*	7.39	56	0.04	3	0.34	47	7	6	37	4	0.45	1.67	26	137

4

Anthropogenic disturbances of natural ecohydrological processes in the Matlabas mountain mire, South Africa*

Matlabas is a mountain mire in Marakele National Park, located within the headwaters of the Limpopo River in South Africa. This mire consists of a complex of valley-bottom seepage wetlands with small elevated peat domes. The occurrence of decaying peat domes and desiccated wetland areas with terrestrial vegetation has raised concerns. The aim of this study was to understand the mire features and water flows in order to identify the potential drivers causing wetland degradation. Wells and piezometers were installed to monitor the hydraulic head and collect water samples for analysis of ion composition, ^{18}O and ^{2}H stable isotope content, and $\delta^{13}C$ and ^{14}C isotope content for radiocarbon dating. Moreover, peat temperature profiles were measured and peat deposits were also dated using radiocarbon. Results indicate that the Matlabas mire developed in the lowest central-east side of the valley by paludification at the onset of the Holocene. During the Mid-Holocene, peat development was extended laterally due to autogenic and allogenic processes. Three types of water flows driving peat development were identified: sheet flow, phreatic groundwater flow and deep groundwater flow. The recent occurrence of decaying peat domes and desiccated wetland areas are possibly related to loss of sheet water and lateral phreatic flows that have resulted from interception of water by an access road and head-cut channels in the mire. Interventions should be undertaken to prevent further degradation of the mire.

* This chapter is submitted as: Bootsma, A., Elshehawi, S., Schot, P., Butler, M., Brown, L., Grundling, P.L., Grootjans, A. (in review) Anthropogenic disturbances of natural ecohydrological processes in the Matlabas mountain mire, South Africa.

INTRODUCTION

Peatlands play a crucial role as carbon sinks in the regulation of atmospheric CO_2 concentrations, which in turn influence climate (Clymo *et al.,* 1998) They also provide ecosystem services like water storage, nutrient cycling and high biodiversity (Joosten & Clarke, 2002). Over the past two centuries, the health of peatlands and their ecosystem functions have been affected by direct and indirect use of these systems, e.g. use of peat for fuel, agriculture and groundwater extraction for drinking water (Joosten & Clarke, 2002; Mitsch & Gosselink, 2000a). Hence, there is growing attention for the assessment, conservation and restoration of peatlands on a global scale (Bonn *et al.,* 2017). Mires are peatlands that are still actively accumulating peat, and this process is controlled by climate, hydrology and vegetation (Joosten & Clarke, 2002) While near-natural mires are still widespread in the northern hemisphere, such as in Canada, Russia, Siberia and Finland (Joosten *et al*., 2017), they are relatively scarce in the southern hemisphere (Joosten & Clarke, 2002). Nevertheless, the southern hemisphere's peatlands play an important role in the global carbon cycle (Yu *et al*., 2010).

Pristine peatlands are rare in South Africa (Grundling & Grobler, 2005). The best examples of pristine peatlands here are found along the eastern coast and in the central mountain areas. Two-thirds of South African peatlands occur along the north-eastern seaboard of the Indian Ocean, known as Maputaland, in KwaZulu-Natal Province (Grundling & Grobler, 2005). Maputaland contains both the largest peatland, the Mkuze peatland complex at 8,800 ha, and the oldest mire, Mfabeni at 48,000 years (Thamm et al., 1996; Meadows, 2001; Grundling *et al.,* 2013b; Baker *et al.,* 2014). The Matlabas mire, however, is situated in Marakele National Park in Limpopo Province, and is part of the Central Highlands Peatland Eco-Region (Grundling *et al.,* 2017). Matlabas is one of the largest and least impacted spring mires known to exist in South Africa. The mire falls within the reaches of the Limpopo River, which suffers events of severe drought (Trambauer *et al.,* 204). While the mire is largely in a good state, some signs of erosion were observed during a wetland inventory project undertaken in the park in 2008 (SANPARKS, 2008). These signs included head cuts and gully erosion. Previous land-use practices (cattle farming) and road construction, which took place in 1960s up to early 1980s may have affected the mire's natural processes (Van Staden, 2002). However, it is not known whether this erosion is increasing or what has caused it. These head cuts and gully erosion are expected to further increase peat drainage in the future, which could result in the loss of large sections of the mire. The present study aims to determine how the Matlabas peatland developed over time in relation to the principal water flows and recent changes in land use, as this knowledge would serve as a strong basis for effective conservation and rehabilitation planning.

Study area

Figure 1 shows the location of the Matlabas mire in the Waterberg Mountains, within Marakele National Park (area of approximately 290.5 km²). The altitude of the

Matlabas mire is around 1,200 m above sea level, and it has a total surface area of 64 ha. It has been managed as a national park since 1988 but was only officially proclaimed a national park on 11 February 1994. Before 1988, the area was used for agriculture with both farming of crops and cattle grazing (Van Staden, 2002).

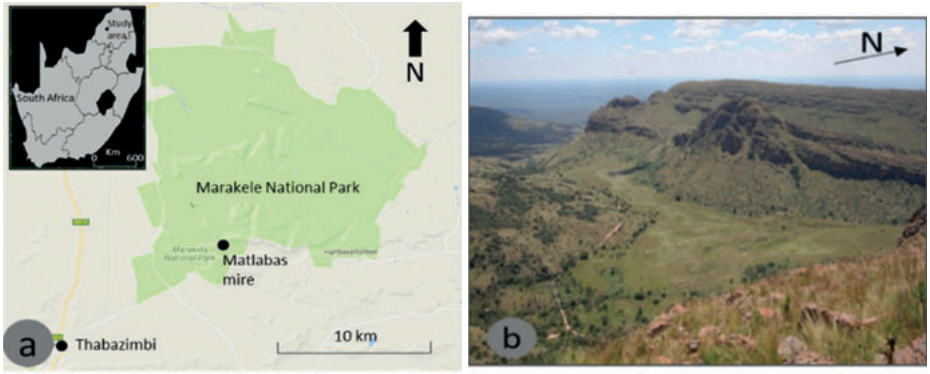

Figure 1: a) Location of the Matlabas mire in Marakele National Park in South Africa (24°27'33.24"S, 27°36'1.28"E), b) Overview of the Matlabas mire from a high plateau in the east.

The mire can be divided into two sides: a western one (6 ha) and an eastern one (8 ha). The western side of the mire drains from west (from 1621 m a.m.s.l.) to east along a slope of 4 %, while the eastern side of the mire drains primarily to the north (from 1614 m a.m.s.l.) along a slope of 5 % (Bootsma, 2016). Two seepage wetlands upslope of the mire were intersected in the late 1960s by a road that runs along the southern edge of the mire. The mire is located close to a watershed within a major east to west stretching valley.

Matlabas is underlain by sandstone bedrock of the Aasvoëlkop Formation, part of the Matlabas Subgroup in the Waterberg Supergroup (with shale and mudstone), and the Sandriviersberg Formation, part of the Kransberg Subgroup also in the Waterberg Supergroup (SACS, 1980). The formations developed on the parent materials range from shallow to deep sandy soils on sandstone and clayey soils on diabase dykes and mudstone (Van Staden, 2002). Wetlands in the Waterberg Mountains mainly occur in the valleys, arranged in a prominent kite-like pattern as a result of the diabase dykes intruding along faults striking west-northwest to east-southeast and northeast to southwest into the Waterberg Supergroup sandstones (Bootsma, 2016).

Average daily ambient temperatures range between a high of 19.5 °C and a low of 5.1 °C, with the maximum daily temperature reaching 22.8 °C and minimum night temperature reaching -1.7 °C. The average annual ambient temperature was 17.6 °C during the period of 2011–2013 (Bootsma, 2016). Average rainfall during the same period was around 1000–1200 mm/year, with an average daily rainfall of about 5.5 mm/day during the hot and wet season, which takes place from October to April (Bootsma, 2016).

METHODS

Surface elevation and channel tracing

Elevations were determined with a differential GPS method, using a network of fixed, ground-based reference stations to broadcast the difference between the positions as indicated by the GPS and a known fixed position to obtain accurate contour lines at 50-cm intervals. Data for 290 points were obtained in February 2012 by F.J. Loock Surveyors Inc from South Africa. The data were calibrated to height above sea level (a.m.s.l). Channelled surface water flows were recorded in the field by a hand-held GPS, visually plotted using aerial imagery and classified as either permanent or intermittent. Moreover, historical aerial images of the mire surface from 1956 and 1972, i.e. before and after road construction, were visually analysed.

Vegetation description

The different plant communities present in the area were mapped to determine their spatial spread as an indication of the direction of water flows and their origins. The Braun-Blanquet approach was followed to describe the vegetation (Westhoff, 1978). Using aerial images, the area was divided into homogeneous units, in which a total of 54 sample plots (4x4m) were placed in a randomly stratified manner per unit (Brown *et al.,* 2013). Plant species within the sample plots were identified and cover abundance values were assigned using the modified Braun-Blanquet scale (Peet *et al*., 2013). Thereafter, a modified TWINSPAN was performed to classify the different plant communities present (Roleček *et al.,* 2009). These vegetation patterns were used as environmental indicators to locate the zones of hydrological changes, and therefore, identify the most prominent sampling targets.

Peat thickness and dating

The thickness of the peat in the mire was recorded along four south to north running transects (A, B, C and D) covering the eastern side and at five points (W1 to W5) covering the western side (Figure 2). A Russian hand auger was used to sample peat cores, 50-cm increments at a time, down to the top of the mineral soil.

Fourteen peat samples (thickness of 1 cm) were collected for radiocarbon (^{14}C) dating to estimate the age at the bottom of the peat (at five locations) and to determine accumulation rates along two vertical profiles at points B3 (3 samples, a to c), B4 (6 samples, a to f) and C (2 samples, a and b). Samples from the vertical profiles were taken at the observed boundaries of facies change, e.g. degree of decomposition. Also, $\delta^{13}C$ content in the peat was measured to estimate the type of plant remnants forming the peat, i.e. C3, C4 or CAM plants (O'Leary, 1981). Each plant type has a different photosynthesis process, which leads to different $\delta^{13}C$ values due to the isotope fractionation (O'Leary, 1988). C3 plants indicate wetter conditions with $\delta^{13}C$ values ranging from -22 to -25, and C4 plants indicate dry conditions with $\delta^{13}C$ values ranging from -11 to -14 ‰ (O'Leary, 1981; 1988). The colour and texture of each peat sample were described according to the Von Post Humification Scale (Von Post, 1922), and then sealed in a plastic bag. These samples were sent to the Centre

for Isotope Research (CIO) at the University of Groningen in the Netherlands for analysis.

All the samples were treated using the Alkali-Acid-Alkali (AAA) method to remove any contaminating material (Aerts *et al.,* 2001). Then the $^{14}C/^{13}C$ content was measured by atomic mass spectrometry (AMS) at the facility (Aerts *et al.,* 2001). Most of the ^{14}C measurements were reported in Before Present (BP) units (Mook & van der Plicht, 1999), except for the samples with bomb effect backgrounds (^{14}C > 100%), while the $\delta^{13}C$ values were reported in permil (‰). The results in BP were calibrated to calendar age (CalBP) using the OxCal calculation model (Bronk Ramsey, 2008). The calibration curve used for most of the samples was SHCAL13 for zone1–2 (Hogg *et al.,* 2013). For the samples with ^{14}C content >100 %, the calibration curve accounting for the bomb effect was used (Hua *et al*., 2013).

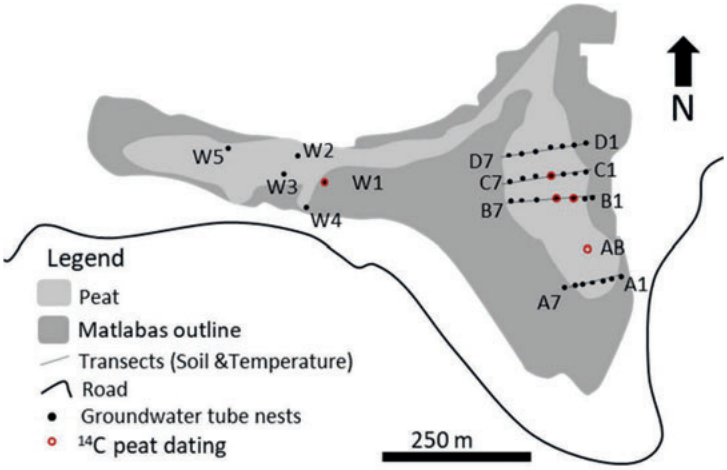

Figure 2. Location of sites used for soil description, radiocarbon peat sampling, groundwater wells for head measurement and groundwater samples for analysis of ion composition, stable isotopes and radiocarbon dating.

Groundwater flow

Phreatic and piezometric water levels

Polyvinyl chloride (PVC) groundwater tubes were installed to measure phreatic and piezometric water levels at various depths. Phreatic groundwater levels were measured using wells, with perforated screens placed along the entire tube, 60 to 80 cm deep, in the peat layer. Piezometric water levels were measured using piezometers, with a 20-cm screen at the bottom of the tube placed in the underlying mineral soil. Observation nests consisted of 1 well and 2 piezometers and were installed at transects A, B, C and D on the east side and at points W1 to W5 on the west side (Figure 2). The 20-cm-screens of the piezometer were inserted at two depths: the first was at a shallow depth of 60–80 cm in the peat layer (referred to as "a" in the code and the second in the mineral soil beneath the peat as "b"). Appendix

1 shows the depths of all the groundwater tubes. Water levels within the wells and piezometers were monitored manually on a monthly basis from 2011 to 2013 to obtain 24 months of consecutive readings.

Peat temperatures

Peat temperatures were measured to identify the direction of the groundwater flows in the peat layer (Van Wirdum, 1991). They were measured using a steel probe of 2 m in length along the 4 transects on the eastern side (A, B, C and D) at 20-cm depth intervals. The measurements were carried out at each transect during a cold and dry period in June 2011, with ambient air temperatures around 12 °C.

Ion composition

Water samples were collected from piezometers during a wet summer season in October 2011 and a dry winter season in June 2012, with 54 samples taken for each season. Another sampling round was added in October 2017, but there were only 29 samples as many piezometer tubes had been burnt by a natural fire. All piezometers were emptied with a hand pump one day before sampling to replenish the water before sampling. The sampled water was then stored in PVC bottles of 100 ml and 50 ml for cation and anion analyses, respectively, and kept in the dark at a temperature of 4° C.

These water samples were analysed at the Agricultural Research Council (ARC) laboratory in Pretoria, South Africa. The samples were passed over a 0.45 mu membrane vacuum filter to remove sediments and impurities. Water pH was measured by titration, and ion composition of Ca, Cl, NO_3, SO_4, PO_4, HCO_3, Mg, Na and K were measured by inductively coupled plasma mass spectrometry (ICP-MS). In the third round of sampling, Fe and SiO_2 ions were also measured. The results were checked for deviations in ionic balance, and samples with deviations higher than 20–30% were disregarded in further analyses.

$^{18}O/^{2}H$ stable isotopes

In March 2014, 22 water samples were collected to measure the stable isotopes of oxygen and deuterium (^{18}O and ^{2}H) in the water (Figure 2, Appendix 2). These water samples were collected in dark glass bottles of 50 and 30 ml per tube and stored in the dark at a temperature of 4° C. Later, they were analysed at the CIO laboratory at the University of Groningen in the Netherlands by dual inlet isotope ratio mass spectrometry (DI-IRMS; Meijer, 2009). The sampling was repeated in October 2017 (29 samples), and these were analysed at the environmental isotope laboratory at Witwatersrand University, South Africa. The stable isotope ratios in the samples ($\delta^{18}O$ and $\delta^{2}H$) were reported in ‰ w.r.t. VSMOW, i.e. the reference used was the Vienna convention material (Meijer, 2009).

Carbon isotopes

The radiocarbon content of water samples is an indication of the residence time of groundwater in the soil (Mook, 2006). Six water samples were taken from the

piezometers in the sand layer at the end of the dry season in October 2017 using 500 ml dark glass bottles to measure their radiocarbon content. Five points were selected on the eastern side at transects A, B and D (A2, B4, B6, D4 and D5) and one point on the western side of the mire at W5 (Figure 2). These samples were analysed for their carbon isotope content ($\delta^{13}C$ and ^{14}C) at the CIO laboratory. $\delta^{13}C$ values of the samples were analysed using DI-IRMS and reported in ‰ w.r.t. VSMOW, similarly to the stable isotopes. The ratios were then used to infer whether there had been dilution of the ^{14}C values due to infiltration through the peat layer, which is indicated by $\delta^{13}C$ values lower than -16 ‰ (Mook, 2006)

RESULTS

Elevation and peat thickness

The peat soils in Matlabas cover a total of 14 ha, which is only 22% of the larger mire area of 64 ha. Peat depth varied from 30 cm at the steep slopes to almost 5 m in the central parts of the eastern side of the mire, while average peat thickness was 1.5 m. Hence, the estimated volume of the peat layer was around 150,000 m^3. Most of the peat layers were fibrous, and they were interrupted by clay and sand layers at the bottom, at which also some layers of gravel occurred, e.g. at B4.

Six channels with concentrated surface water flow were identified (Figure 3). Two of these are permanent water flow channels on the eastern side. A third channel starting from the western side also has a permanent flow. The permanent channels are incised about 40–50 cm into the peat. Surface water drains the mire in a northerly direction.

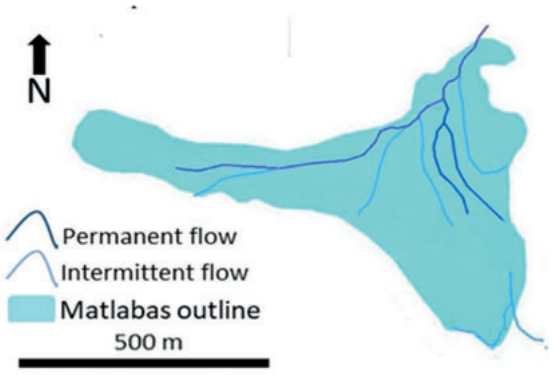

Figure 3. Map of water flow channels.

Aerial images taken in 1956 and 1972 show the mire before and after the road was built. These images show that some channel formation was already apparent in 1956 (Figure 4a). Since construction of the road in the late 1960s, however, channel formation in the eastern section of the mire had increased in number and volume by

1972 (Figure 4b). Furthermore, the extent of two seepage wetlands visible on the 1956 images south of the later constructed road are largely reduced in the 1972 images.

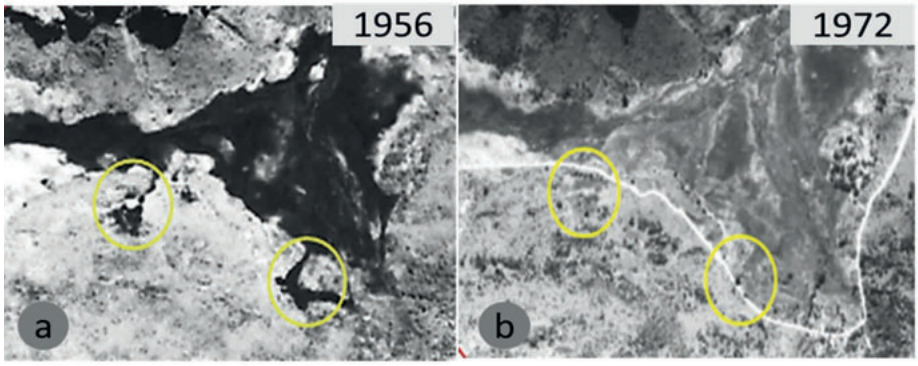

Figure 4. (a) Aerial image of the Matlabas mire taken in 1956, (b) aerial image from 1972. The yellow circles show the location of seepage wetlands, which appear to have been significantly reduced after construction of the road, indicating changes to the hydrological processes of the mire.

Moreover, the mire has developed a series of elevated peat domes, with heights of approximately 1 m above the surrounding landscape and widths between 3 and 9 m (Figure 5a). Most domes are situated along a fault line in a northwest-southeast direction, shown in a geological map of the area,[17] but some are also aligned in an east-west direction (Figure 5b).

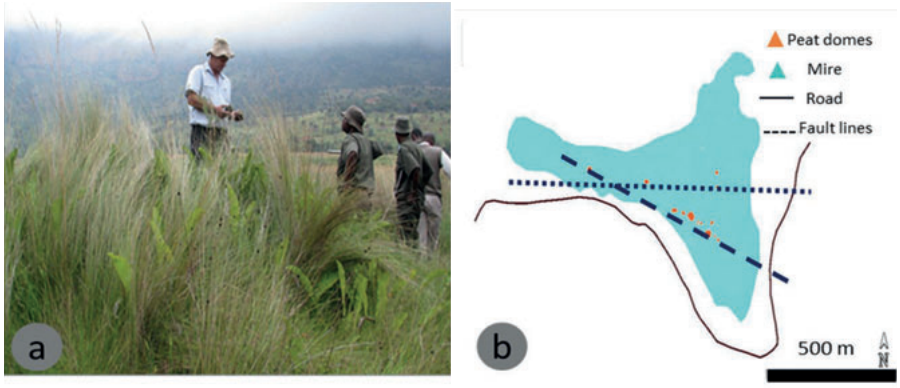

Figure 5. (a) Photograph of one of the small peat domes and (d) the peat dome occurrences and their alignment in the NW-SE direction along a previously identified fault line (dashed line); another alignment of peat domes in the E-W direction that might indicate another fault line (dotted line).

Vegetation description

From the TWINSPAN analysis, three major plant communities were identified (Figure 6). The three major communities are briefly described below:

1. *Andropogon eucomus-Aristida canescens* community. Most of the elevated peat domes were covered with this vegetation community. This vegetation community contained the largest number of species, with common wetland species as well as species generally associated with drier conditions.
2. *Kyllinga melanosperma-Miscanthus junceus* community. This community occurred in the wettest part of the mire and was closely associated with peat deposits. A stand of *Phragmites australis* reeds on transect B at B3-B4 was found in this vegetation community.
3. *Pteridium aquilinum* community. This community occurred along the edges of the mire and is characterized by species-poor patches dominated by the fern *Pteridium aquilinum*.

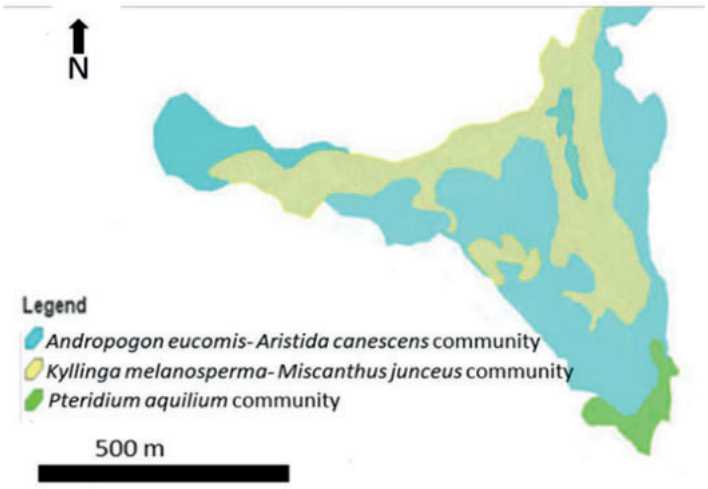

Figure 6. Vegetation map of the mire showing three dominant vegetation types.

^{14}C dating

Table 1 lists the results of the radiocarbon dating of the 14 peat samples, their δ^{13}C content and descriptions of the depth intervals; the ages are given as median calibrated age. The mire's oldest basal peat sample, with a radiocarbon age of 11,160 CalBP, was taken from point B4f, which is the second lowest point in altitude. The valley flank basal peats all had younger ages, ranging between 5120 CalBP on the south-eastern side (AB), 3860 CalBP on the western side (W1) and 690 CalBP on the north-eastern side (C3b). Modern dates with bomb values were observed at point B4a (-55 CalBP) and point C3a (-6.5 CalBP), while point B3a dated back to 130 CalBP. The δ^{13}C values show that C3 plants were limited to the top layer in core B4 (point B4a), whereas the rest of the samples had values indicating C3 plants.

Groundwater flow

The groundwater phreatic head in the peat layer showed a decrease from east to west along transect B (Figure 7a). At transect C, however, there was a downward direction

of the phreatic head isohypse with most of the flow being directed to point C5, which is at the head of a permanent channel. The channel at C5 was shown to be draining from points C4 and C6, which had higher phreatic heads (Figure 7b).

Table 1: Results of ^{14}C dating of the peat samples taken from transects A, B, C on the eastern side and point W1 on the western side.

Code	Sample depth (cm)	Altitude (m a.m.s.l)	Sample description & Von Post scale (H1-H10)	$\delta^{13}C$ (‰)	Median age (CalBP)	Thick-ness (m)	Accumulation rate (mm/yr)
W1	200	1590.4	peat with gradual increase of clay content with increasing depth in the 50-cm core, low water content	-12.22	3860	--	--
AB1	250	1584.65	decomposed peat (H8)	-13.26	5120	--	--
B3a	37	1579.7	decomposed peat (H6)	-11.62	130	1.00	1.56
B3b	136	1578.03	peat with high clay content (>H6)	-10.33	590	0.72	0.61
B3c	208	1577.31		-11.43	1780	--	--
B4a	35	1577.63	red amorphous peat, (H1-H3)	-25.88	-55	0.46	1.31
B4b	79	1577.17	recomposed peat (H6)	-12.29	295	1.42	1.76
B4c	227	1575.75	radicel Peat (H1-H3)	-13.31	1100	0.62	0.66
B4d	282	1575.13	radicel Peat (H1-H3)	-14.46	2040	1.18	1.37
B4e	399	1573.95	peat with clay and sand interval at 415-425 (>H6)	-15.92	2900	1.00	0.12
B4f	499	1574.95		-13.97	11,160	--	--
B5	155	1575.31	peat with high clay content (>H6)	-11.53	1225	--	--
C3a	80	1575.52	decomposed peat (H6)	-10.07	-6.5	1.15	1.65
C3b	195	1574.37	peat with high clay content (<H6)	-12.96	690	--	--

Differences between the piezometric head and the phreatic head were higher at points B2 and B3, 0.01 to 0.04 m respectively. Such differences indicate potential discharge of groundwater, in line with the depressions visible on the ground surface. The head differences were largest at B4, where differences in the sand piezometric head and peat phreatic head equalled 0.14 m. Similar differences in head were observed along transect C, with the highest piezometric head found under one of the peat domes at point C4. In contrast, the piezometric heads in the sand were lower (c. 0.03 m) than those in the peat further west from B4 and C4 at both transects. At C5, the head difference was also significantly lower at 0.4 m. Lastly, the water levels in the peat domes were found 30–50 cm below the surface. This is different from other parts with no dome structures, where the water levels were close to the surface. In the south to north direction, the phreatic head decreased northwards following the height gradient of the mire surface and the drainage direction of the surface water channels.

Peat temperature

Peat temperature showed an increase with depth, with the temperature gradients generally following the gradient of the peat surface slope. However, the discharging

groundwater at B4 showed input of warmer water about 1.5 m away from the surface: > 14˚C when the ambient temperature was 10 °C (Figure 8). These measurements were taken at night during the dry and cold season in August 2013. Such patterns were also found along transects A and C, where warmer temperatures appear to be associated with discharging groundwater flows.

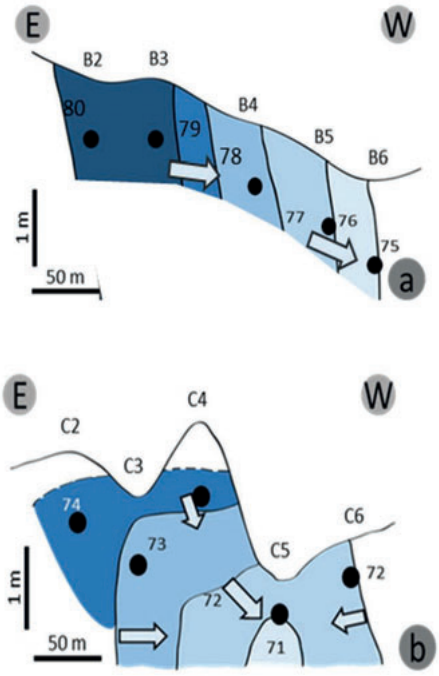

Figure 7. Groundwater phreatic head isohypse in March 2012 along (a) transect B and (b) transect C.

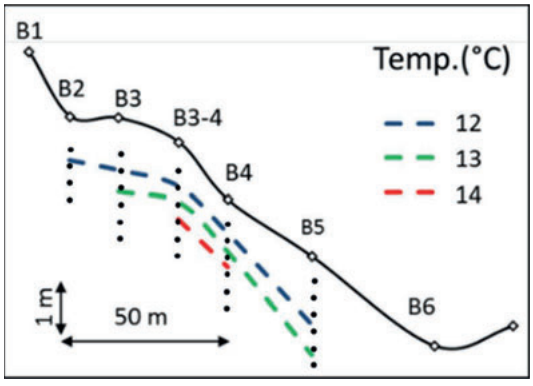

Figure 8. Peat temperature patterns along transect B measured in August, 2013.

Ion composition

Chloride ion concentrations changed by three- to four-fold with season in the top one to two meters of the peat layer. In deeper layers, the changes in concentration were smaller and less than one-fold, e.g. at the sand piezometer at B4 (Figure 9a to c). Calcium ion concentrations also increased in the dry seasons, with magnitudes of change similar to patterns in the chloride ion. Calcium values increased by more than three-fold within the top two meters, while it remained one- to two-fold higher in the deeper parts, except for B6 which showed higher calcium values in the deeper layers (Figure 9d to f).

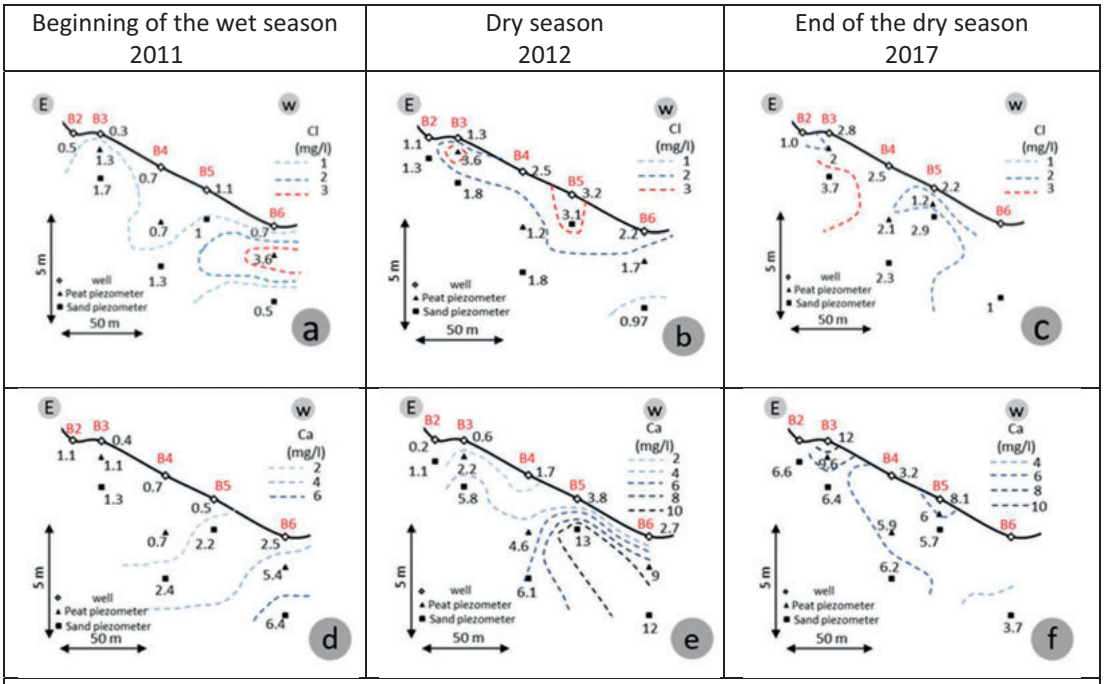

Figure 9. Ion tracers in transect B: (a) chloride at the beginning of the wet season in October 2011, (b) chloride during the dry season in June 2012, (c) chloride at the end of the dry season in October 2017, (d) calcium at the beginning of the wet season in October 2011, (e) calcium during the dry season in June 2012, and (f) calcium at the end of the dry season in October 2017.

In transect C, the calcium-rich and chloride-poor groundwater remained in the deeper soil layers. In the central peat dome, relatively large changes in ion composition occurred. During the wet season the calcium values were low under the peat dome (point C4), while in the dry season the calcium values were higher. There was also an increase of nitrate concentrations (0.73 mg/l relative to the average of 0.16 mg/l) in the groundwater below the peat domes at points C2 and C4 during the wet season (see Appendix 1).

Stable isotopes

The stable isotope content in the water sampled in March 2015, which was at the end of the hot summer season, were significantly enriched compared with those sampled in October 2017, which was at the end of the cold winter season (Figure 10). The samples from March 2015 had $\delta^{18}O$ values ranging from -4 to -6 ‰ and $\delta^{2}H$ values ranging from -20 to -30 ‰, while the samples from October 2016 had $\delta^{18}O$ values ranging from -4 to -3 ‰ and $\delta^{2}H$ ranging from -10 to -20 ‰/. Samples from the western side of the mire appear to be mostly below the global meteoric water line (GMWL), with more indications of enrichment.

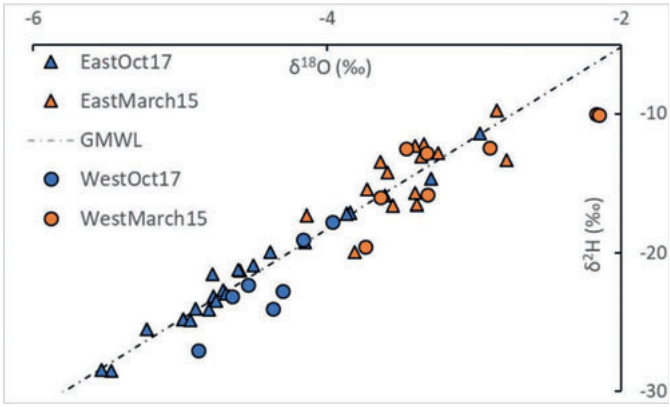

Figure 10. Stable isotope content in water samples from Matlabas. There were 22 water samples from March 2015 and 29 water samples from October 2017. These samples are labelled by the side of the mire from which they were sampled: west samples and east samples.

Carbon isotopes

Table 2 shows that four water samples (A2b, B6b, D4b and w5b) had uncorrected ^{14}C values above 100%, indicating infiltration after 1950 and short residence times. Their $\delta^{13}C$ values differed 0 to -15 ‰. Two samples (B4b and D5b) had $\delta^{13}C$ values around -13 ‰ and ^{14}C values between 95 to 100 %, which indicate infiltration before 1950 and longer residence times.

Table 2. Radiocarbon dating content in six groundwater samples from Matlabas. The samples were taken in October 2017.

No.	Code	Lab no. (GrM)	^{14}C uncorrected (%)	Error ±	$\delta^{13}C$ (‰; IRMS)	Error ±
1	A2b	11547	104.26	0.19	-14.27	0.15
2	B4b	11548	96.42	0.18	-13.38	0.15
3	B6b	11549	104.91	0.19	-10.10	0.15
4	D4b	11550	106.3	0.19	0.43	0.15
5	D5b	11552	95.31	0.18	-13.06	0.15
6	w5b	11554	105.25	0.18	-6.31	0.15

DISCUSSION

Mire development

Based on radiocarbon dating, peat accumulation began at the lowest parts of the valley on the central eastern side during the transition from the Late-Pleistocene to the Holocene. This onset was observed in the thickest peat core obtained at Matlabas, a 5-m peat layer underlain by sand and clay, which was sampled from point B4. Peat accumulation started directly over the mineral soil by paludification processes (Charman, 2002). The observed sand/clay layers indicate high energy flows during the Early to Mid-Holocene, coupled with an apparently slow peat accumulation rate in the first meter of peat. This indicates initially unstable conditions for accumulating peat.
By the Mid-Holocene lateral expansion of peat formation had occurred in the higher parts of the valley bottom in the south and west, possibly due to a mixture of both autogenic and allogenic factors (Anderson *et al.,* 2003). Autogenic factors include the clogging effects of peat accumulation on the slope of transect B, with a low hydraulic conductivity leading to a higher water table upslope at transect A in the south and point W1 in the west. With respect to allogenic factors, expansion to the north occurred due to the shift to a wetter climate during the Late-Holocene (Anderson *et al.,* 2003).

In the current vegetation, the wettest vegetation type, which possibly contributes to peat formation, is dominated by the large tussock species *Miscanthus junceus* and also includes stands of *Australis phragmites* at B3 to B4, although *Kyllinga melanosperma* and *Thelypteris confluens* are also abundant. However, the plant remnants in the peat cores were dominated by $\delta^{13}C$ values of C4 plants, which indicates lower water availability (O'Leary, 1981; O'Leary, 1988; Scott, 2000). However, the recent vegetation shows shifts to C3 plants in the best developed and wettest parts of the mire (B4). This modern shift in $\delta^{13}C$ values highlights the role that stable discharge of groundwater flow coupled with the maturity of the peat development plays in sustaining wetter conditions in the mature parts of the mire.

Natural dynamics: water origin and flow

Piezometric head data indicate that groundwater discharge is limited to the central eastern parts of the mire, e.g. at B2 to B4 and C2 to C4. Three major water flows were shown to control mire development (Figure 11). The first one is sheet flow over the peat surface that occurs in the wet season when precipitation exceeds peat infiltration capacity and the peat is often already saturated. The second is the phreatic groundwater flow in the peat layer, which is often also supplied by the intermittent channel in the south that flows in the mire during the wet season with relatively high energy flows, i.e. sand deposits in the soil profiles at transects A and B. The third is the seepage discharge of deeper groundwater at certain points in the mire, e.g. B4 and C4, which is stable and shows little change over the seasons.

The ion composition indicates that the groundwater in Matlabas is generally poor in dissolved minerals, similar to the precipitation water in the Limpopo region (Van Wyk, 2011). Infiltrating water that passes through the colluvium layer at the valley

slopes hardly dissolves any minerals. Hence, the water flows have low concentrations of calcium and mostly depleted stable isotopes, especially during the wet season when the occurrence of rainwater lenses in the top peat layers increases (Schot *et al*., 2004). After a dry period, higher mineral concentrations are evident due to concentration by evapotranspiration, particularly in the top layers.

The effects of evaporation could also be observed in the stable isotopes values. The variations at the end of the wet period were minor, indicating the stable upward flow of groundwater that is not affected by evaporation. This was, however, not the case for the water flows in the western side of the mire, which has lower hydraulic conductivity in its peat layer. Hence, signs of evaporation were observed in the samples taken from its middle parts during both the hot-wet periods and the cold-dry periods, where the hillslope water enters from the sides, showing a slower flow subject to evaporation processes (Gat, 1996), and follows the relief to the east side of the mire.

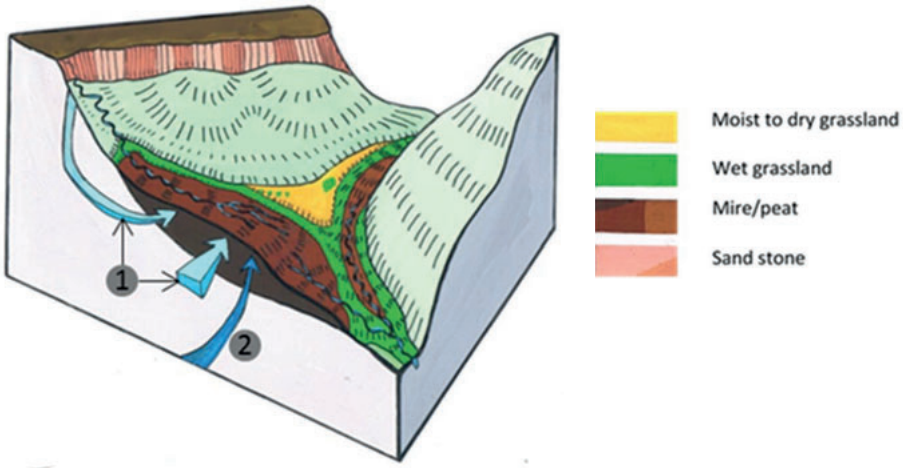

Figure 11. An illustration of the major water flows: 1) lateral sheet and phreatic groundwater flow from the hillslopes, 2) sheet flow above the peat surface during the wet season and 3) deep groundwater flow with a continuous discharge, especially dominant in the dry season.

The observed discharges of deep groundwater flow generally had short residence times; however, they had longer flow lines and deeper origins than the phreatic ones. This is indicated by the radiocarbon values of the water samples. Hence, the sources of these deep discharging groundwater flows are most likely the adjacent hillslopes, which consist of unsorted rock boulders and coarse fragments that form highly permeable layers acting as recharge areas for subsurface water flow to the mire. The groundwater discharges are diluted in the wet period by input from the phreatic and sheet flows, resulting in low calcium and chloride concentrations. However, their chemical characteristics are more nuanced in the dry period with their calcium and bicarbonate-rich groundwater moving vertically upwards, especially at point B4. This deeper groundwater differs distinctly from the shallow groundwater, and their

dynamic interactions are most likely to control the vegetation zones, e.g. the *Phragmites australis* reed zone (De Mars *et al.,* 1997).

Mire features

Geological structures and vegetation also play an important factor in regulating and maintaining the sheet flow during the wet season. The geological fault lines appear to be linked with an upward flow of groundwater, in that the alignment of the peat domes in the northwest-southeast direction resemble the position of a fault line indicated on the 1:250.000 Geological Map (SACS, 1980) There is also another alignment of peat domes in an east-west direction, which could point to the presence of another fault line.

The large tussocks of the grass *Miscanthus junceus* and the thick rhizomes of the sedge and fern species appear to prevent soil erosion during storm flood events caused by the intermittent stream from the south. The large tussocks are elevated above the water surface, in some instances by as much as 50 cm. They probably reduce the flow velocity and prevent further erosion during storm flood events, with the tussocks and rhizomes dispersing surface water flow so that it does not directly flow into adjacent erosion channels. The vegetation, therefore, is exhibiting a self-organization mechanism, providing a local positive feedback to stabilize soil against erosion processes (Eppinga *et al.,* 2007)

Anthropogenic disturbance

There are signs of desiccation and release of nutrients, e.g. nitrates concentrations in the dry season, especially in nearby peat dome areas. The desiccation seems to be related to the head cuts in the peat, e.g. at C5. The head cuts not only drain the peat but also expose soil layers to oxidation and infiltration of precipitation water, thus stimulating the presence of acid components in the soil (Brady & Weil, 1998; Madaras *et al*., 2012). The water pressure data indicate that desiccated peat domes become infiltration areas that lose water to the stream. Also, calcium concentrations in the groundwater below some of the drained peat domes increase significantly during dry periods.

The desiccation can be attributed to the change in the land-use practices that have intercepted the sheet flow and the phreatic water supply during the wet seasons. This is also evident from the data available from the unaffected parts of the mire, which reflect stable conditions of groundwater discharge and wetness. The constructed road is a major factor in intercepting the sheet flow, which is also evident in the disappearance of the seepage wetlands in the south that have now been replaced with non-wetland plant species. Another factor responsible for the head cuts is past grazing practices and the current increase in the local elephant population. The vegetation was often burnt in winter to encourage grazing, thereby leading to poor vegetation growth and higher runoff due to reduced vegetation interception of storm flows. Currently, these two factors may be coupled with the appearance of elephant walking paths towards the wet peat areas, where they make bathing pools, which is due to the increasing numbers of elephants since the area became a national park.

These paths may lead to accelerated flow resulting in the initiation of more head cuts. However, these processes require further investigation.

CONCLUSION

The Matlabas mire started accumulating peat during the Early-Holocene. However, the average measured accumulation rate remained very low (0.011 mm/yr) until the Mid-Holocene assuming a continuous accumulation or due to loss in accumulated peat caused by erosion phases. The maturity of peatland development drives a positive feedback on sustaining wetter conditions for higher accumulation rates. Water availability for plants seems to have shifted to more positive conditions for wetland species in the present, especially in the oldest part of the mire at transect B. Three major water flows were found to support functioning of the mire, namely phreatic groundwater combined with intermittent sheet flow and discharges of locally permanent deep groundwater. The first type of flow had higher water quality during the wet season, where ion composition was diluted by the sheet flow originating from the intermittent channel in the south east of the mire. During the dry season, this phreatic flow increased in ion concentrations due to evaporation processes. The deep groundwater flow was dominant during the dry period, and areas with this type of discharge had more or less stable ion composition throughout the year, e.g. at B4. Land-use practices have had an effect on the less mature parts of the mire by intercepting water from the intermittent channel in the south through the constructed road and formation of head cuts in areas of the mire with grazing and walking paths for cattle and elephants.

ACKNOWLEDGEMENT

We would like to acknowledge the staff at SANPARKS for arranging access and assistance in the park; ERA and the WRC (Project K5/2346) for their partial funding. We thank Ola Abulshalashel for her help with the illustrations, Esther Chang for language editing. We thank Althea Grundling and Agricultural Research Centre laboratory in Pretoria for the macro ions analysis. We also appreciate the support of Harro Meijer, and Rien Herber and for the radiocarbon analysis done by Sanne Palstra, and the people at the CIO Laboratory at University of Groningen.

APPENDIX

Appendix 1. Results of ion composition analyses of the water samples (mg/l) from (a) October 2011, (b) June 2012, and (c) October 2017.

(a)

No.	code	pH	Ca	Cl	NO_3	SO_4	PO_4	HCO_3	Mg	Na	K
1	A1w	6.43	3	3	0.07	1	0	43	1	5	1
2	A2w	5.6	0	1	0.53	1	0	6	0	1	1
3	A1a	5.63	1	2	0.49	0	0	10	0	3	1
4	A1b	5.46	1	2	0.18	0	0.04	10	0	2	1
5	A2a	5.61	1	2	0.16	1	0	13	0	4	1
6	A2b	5.38	1	2	1.12	0	0.13	7	0	2	1
7	A3w	5.18	1	1	0.05	0	0	12	0	1	1
8	A3a	5.57	1	3	0.57	9	0	15	1	4	4
9	A4w	5.33	1	1	0.05	0	0	11	1	2	1
10	A5w	5.81	1	1	0.15	0	0	18	1	3	1
11	B2w	4.96	1	1	0.19	0	0	12	0	2	1
12	B3a	5.52	1	2	0.49	1	0	10	0	2	1
13	B3w	5.37	0	1	0.34	0	0	7	0	3	0
14	B3b	5.13	1	1	0.19	0	0	9	0	1	1
15	B4w	5.58	1	1	0.05	0	0	7	0	1	1
16	B4a	5.5	1	1	0.51	0	0	5	0	2	1
17	B4b	6.48	2	1	0	0	0	44	1	4	2
18	B5w	5.48	0	1	1.12	0	1.01	10	0	3	1
19	B5b	5.87	2	1	1.26	1	0	16	1	3	1
20	B6a	6.34	6	0	0.04	1	0.03	110	3	6	1
21	B6a	6.62	6	4	0.03	3	0	52	2	6	1
22	B6w	5.66	3	1	0.26	1	0.01	16	1	2	1
23	C2w	6.1	2	1	0.07	0	0.09	26	0	2	1
24	C2b	6.05	2	7	0.17	2	0.27	40	1	6	6
25	C3w	6.62	3	1	0.2	1	0.05	104	1	5	2
26	C3a	5.8	3	1	0.05	1	0.06	28	1	3	1
27	C3b	6.01	3	1	0.02	0	0	29	1	4	1
28	C4a	5.58	4	1	0.03	0	0	23	2	2	1
29	C4b	5.75	3	1	0.73	1	0.81	27	1	2	1
30	C5b	6.14	10	1	0.09	1	0	104	6	10	1
31	C5w	6.25	2	1	0.17	0	0	110	0	4	1
32	C6w	6.44	6	2	0.19	2	0.34	56	3	5	1
33	D3w	5.73	2	1	0.25	1	0.03	11	1	2	1
34	D3a	6.12	2	2	3.21	2	0	20	0	5	2
35	D3b	6.17	5	1	2.16	1	0	27	1	4	1
36	D4w	6.16	3	1	0.11	0	0	38	1	3	1
37	D4a	5.73	3	2	1.12	0	0	26	1	4	1
38	D4b	6.65	2	2	0.18	1	0	88	1	8	2
39	D5w	6.21	4	2	0.04	1	0	32	1	6	1
40	D5a	5.56	1	3	0.31	5	0.1	18	1	5	2
41	D5b	5.67	2	2	0.72	1	0.06	26	1	6	1
42	D6w	6.48	6	0	0.06	1	0.02	90	3	5	1
43	W1w	4.92	0	1	0.3	0	0.22	9	0	3	1
44	W1a	5.77	0	0	0.01	0	0	0	0	0	0
45	W2w	5.94	1	0	0.04	0	0	28	1	3	1
46	W2a	5.93	1	1	0.62	1	0	7	0	1	1
47	W2b	6.81	9	2	0.47	4	0	206	6	7	2
48	W3w	5.28	1	1	0.08	1	0	24	1	3	1

49	W3a	5.36	2	1	0.11	1	0.05	21	2	3	1
50	W4w	6.18	6	2	0.22	7	0	83	2	7	2
51	W4a	5.96	4	4	0.26	8	0	49	2	8	4
52	W4b	5.31	1	1	0.15	0	0	12	1	2	1
53	W5w	6.49	6	1	0.18	0	0	40	2	5	1
54	W5b	6.59	4	1	1	0	0	34	2	6	1

b)

No.	code	pH	Ca	Cl	NO3	SO4	PO4	HCO3	Mg	Na	K
1	A2a	5.54	1	4	0.43	0.19	0	6	1	3	1
2	A2b	5.75	1	3	0.26	0.3	0	5	1	3	0
3	A3w	5.55	1	4	0.28	0.48	0	6	1	4	2
4	A3a	5.37	0	1	0.11	0.24	0	5	1	2	1
5	A4w	5.59	1	3	0.24	0.74	0	9	0	4	0
6	A5w	5.18	1	1	0.47	0.67	0	5	0	2	1
7	B2a	5.23	0	1	0.29	0.41	0	5	0	2	2
8	B2w	6.07	6	1	0.78	0.13	0	32	1	4	1
9	B3a	5.68	2	1	0.41	0.34	0	15	0	2	0
10	B3a	6.15	2	4	0.24	0.39	0	14	1	2	1
11	B3b	6.15	2	2	0.28	0.26	0	9	1	2	0
12	B4w	6.15	5	1	0.2	0.23	0	28	1	5	1
13	B4a	6.27	6	2	0.27	0.62	0	38	3	3	1
14	B4b	6.1	4	3	0.19	0.31	0	20	2	3	0
15	B5w	6.32	13	3	0.48	0.7	0	95	2	8	3
16	B5b	6.72	18	1	0.25	0.24	0	104	2	7	1
17	B6a	6.75	9	2	0.27	0.73	0	55	3	5	1
18	B6b	6.74	3	2	0.12	0.44	0	21	1	5	1
19	B6w	6.09	1	1	0.24	0.47	0	15	1	2	1
20	C2w	5.83	0	1	0.14	0.58	0	2	0	0	1
21	C2b	6.42	0	1	0	0.41	0	6	0	0	1
22	C3w	6.07	0	1	0.18	0.09	0	46	0	0	1
23	C3a	6.34	9	2	0	0.01	0	99	1	0	1
24	C3b	5.93	9	1	0.23	0.25	0	62	2	6	1
25	C4a	5.89	9	2	0	0.16	0	82	2	7	2
26	C4b	6.45	12	2	0	0.16	0	129	3	8	1
27	C5a	6.49	14	0	0.22	0.31	0	120	6	12	1
28	C5b	6.4	3	1	0	0.33	0	37	1	4	0
29	C5w	6.38	5	3	0.24	0.6	0	82	3	10	2
30	C6w	5.9	2	2	0	0.11	0	31	1	5	0
31	D3w	6.37	9	1	0.1	0.24	0	64	1	8	1
32	D3a	6.41	23	2	0	0.18	0	101	2	7	1
33	D3b	5.93	3	2	0.18	0.61	0	42	1	6	0
34	D4w	6.38	3	1	0.16	0.13	0	14	1	1	0
35	D4a	6.52	4	2	0	0.23	0	28	1	8	1
36	D4b	5.84	1	2	0.42	0.64	0	8	0	2	0
37	D5w	6.02	2	1	0.31	0.52	0	42	1	6	1
38	D5a	6.24	4	1	0.11	0.18	0	41	2	5	0
39	D5b	6.2	2	2	0	0.38	0	21	1	4	0
40	D6w	5.15	0	1	0.19	0.33	0	10	1	1	4
41	W1w	5.95	3	2	0.22	0.34	0	20	1	4	3
42	W1a	5.74	1	0	0.28	0.54	0	26	1	3	0
43	W2w	5.36	0	0	0	0.2	0	6	0	1	1
44	W2a	5.87	1	2	0	0.6	1.09	17	1	2	5
45	W2b	5.92	3	0	0.34	0.55	0	17	2	2	2
46	W3w	6.16	2	1	1.75	2.87	0	26	1	4	3

47	W3a	6.85	4	2	0.4	2.16	0	34	4	3	3
48	W3b	5.91	1	1	0	0.28	0	30	4	3	4
49	W4w	6.26	4	5	0.42	1.82	7.82	21	1	5	5
50	W4a	5.31	2	1	0.62	1.03	0	78	5	3	21
51	W4b	6.33	5	0	0	0.17	0	42	2	6	0
52	W5w	6.47	5	1	0.84	0.76	0	45	2	6	1
53	W5a	6.32	5	1	0.34	0.42	0	43	2	6	0
54	W5b	6.16	1	0	0	0.21	0	12	1	2	0

c)

No	code	pH	Ca	Cl	NO_3	SO_4	PO4	HCO_3	Mg	Na	K	Fe	SiO_2
1	A2a	5.12	4	4	0.0	1	0.8	5	1	5	1	0.2	10
2	A2b	6.16	5	2	0.3	1	0.6	13	2	9	1	0.7	11
3	B2	6.17	7	1	0.0	1	0.0	12	1	12	1	13.5	16
4	B3w	6.46	12	3	0.0	1	5.7	32	1	8	2	1.3	16
5	B3a	5.81	10	2	<0.01	1	4.3	51	2	11	3	6.0	16
6	B3b	6	6	4	0.1	0	1.5	33	2	9	3	2.1	13
7	B4w	5.81	3	3	0.0	1	0.6	9	1	8	1	1.6	18
8	B4a	6.17	6	2	0.1	1	0.3	16	2	12	1	<0.01	17
9	B4b	7	6	2	0.0	1	0.5	28	2	8	2	0.3	23
10	B5w	6.43	8	2	0.1	1	0.4	20	2	15	2	5.6	23
11	B5a	6.19	6	1	0.1	9	0.5	16	2	6	1	7.2	19
12	B5b	6.55	6	3	0.2	1	0.5	25	2	12	3	0.1	31
13	B6	6.6	4	1	0.0	1	0.5	13	1	9	1	4.4	12
14	D2a	7	10	2	0.0	2	11.3	73	4	13	2	1.1	17
15	D2b	7.57	20	9	0.1	9	29.9	269	5	15	6	0.3	16
16	D3a	5.76	4	2	0.0	1	0.6	7	1	7	1	1.1	13
17	D3b	6.73	5	1	0.4	1	0.3	20	2	8	1	<0.01	15
18	D4a	6.59	5	1	0.1	1	0.4	18	2	8	1	0.4	20
19	D4b	6.79	5	2	0.3	1	1.6	20	1	10	1	0.5	22
20	D5a	7.2	8	1	0.0	0	0.3	40	3	12	1	<0.01	3
21	D5b	6.99	10	2	0.1	1	1.0	46	4	11	1	<0.01	34
22	w5b	6.58	7	2	0.1	1	0.7	21	3	8	2	0.4	144
23	w5a	6.09	4	5	0.4	2	2.1	10	1	8	1	0.5	5
24	w4b	6.42	11	12	0.2	0	0.6	23	3	12	3	2.3	12
25	w4a	6.22	8	7	0.0	1	0.1	23	1	8	2	3.4	7
26	w2b	6.17	4	1	0.0	1	0.4	9	2	12	2	1.7	27
27	w2a	6.36	3	1	0.1	1	0.6	15	2	3	1	0.8	12
28	w1a	6.65	4	1	0.0	1	0.4	16	2	7	2	2.1	22
29	E1	6.71	4	2	0.1	3	0.2	14	2	19	2	1.0	30

Appendix 2. Results of the stable isotope content in groundwater samples taken on (a) March 2015 and (b) October 2017.

No.	Date	Sample code	Depth (m)	$\delta^{2}H$ (‰)	$\delta^{18}O$ (‰)
1	October 2017	A2a	1.05	-24.80	-4.98
2	October 2017	A2b	1.35	-25.55	-5.23
3	October 2017	B2	0.5	-21.26	-4.59
4	October 2017	B3a	0.5	-19.92	-4.39
5	October 2017	B3b	2.3	-23.17	-4.77
6	October 2017	B3well	0.1	-17.15	-3.85
7	October 2017	B4well	0.1	-14.72	-3.29
8	October 2017	B4a	1.5	-24.10	-4.81
9	October 2017	B4b	4.5	-20.93	-4.50
10	October 2017	B5w	0.5	-22.72	-4.71
11	October 2017	B5a	0.9	-22.97	-4.69
12	October 2017	B5b	1.8	-23.44	-4.76
13	October 2017	B6	1.25	-11.42	-2.96
14	October 2017	D2a	2.5	-21.22	-4.61
15	October 2017	D2b	3.2	-21.57	-4.78
16	October 2017	D3a	0.7	-19.22	-4.15
17	October 2017	D3b	1.7	-24.80	-4.98
18	October 2017	D4a	1	-24.02	-4.90
19	October 2017	D4b	1.65	-24.87	-4.93
20	October 2017	D5a	1.25	-28.56	-5.47
21	October 2017	D5b	2.5	-28.47	-5.54
22	October 2017	EastChannel2	0.2	-17.22	-3.87
23	October 2017	W5b	1.65	-19.04	-4.16
24	October 2017	W5a	0.8	-17.79	-3.96
25	October 2017	W4b	1.7	-23.13	-4.65
26	October 2017	W4b	1.7	-22.33	-4.54
27	October 2017	W2b	3	-27.08	-4.88
28	October 2017	w2a	0.7	-24.02	-4.37
29	October 2017	W1a	0.5	-22.75	-4.30
30	March 2015	W3	0	-12.46	-2.90
31	March 2015	W5a	0.8	-19.59	-3.74
32	March 2015	W4b	1.9	-10.03	-2.17
33	March 2015	W2b	3	-12.83	-3.33
34	March 2015	W1b	3.1	-10.10	-2.15
35	March 2015	W3	0	-16.06	-3.64
36	March 2015	W1	0	-12.55	-3.46
37	March 2015	B3	0	-15.66	-3.30
38	March 2015	B3well	0.1	-16.56	-3.39
39	March 2015	A2b	2	-15.45	-3.73
40	March 2015	A4	0	-16.62	-3.55
41	March 2015	B1a	0.5	-17.33	-4.14
42	March 2015	B2	0	-12.20	-3.34
43	March 2015	B3a	0.5	-15.94	-3.61
44	March 2015	B3b	2.3	-19.97	-3.81
45	March 2015	B4	0	-9.78	-2.85
46	March 2015	B5a	0.5	-13.49	-3.64
47	March 2015	B6	0	-13.11	-3.36
48	March 2015	C5	0	-13.33	-2.78
49	March 2015	ChannelEast1	0	-12.31	-3.40
50	March 2015	ChannelEast2	0	-12.84	-3.25
51	March 2015	ChannelEast3	0	-15.70	-3.40

5

Natural isotopes identify origin of groundwater flows influencing wetland vegetation in the Drentsche Aa brook valley, the Netherlands*

This study uses groundwater isotopes and ion composition to verify model simulations and ecohydrological studies in the Drentsche Aa nature reserve in The Netherlands, which is representative for the north western wetland areas in the Ice Marginal Landscape zone. At eight field sites, a total of 24 samples were analysed for their ^{13}C, ^{14}C, ^{2}H, and ^{18}O isotopes and ionic composition. The isotopes indicate that most of the fen peatlands in the area depend on the exfiltration of sub-regional groundwater flows, which confirmed the previous model simulations and ecohydrological studies. At three sites, isotopes and ionic composition indicate that the groundwater from the sub-regional system has been replaced by local infiltrated rainwater, due to nearby groundwater abstractions for drinking water, which influenced the success rates of the restoration measures. Furthermore, the evidence from chloride and ^{14}C contents was found to indicate the presence of more saline groundwater, which are influenced by the groundwater flows near salt diapirs. Groundwater abstractions may enhance the upward flow of the saline groundwater to eventually exfiltrate at the wetlands, affecting the biodiversity of the nature reserve.

* This chapter is submitted as: Elshehawi, S., Bregman, E., Schot, P., Grootjans, A. (in press) Natural isotopes identify origin of groundwater flow influencing wetland vegetation in the Drentsche Aa brook valley, The Netherlands. *Journal of Ecological Engineering.*

INTRODUCTION

Wetland vegetation is strongly influenced by hydrology (Wheeler & Shaw, 1995; Gilvear & Bradley, 2009), notably by the interactions between local, sub-regional and regional groundwater flow systems (Tóth, 1963; Schot & Molenaar, 1992; Dahl *et al*., 2007; Van Loon *et al*., 2009). Such interactions among the groundwater flows lead to different types of groundwater-dependent ecosystems (Wassen *et al*., 1990). An example of such systems is the Drentsche Aa Brook Valley, which is a nature reserve in the north of the Netherlands. This valley is characterized by various types of wetlands, agricultural fields, heathlands and small villages. The heathlands, forests and wetlands are all part of a protected nature reserve (Van Diggelen *et al*., 1995). Different types of wetland vegetation are dependent on various water sources, with the biodiversity-rich fen peatlands primarily depending on the groundwater flows from phreatic and semi-confined groundwater aquifers (Grootjans *et al*., 1993; Van Diggelen *et al*., 1995). Everts & De Vries (1991) illustrated the hypothetical groundwater systems in Drentsche Aa based on the vegetation gradients using the theoretical framework from the groundwater systems by Toth, (1963) (Figure 1). These local and sub-regional groundwater systems have been intensively studied and the results have been used for nature and landscape policy plans.

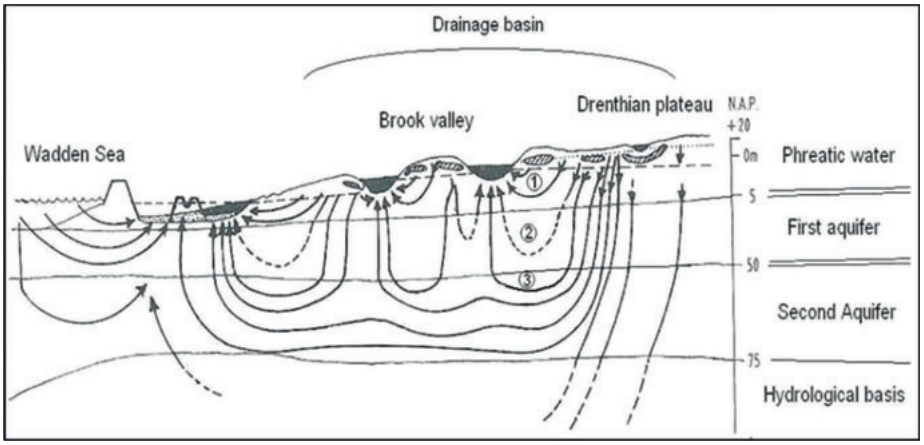

Figure 1. An illustration of the hypothetical groundwater flow systems conditioning the ecohydrological systems in Drentsche Aa Brook Valley (Source: Everts and De Vries, 1991).

However, the area is part of the Ice Marginal Landscape zone, and geological proccesses such as the pro- and postglacial differential Saalian and Weichselian rebound and the sub-glacial deeply eroded Elsterian channel systems are not well understood, especially in relation to the groundwater flows (Figure 2a) (Smit *et al*., 2015). On the basis of better geological input, Magri & Bregman (2011) simulated the groundwater flows in the area using particle tracking, where they indicated the areas of infiltration and exfiltration of groundwater on sub-regional and local scales. One of

the model outcomes was that salt diapirs might diffuse into the groundwater exfiltrating into the wetlands, due to the influence of double diffusive convection (DDC) processes (Diersch & Kolditz, 1998), and compromise the wetland biodiversity under increased groundwater abstraction rates (Figure 2b). These salt plume formations originate from the intrusive salt diapirs of the Zechstein formation (De Vries, 2007; Magri & Bregman, 2011).

Another threat to the nature reserve involves the groundwater abstractions for drinking water production from the semi-confined aquifers (Mendizabal & Stuyfzand, 2009; Mendizabal *et al*., 2011) at two locations adjacent to the brook valley (Figure 2). These may change the natural groundwater flow patterns, which in turn may affect the wetland vegetation and biodiversity. Such impacts have been reported for European wetlands (e.g. Wassen et al., 1990; Schot & Van der Wal, 1992; Grootjans *et al*., 1993).

Although the Drentsche Aa nature reserve has been widely studied, uncertainties remain, i.e. regarding the reliability of the simulated flow patterns and possible up-coning of salt plumes. The accuracy of the groundwater simulation models depends on the underpinning assumptions and the availability of adequate data. The ecohydrological studies using plant species occurrence as indicators for groundwater flow systems may disregard the time lag in the response of plant species following groundwater flow changes due to e.g. buffering of soil water quality due to the buffering processes in the soil.

Simulated groundwater flows may be validated by independent hydrological tracers, such as chloride and natural isotopes (Schot & Molenaar, 1992; Gibson *et al*., 2005; Mayer *et al*., 2014). The natural isotopes used as tracers in the ecohydrological research related to groundwater, have been mostly limited to the stable isotopes of oxygen and hydrogen (e.g. Schot & Wassen, 1993; Isokangas *et al*., 2017). Radioactive isotopes, especially radiocarbon, are less commonly used due to practical reasons, e.g. sample volumes and analysis costs (Mook, 2006). In the study area, the radiocarbon age dating of groundwater may provide insight into the residence times which reflects the groundwater flow systems affecting the wetland vegetation. Young groundwater will generally reflect the local flow systems with recently infiltrated water from the vicinity and possibly showing the human pollution signs in their ionic composition. Old groundwater may, however, indicate the deep groundwater flow from sub-regional to regional systems, which would have recharged long ago showing enhanced mineral dissolution and free from human pollution. Additionally, deep groundwater affected by the DDC near the salt domes would show lower ^{14}C activity, and enriched $\delta^{18}O$ values and/or high salinity from the evaporites present in the salt diapirs. Stable isotopes may also indicate increased stable isotope values as a result of increased evaporation during slow infiltration through peat layers, as compared to present-day rain water, or signal different rain water isotope characteristics in ancient recharge water.

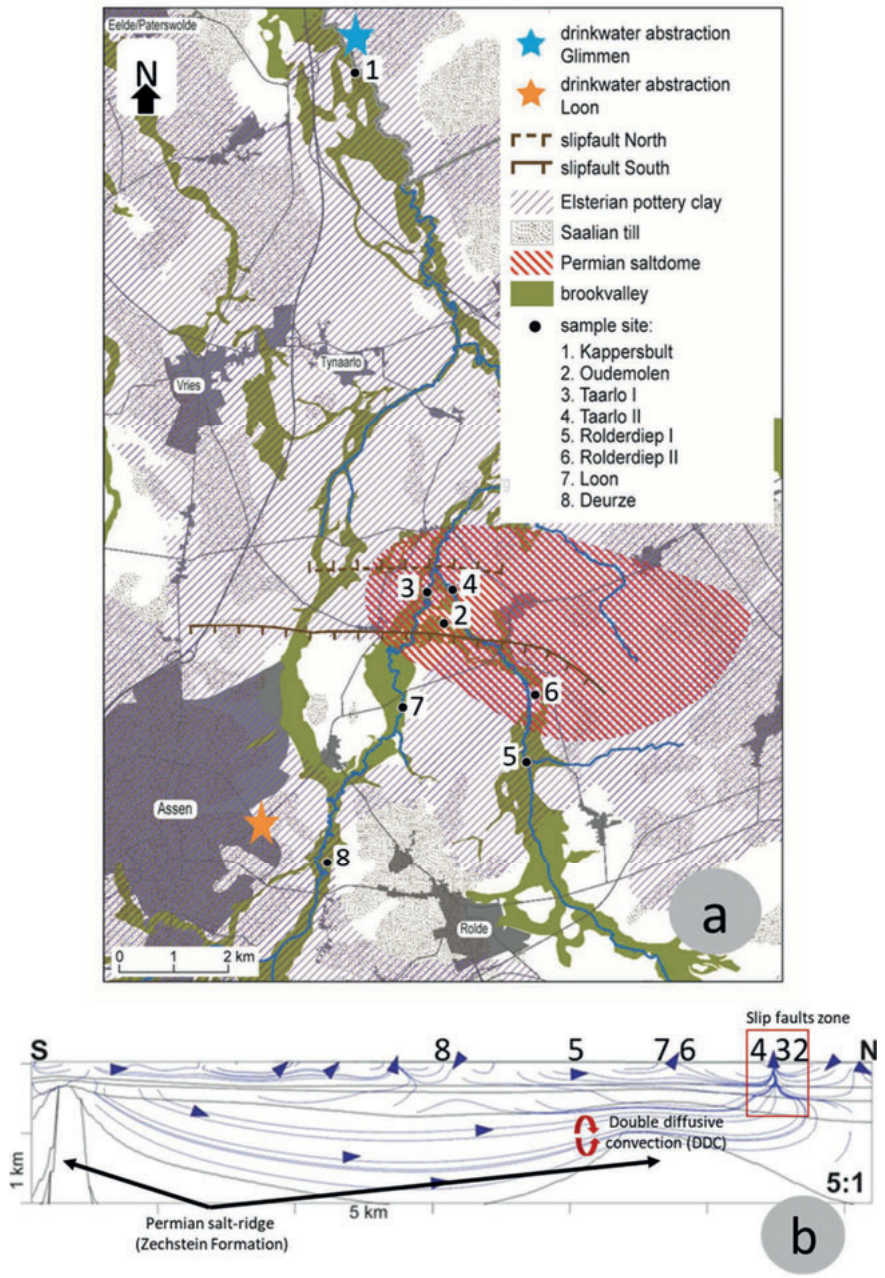

Figure 2. Groundwater sampling sites and geological features that control the regional, sub-regional and local flow patterns in the groundwater (a), simulation model results show the effect of the double diffusion convection, which affects groundwater reaching the surface (b).

This study uses groundwater isotopes in the Drentsche Aa brook valley to validate (i) the origin of groundwater flows to the fen peatlands as indicated by the model simulations by Magri and Bregman (2011) and by ecohydrological studies (e.g. Everts & De Vries, 1991; Grootjans *et al*., 1993 and Van Diggelen *et al*., 1995), (ii) the influence of groundwater abstractions on the groundwater flow, and (iii) the possible salination of shallow groundwater in the nature reserve by up-coning water from salt diapir evaporites. Furthermore, the study aims to assess restoration success in light of these investigations.

Study Area

The Drentsche Aa brook valley is the best-preserved brook valley landscape in the Netherlands (53°1'52.18"N. 6°38'17.10"E, Figure 3). Almost all the streams still meander in a natural way and the heathlands, fen meadows, forests and cultural aspects of the landscape are still in good condition and were partly restored to a former state (Bakker *et al*., 1980). The total catchment area of the Drentsche Aa is about 30,000 ha. Out of these, only 3,500 ha are managed to restore the semi-natural landscape of c. 1900. The topography of the landscape consists of a plateau at a height of about 28 m AMSL in the upper reaches, with the brook valley following the topographic relief to reach the height of about 0 m AMSL in the lower reaches at Kappersbult.

According to De Vries (2007), the rainfall averages in the Netherlands are relatively constant with a precipitation surplus of 250-300 mm a year that mostly falls during winters. The fresh groundwater flows in the eastern parts of the Netherlands, including the Drentsche Aa valley, are within the Plio-Pleistocene sandy aquifer. This aquifer is mostly unconfined, with the thickness ranging between 150-250 m in Drenthe (De Vries, 2007; Mendizabal *et al*., 2011). The aquifer sediments are mainly medium-sized, with intercalation of finer sediments (De Vries, 2007). The Breda formation is a clay layer of marine origin that exists at a depth of 150-250 m in Drenthe, which represents the hydrological basis of the fresh water systems (De Gans, 2007). The sub-regional and regional groundwater flows are controlled by four elements: slip-fault systems that border a tilted tectonic block (Smit *et al*., 2018), the Zechstein salt diapir, the interspaced lacustro-glacial Elsterian clay layers (Peelo 1 and Peelo 2 formations), and the Saalian tills (boulder clay) (Figure 2a). The slip-faults are difficult to trace due to (un)consolidation of the sediments (De Gans, 2007); however, it has been improved by new interpretation techniques: such as extrapolation of deep faults in 3D and SKY-TEM data (Smit *et al.*, 2018). Bregman *et al*., (2015) indicated that the faults influence the morphology of the surface area, as well as the functioning of the regional hydrological systems which is based on top of the Zechstein Formation. This formation is strongly undulating with salt diapirs present in some areas.

METHODS

Selected sites

We selected eight study sites based on four hydrogeologic drivers and/or controllers: traced fault structures, Zechstein salt diapir depth, the Saalian tills (boulder clay) and Peelo-I and II clay formation(s) (Figure 2). The fault structures were obtained from Bregman *et al*. (2015). The thickness and locations of the Zechstein and Peelo formations in the study area were obtained via "Dinoloket", which is an online platform for 2D and 3D models of geological layers in the Netherlands (Dinoloket, 2014).

The following eight study sites were selected (Figure 2a):

Lower reach

The first one was Kappersbult in the lower reaches of the valley. It has a 6m-thick peat layer that indicates paleo groundwater exfiltration, although it was identified as an infiltration area when investigated by Van Diggelen et al. (1994). Restoration measures were applied to allow flooding in the Kappersbult reserve, but the effects of drainage by agriculture and water abstraction could not be prevented (Bakker *et al*., 1980; Van Diggelen *et al*., 1994). Furthermore, it was indicated as an infiltration area by groundwater flow simulation, due to the groundwater abstraction from the station in Glimmen (Figure 2) (Magri & Bregman, 2011).

Middle reach

Six sites were investigated: Oudemolen, Taarlo-I and -II, Rolderdiep-I and -II and Loon. In this area, the fault structures are traced in the northern part of the area. On top of the raised tectonic block, which is slightly sloping to the north and borders with the two slip faults (Figure 2a) (Smit *et al.,* 2018). The Peelo-1 layer is present at Taarlo-II at a depth of about 10 m below the surface and Peelo-II layer at a depth of about 42 m below the surface. On top of the raised block, the peat layers have a thickness of 1.5 meter in the small river valley. The situation in this location is in strong contrast to Loon and Rolderdiep-I. These two sites are just above a lowered tectonic block and part of the rim syncline of the Anloo salt dome. At Loon, only the Peelo-2 layer is present at the depths of about 40-50 m below the surface. The peat thickness in this part of the study area with a broad valley reaches up to 6.5 m. The differences in geology and morphology in this part of the study area and the downstream part on top of the (raised) tectonic block are also reflected in the hydrological situation with strong seepage. In spring, this part of the study area is impassable because of floating peat layers caused by stagnation of drainage. Loon, is described by Grootjans et al. (1993) as a valley with groundwater exfiltration from the sub-regional groundwater system. However, the groundwater simulations indicated the influence of groundwater abstraction from the nearby pumping stations, i.e. Assen (Figure 2), which could have changed the groundwater flow paths (Magri & Bregman, 2011). All of these sites, except for Oudemolen, receive higher rates of groundwater discharge, ranging from 1.4 to 4.2 mm/day (Grootjans *et al.,* 1993). Oudemolen, is a small bog

situated in a heathland within an infiltration area (Grootjans *et al.,* 1993). It is characterized by very low productivity and only receives acidic rainwater poor in minerals (Van Diggelen *et al.*, 1995). The site has a podzolic B-horizon that prevents rapid infiltration of precipitation water.

Upper reach

Deurze is located in the upper reaches of the Drentsche Aa valley. The depth of the Peelo-I layer is about 10 m from the surface, where it prevents deep groundwater exfiltration (Grootjans *et al.,* 1993; Van Diggelen *et al.,* 1995). The seepage intensities of groundwater were estimated to be around 0.7-1.4 mm/day (Grootjans *et al.,* 1993). This area was indicated by the model to be limited to local groundwater flows, due to the shallow depth of the Peelo Formation (Magri & Bregman, 2011).

Groundwater sampling

We installed Poly-Vinyl-Chloride (PVC) piezometers using a hand auger. Each piezometer had a 20-cm filter at the bottom. The piezometers were installed at each site at a depth of 1 m in the organic soil and underlying mineral soil, depending on the thickness of the peat. At the Ta-II site, we sampled water from a provincial well (reference number: B12D0281). This well had 8 piezometers at different depths up to 95 m. We sampled water at 5 depths: F2, 9 m; F3, 17 m; F4, 40m; F5, 58 m; F7, 82 m; and F8, 95 m. We also sampled the surface water in the streams at Kappersbult and Taarlo. All the pipes were flushed a day before sampling. The samples were collected at the end of October 2014, December 2014 and January 2015. The samples were stored in polyethylene bottles of 50 and 100 ml for chemical analyses, and in 30 ml bottles for oxygen and deuterium isotopes. The samples for radiocarbon dating were collected in 500 ml dark glass bottles. All the samples were stored at the temperatures between 4 and 10°C.

Laboratory analyses

Isotopes

Radiocarbon dating

Dissolved Inorganic Carbon (DIC) in the samples was extracted and trapped into CO_2 gas, which was then converted into graphite. An Accelerator Mass Spectrometer (AMS) was used to count the carbon activity per second. The results are presented as ^{14}C %, which is the sample activity compared to a reference material with a known activity: $^{14}C_{sample} = (^{14}C_{measured} / {}^{14}C_{reference})$ % (Mook, 2006).

Stable isotopes ($\delta^{18}O/\delta^{2}H$)

The water samples were combusted and trapped into CO_2 gas, which was then calibrated with the CO_2 level of a reference material. The CO_2 content was then measured using a Dual Inlet Isotope Ratio Mass Spectrometry "DI-IRMS" (Meijer, 2009), and standardized using the Vienna Standard Mean Ocean Water Reference "VSMOW", which has a set reference value of ocean water at 0 ‰ (Mook, 2006).

The quantification of the stable isotopic elements in a sample is based on comparing the measured sample to a standard with the following equation:

$$\delta_{sample} = (R_{measured} - R_{reference}) / R_{reference}$$

where $R_{measured}$ is the ratio of the measured heavy isotope content to the lighter one in a sample; $R_{reference}$ represents the global reference sample, which is "VSMOW" in this case; and δ is the standardized measurement of the sample isotopic content.

Ion composition

The ion composition analyses were conducted at the Department of Experimental Plant Ecology at the University of Nijmegen in January 2015. The samples were filtered and analyzed. One sub-sample was used to measure the pH and total alkalinity by titration. Cations were measured by means of inductive coupled plasma spectrometry. Nutrients, as well as the chloride and sodium contents were analyzed using an auto-analyzer scalar (AAS). Total inorganic carbon (TIC) was measured with 1-ml fractions of the samples using an Infrared Gas Analyzer (ABB Advance Optima). The water samples with errors in the ionic balance of more than 10% were discarded.

Data analyses

^{14}C correction and graphical representation

Radiocarbon age is a function of the radiocarbon percentage in the samples, where the sample ages are inversely proportional to the radiocarbon percentage. The calculation of radiocarbon age is based on the following formula: sample age = -8033 ln ($^{14}C_{measured}$ /A_o), where A_0 is the initial activity of radiocarbon at infiltration (Geyh, 2000; Mook, 2006). We used two models for A_0: (i) Tamer's alkalinity model to estimate A_0 (Tamers, 1975) and (ii) the correction model by Vogel (1970) for the Netherlands, which assumes A_0= 85 pMC. The samples with the values >100 pMC are assumed to have been influenced by the bomb effect, indicating recent infiltration (after 1950). The samples with values < 100 pMC indicate possible infiltration before 1950.

Stable isotopes

In order to present the stable isotope data, we plotted the values of the $\delta^{18}O$ and $\delta^{2}H$ against the Global and Local Meteoric Water Lines (GMWL and LMWL). The data for the GMWL and LMWL were obtained from the isotope observation network of the International Atomic Energy Agency (IAEA/WMO); the LMWL data were measured at the Groningen station in the network (IAEA/WMO, 2017). The recent rainwater values for $\delta^{18}O$ range around -7.5 ± 0.5 ‰ (IAEA/WMO, 2017). These meteoric water lines were then used for the evidence of evaporation processes resulting from the exposure to the surface or high temperatures (Gat, 1996; Mook, 2006), which could indicate the DDC effect.

Ion composition and Principal Component Analysis (PCA)

In order to identify whether the water from various sources (different aquifers or DDC upwelling) exfiltrates into the fen peatlands at the Drentsche Aa, we used the multivariate statistical technique Principal Component Analysis (PCA). The *Factoextra* package in R was used to run PCA (Kassambara, 2017). The data input consisted of the water concentrations of 15 ions and TDS (16 variables in total) measured in 32 water samples (26 plus the 6 repeated samples).

RESULTS

Radiocarbon dating (^{14}C)

Table 1 shows the results from the radiocarbon dating and the corresponding calculated ages using both conventional calculation (Tamers, 1975) and the Vogel (1970) model. The samples that have the ^{14}C values higher than 85 pMC and bomb ^{14}C values were interpreted as indicating the infiltration areas (Kappersbult, Deurze, Oudemolen and Loon). The relationships of the ^{14}C values with $\delta^{13}C$ (Figure 3a) and the reciprocal of HCO_3 (Figure 3b) can be classified into two groups for the groundwater with ^{14}C between 45 to 65 pMC. The first group includes the samples from Taarlo II and Rolderdiep I, which have the $\delta^{13}C$ values between -14 to -16 ‰ and high HCO_3 content ($1/HCO_3$ lower than 0.006 mg/l). Meanwhile, the other group includes the samples from Taarlo I and Rolderdiep II.

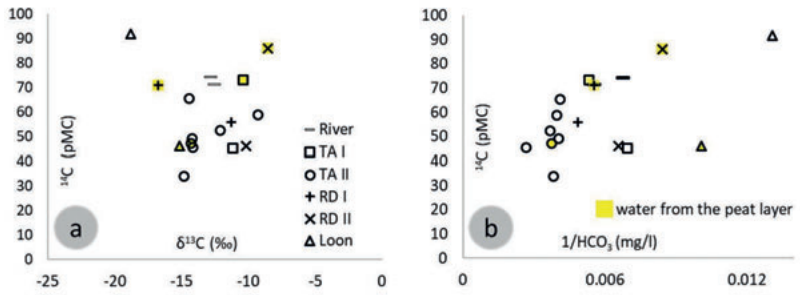

Figure 3. Relationships of the ^{14}C (pMC) content in the water samples with (a) $\delta^{13}C$ (‰), and (b) the reciprocal of HCO_3 (mg/l).

Stable isotopes (^{18}O and ^{2}H)

Figure 4 shows the results of the $\delta^{18}O$ and $\delta^{2}H$ values with the GMWL and LMWL. We identified three groups (A, B and C) based on their $\delta^{18}O$ values and their location with respect to the LMWL. Their $\delta^{18}O$ values were -7.5 to -7, -7 to -6.5 and -6.5 to -6 ‰ respectively. On the other hand, most of the samples in group A are above or right on the GMWL and the LMWL, the samples in groups B and C are mostly below the meteoric water lines, which indicates the possible effects of evaporation processes. Group A included the samples from Rolderdiep-II and Taarlo-I sites, while group B included the river water samples and some peat water samples from Rolderdiep-I and

II, as well as Deurze. Lastly, group C included all the samples from Taarlo-II, and the samples from the mineral soil at Rolderdiep-I (RD-Ib) and Kappersbult (KB-d). The samples collected earlier in October showed only slightly different values from the ones sampled later in January.

Table 1. Age of groundwater calculated using (1) the alkalinity correction model (Tamers, 1975), where the A_0 values ranged from 50 to 70%, except for L-a, and (2) Vogel's model, which assumes A_0= 85±5 % (Vogel, 1970). Site codes are: RD-I= Rolderdiep-I, RD-II = Rolderdiep-II, TA-I = Taarlo-I, TA-II = Taarlo-II, OM = Oudemolen, L = Loon, De = Deurze, KB = Kappersbult and SU= surface river water, while the peat samples codes are annexed with "a".

#	Code	Depth (m)	pH (at 20˚C)	^{14}C (%)	$\delta^{13}C$ (‰)	Tamers Model		Vogel model (A_0 = 85 %)
						A_0 (%)	Age (yrs)	Age (yrs)
1	Oudemolen	0.2	4.76	109.3	-10.2	--	--	--
2	TA-SU	0	7.59	71.01	-12.56	*55*	--	1490
3	TA-Ia	0.9	7.08	73.19	-10.41	*58*	--	1240
4	TA-Ib	3.5	7.38	45.26	-11.17	*55*	*1610*	5210
5	TA-IIa	1	7.30	47.32	-14.33	*55*	*1245*	4845
6	TA-IIb	3	7.42	65.39	-14.43	*55*	--	2170
7	TA-IIc F2	9	7.54	58.95	-9.3	*55*	--	3025
8	TA-IIc F3	15	7.58	102.2	-15.37	--	--	--
9	TA-IIc F4	25	7.50	49.08	-14.18	*55*	*940*	4540
10	TA-IIc F5	38	7.57	45.33	-14.16	*55*	*1600*	5110
11	TA-IIc F7	82	7.52	52.38	-12.1	*55*	*405*	4005
12	TA-IIc F8	95	7.75	33.82	-14.84	*55*	*4020*	7620
13	RD-Ia	0.9	6.93	71.03	-16.75	*64*	*0*	1485
14	RD-Ib	5	6.84	55.78	-11.26	*64*	*1135*	3485
15	RD-SU	0	6.53	103.7	-12.81	--	*0*	--
16	RD-IIa	0.9	7.1	86.05	-8.55	*58*	*0*	--
17	RD-IIb	3.5	6.74	46	-10.14	*68*	*3230*	5080
18	L-a	1	6.01	46.03	-15.14	*85*	*5070*	5070
19	L-b	4	6.99	91.8	-18.79	*58*	--	--
20	De-b	5.5	7.13	104.0	-20.8	*58*	--	--
21	KB-SU	0	7.75	73.9	-11.45	*52*	--	1160
22	KB-a	1	6.69	104.2	6.54	--	--	--
23	KB-c	3	6.87	106	-10.08	--	--	--
24	KB-d	6.3	7.16	108	-3.42	--	--	--

Ion composition

The PCA resulted in 16 principal components (PC) with the first two explaining 56.23 % of the data variation: 35.7% for PC1 and 20.5% for PC2, respectively. Figure 5 shows the ion variable loadings onto the principal components PC1 and PC2. The arrow lengths represent the magnitude of the variable loadings onto the PCA axes. Ion variables are grouped into clusters: cluster 1 contains most of the ions inversely proportional to PC1, cluster 2 contains the ions directly proportional to PC1 but inversely correlated to PC2 with the exception for NH_4, and cluster 3 contains the ions directly proportional to both PC1 and PC2. For instance, the TDS and the bicarbonate and calcium ions are best represented by the first two components. In contrast, NH_4 in cluster 2 is only explained by PC1, as an increase of a sample NH_4 content correlates with a positive position along PC1 and cannot be explained by changes in PC2.

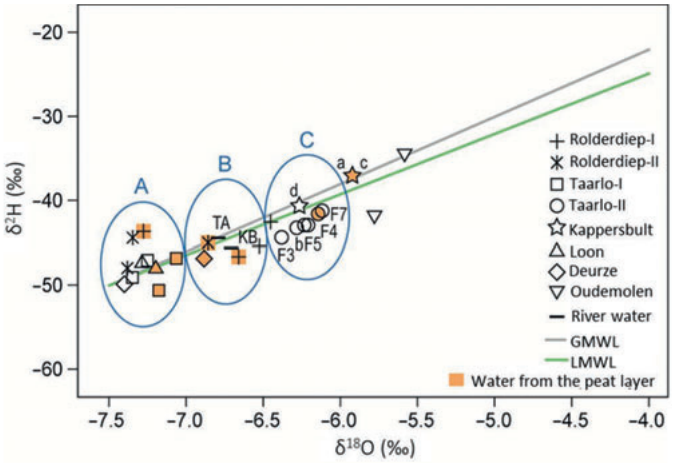

Figure 4. Stable isotopic compositions were plotted with GMWL and LMWL. The water samples collected from the peat layers are indicated with yellow filling.

Figure 6 shows the sample correlation to the first two PCs. Similarly, cos2 also indicates the quality of the sample representation and contribution to the PCs, e.g. the samples 16, 17, 19, 22 and 32 are best explained by the first two PCs, while the samples 5, 7, 11 and 31 are poorly explained. There are distinct differences in ion composition among the bog samples taken from Oudemolen (23 and 24), the deep sample from Taarlo-II (Ta-IIc F8, 22) and the sample from the mineral soil at Kappersbult (KB-D, 32). The samples from Oudemolen are inversely proportional to both PC1 and PC2, which have low ion composition, except for Fe, P and SO_4. The deepest sample at Taarlo-II (Ta-IIF8), however, is directly proportional to PC1 with a distinctive increase in chloride, sodium and potassium. Kappersbult was directly proportional to both PC1 and PC2, with distinctive increases in calcium, bicarbonate, magnesium and overall TDS.

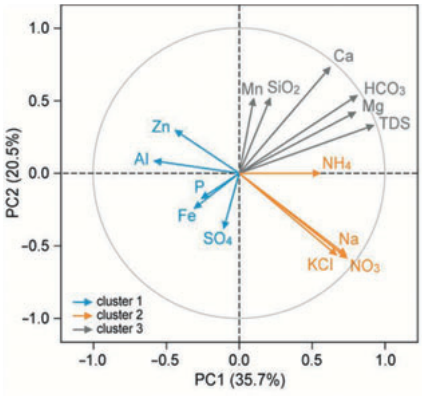

Figure 5. PCA plot of the macro-ionic content of the water samples. The arrow lengths indicate the variable loadings (ion composition) along the PCA axes, where the maximum of each loading is 1. The clusters indicate the proportionality relation between the variables and the PCA axes.

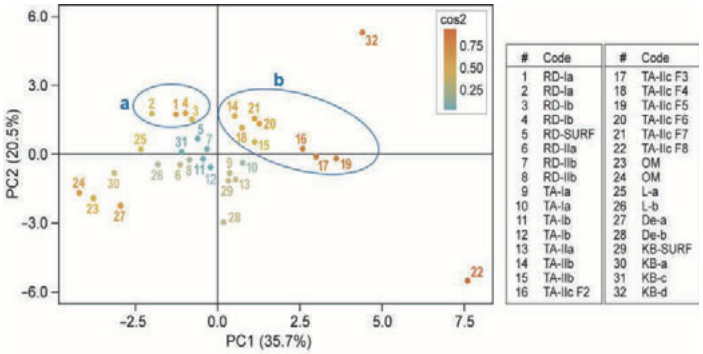

Figure 6. PCA plot of the sampling sites indicating correlations of the water samples to the first two PCA axes. The statistic cos2 indicates the quality of representation (contribution) of the samples by these two PCs. Site codes are: RD-I= Rolderdiep-I, RD-II = Rolderdiep-II, TA-I = Taarlo-I, TA-II = Taarlo-II, OM = Oudemolen, L = Loon, De = Deurze, KB = Kappersbult.

DISCUSSION

Isotopes and origin of water flow

Sub-regional groundwater exfiltration sites

We assumed that the samples with radiocarbon activities >100 pMC represent modern water. We observed that the shallow groundwater samples collected from the Taarlo (I and II) and Rolderdiep (I and II) sites indicate a possible exfiltration of water from the sub-regional aquifer. Using Han's graphical method, the sites with ^{14}C <60 pMC could be separated into two groups: the first group contains Taarlo-II and Rolderdiep-I and the second, Taarlo-I and Rolderdiep-II. These two groups in the ^{14}C data were based on the $\delta^{18}O/\delta^{2}H$ plot (groups A and C) and to a lesser degree, the PCA plots. These differences in stable isotopes could have resulted from the changes in the past climatic conditions during the time of recharge (Gat, 1996; Mook, 2006) or the surface conditions under which the infiltration took place, e.g. slow infiltration through peat layers (Mendizabal *et al.*, 2011). Therefore, it is more likely that the water flows exfiltrating into Taarlo-I and Rolderdiep-II are from similar sources but were influenced by different geochemical reactions from those at Taarlo-II and Rolderdiep-I. Taarlo-II and Rolderdiep-I could be also receiving water flows from the same sources.

Infiltration and local groundwater exfiltration sites

The groundwater samples under present-day infiltration regimes, post 1950, are identified by bomb ^{14}C (>100 pMC) as well as ^{14}C values higher than 85 pMC (Vogel, 1970). Additionally, the $\delta^{2}H$ and $\delta^{18}O$ values for these samples are similar to the rainwater values at the recharge time ($\delta^{18}O$ = -7.5 ± 0.5 ‰ for The Netherlands), which indicates the dominance of modern water (Clark & Aravena, 2005; Mook, 2006). Such values were observed in four sites in this study: Oudemolen, Deurze, Loon

and Kappersbult. The first two are hypothesized already to reflect the infiltration and local system supply regimes; however, earlier studies indicated that Loon and Kappersbult should be supplied by sub-regional groundwater flows (Everts & De Vries, 1991; Magri & Bregman, 2011). Thus, the latter sites likely indicate groundwater abstraction influence on the natural groundwater flow systems.

Oudemolen reflects the sole dependency on rainwater supply. The chemical analysis of the water samples from the small bog at Oudemolen confirmed that this water is acidic (pH = 4.7) and poor in minerals. The low Cl^- content (~ 5-7 mg/l) also indicates rain water infiltration (Appelo & Postma, 2005). However, the stable isotope values indicate enrichment of $\delta^{18}O$ and $\delta^{13}C$ isotopes (5.8 and 10.2 ‰ respectively), which is due to evaporation as the precipitation is hampered by the impervious organic layer (Schot & Wassen, 1993). This site reflects a natural infiltration zone, which is isolated from the surrounding due to the podzol zone formation. Here, it reflects the water quality of rainwater/infiltration patterns. This pattern is then different for the other site, i.e. Deurze, Loon and Kappersbult, which reflect an anthropogenic influence.

The Deurze-b site in the upper reaches of the valley, which is also underlain by thick impervious Elsterian clay layers at shallow depths, is identified as being supplied by the phreatic groundwater flows from a local hydrological system (Magri & Bregman, 2011). The isotopic evidence indicate that the site is supplied by infiltration and local groundwater flow. For instance, the samples show bomb ^{14}C values (>100 pMC) as well as the $\delta^{13}C$ content, which shows a shift towards enrichment by organic material (-20 ‰). However, the groundwater has a higher mineral content, especially in Na^+ and Cl^-. The nutrient content of this site is higher than in the rest of the study sites (NO_3^- > 2.5 mg/l), which indicates possible pollution due to the agricultural activities (Schot & Van der Wal, 1992).

As for Kappersbult and Loon, ^{14}C the data also indicate that they are infiltration sites or locally supplied. Both these sites are situated close to the groundwater abstraction facilities in Glimmen and Assen, respectively. The hydrogeologic setting of these sites would suggest possible exfiltration of the sub-regional groundwater flows similarly to the Taarlo and Rolderdiep sites. Yet, the radiocarbon data in Kappersbult showed the values of bomb ^{14}C, indicating infiltration of water on the surface. The macro-ion composition showed the values of high Ca and HCO_3 compared with the other infiltration areas. This most likely resulted from the dissolution of the minerals from the deeper peat layers, due to infiltration of CO_2-rich groundwater from upper layers (Schot & Wassen, 1993; Brandyk *et al*., 2007). The released CO_2 enhances the dissolution of soil minerals, in our case Ca and HCO_3 (Appelo & Postma, 2005). Therefore, we can conclude that the flow regime has been changed, most likely by the activities of the groundwater abstraction facility near Glimmen (Van Diggelen *et al*., 1993).

The samples at Loon (both at depths of 1 and 4 m) had low concentrations of macro-ions. This was unexpected, since thick peat layers are present here at the depth of 3 m, and indicates strong seepage conditions in the past. The ^{14}C analysis of Loon showed a modern water signature of 91 pMC. Therefore, we argue that a change

in the water regime had also occurred at this site, in which an exfiltration area was shifted towards infiltration. The Loon site now likely receives the groundwater from a nearby extensive heathland infiltration area, Balloerveld. The existing groundwater abstraction facility near the city of Assen has apparently reduced the discharge of groundwater from the second aquifer and consequently increased the inflow of groundwater from more local groundwater systems. It confirms the effect of groundwater abstraction on natural groundwater flows, which was indicated by Magri & Bregman (2011). In their study, different scenarios were computed, which indicated that even lowering the groundwater abstraction from 6 mm^3 to 3 mm^3 did not stop the negative impact on the groundwater system.

Relic situations

There was one unexpected outcome of the ^{14}C measurements. On two occasions while sampling at Loon and Taarlo-II, we found older groundwater in the upper peat layer (at the depth of 1 m below the surface) compared with the groundwater in the underlying mineral sand deposits. We have interpreted this as the presence of older relic groundwater in the peat layer. Under the conditions of changed groundwater flows, sand deposits can react faster to the hydrological changes compared with thick organic peat layers.

Evidence of double diffusive convection (DDC)

The radiocarbon data indicate that the sample from the provincial well (B12D0281 at Taarlo-II) at a depth of 95 m has the lowest ^{14}C content, about 33 pMC. This makes the sample clearly distinct from the groups related to the samples indicating sub-regional groundwater flows. Furthermore, it deviates from the rest of the samples in the PCA plot (sample nr. 22; Figure 6), due to a water type change from $CaHCO_3$ to $NaHCO_3$. This sample, and some other ones all south of the slip-fault (Figure 2a) that were also sampled and reported in 1995 by the province of Drenthe (1995), are the only ones indicating the upwelling of the deep groundwater. It is likely to originate from below the, currently considered, hydrological basis of the regional groundwater, Breda Formation. Despite this, the DDC effect on the fen water quality cannot be confirmed at our sites, as the deep groundwater flows were not shown to mix with exfiltrating sub-regional/shallow flows near the surface. It would still be wise to take more measurements from other deep wells in the valley to check whether salt plumes could exist at the depths shallow enough to affect the vegetation communities at the surface.

CONCLUSIONS

The study area is part of the Ice Marginal Landscape with salt formations in the deeper subsurface. Due to the glaciological processes and geo-hydrological conditions, we expect that the results of our study are important not only for the Drentsche Aa area, but also for other countries and regions in the IML zone from the

Netherlands to Lithuania. We think that the results of our study contribute to a better understanding of groundwater flows as a base for nature conservation and other functions of the landscape.

The data indicated that the groundwater abstraction activities affecting these sites appear to have also affected the restoration success in various sections of the study area. The analysis of 30 years, in 10-year lapses, of vegetation data from 1992 to 2012 indicated good recovery after restoration management in the areas not affected by the abstraction of groundwater, e.g. Taarlo and Rolderdiep (Appendix 2) (Bakker et al., 2015). In contrast, the areas that were affected did not show similar increases in target species, e.g. Kappersbult. Unlike other sites, Kappersbult showed poor results in the restoration of the hydrological conditions and its target species. Although the groundwater abstraction has been reduced, the groundwater flow simulations of lowered abstraction scenarios indicate that the impact still will have a negative influence on the wetland vegetation in future (Magri & Bregman, 2011). However, it could be that the impact of the taken measures would simply take more time to recover. Despite the measures to reduce drainage in the area south of the fault zone, between Loon Oudemolen and Rolderdiep, which leads to drainage and floating of peat, the groundwater system seems to be still in unbalance. However, recovery of the groundwater system seems to be successful.

It is necessary to follow up on the inter-relationship of the deep saline groundwater flows to the relatively shallow fresh groundwater systems. Hence, further monitoring of the groundwater quality in combination with study of the vegetation development is advised.

ACKNOWLEDGEMENT

We would like to acknowledge StaatsBosBeheer (Dutch State Forestry) for allowing us to sample groundwater, the Province of Drenthe for sampling the deep wells, Christian Fritz for analyzing the macro-ion data at Radboud University, Harro Meijer and Hans van der Plicht for allowing the isotope analysis to be conducted at CIO, Groningen, and Rien Herber for his help with this project.

APPENDIX

Appendix 1. Full results of the Ion composition analyses of the water samples. TDS = total dissolved salts. (*) samples taken in October 2014.

#	Code	Depth	pH	Alk. 10^6	TIC	HCO_3	SO_4	Cl	NO_3	P	Ca
		(m)	(20° C)	eq/L	ppm			(mg/l)			
1	RD Ia*	1	6.93	3362	5001	180.5	0.7	10	0.6	0.02	61
2	RD Ia*	1	6.84	2916	4877	167.7	1.2	12	0.7	0.05	57
3	Rd Ib*	5	7.30	3468	4738	196.1	0.6	12	0.8	0.03	56
4	RD Ib	5	7.16	3365	5194	206.4	0.3	5	0.3	0.03	54
5	RD SURF	0	6.53	2456	5269	142.1	0.9	20	1.2	0.03	42
6	RD IIa	1	7.10	2079	3052	118.8	19.3	16	1.0	0.03	41
7	RD IIb*	3.5	6.74	2694	4712	152.2	0.9	17	1.0	0.03	45
8	RD IIb	3.5	7.22	2520	3335	135.1	18.2	16	1.0	0.02	43
9	TA SURF	0	7.59	2621	4136	180.7	14.6	28	1.7	0.04	50
10	TA Ia*	1	7.08	3368	4837	187.1	10.6	20	1.2	0.03	60
11	TA Ia	1	7.24	2925	4687	191.0	4.8	14	0.9	0.10	52
12	TA Ib*	3.5	7.37	2600	3410	143.7	18.7	19	1.2	0.02	48
13	TA Ib	3.5	7.36	2673	3913	164.0	16.3	25	1.5	0.02	50
14	TA IIa	1	7.32	4473	6449	268.1	0.5	10	0.6	0.03	69
15	TA IIb	3	7.42	3954	5729	243.4	0.3	20	1.3	0.02	59
16	TA IIc F2	9	7.54	4163	5837	253.1	2.8	39	2.4	0.02	73
17	TA IIc F3	17	7.58	4135	6029	263.0	3.4	47	2.9	0.02	72
18	TA IIc F4	26	7.50	3808	5751	247.9	0.3	12	0.7	0.02	60
19	TA IIc F5	40	7.57	4250	8633	376.3	0.2	49	3.0	0.02	60
20	Ta IIc F6	58	7.44	4355	6410	273.3	0.1	15	0.9	0.01	70
21	TA IIc F7	82	7.52	4264	6278	271.2	0.2	13	0.8	0.01	72
22	TA IIc F8	95	7.75	4251	5897	262.3	0.2	115	7.1	0.04	35
23	OM*	0.2	4.73	1512	425	0.4	2.6	5	0.3	0.06	1
24	OM	0.2	4.76	1950	408	0.4	2.0	7	0.5	0.03	1
25	L-a	1	6.91	1751	2772	99.3	8.4	5	0.3	0.05	29
26	L-b	4	7.13	1593	1939	76.4	21.3	10	0.6	0.02	27
27	De-a	1	6.01	3883	842	11.7	2.7	37	2.3	0.04	8
28	De-b	5.5	6.99	1493	2120	79.0	50.6	40	2.5	0.07	39
29	KB SURF	0	7.75	2309	3322	147.7	15.4	28	1.7	0.01	44
30	KB-a	1	6.69	1579	2617	81.5	3.2	10	0.6	0.05	32
31	KB-c	3	6.87	3025	5051	176.8	2.5	22	1.4	0.17	54
32	KB-d	6.3	7.16	7461	11205	445.8	1.8	21	1.3	0.02	131

No.	Na	K	Mg	Mn	Fe	Al	Si	NH_4	Zn	TDS
						mg/l				
1	7.5	0.3	4.6	0.25	0.40	0.25	12.01	0.005	0.26	279
2	8.4	0.3	4.5	0.25	0.43	0.35	12.00	0.01	0.44	265
3	9.9	1.2	5.7	0.33	0.04	0.35	12.05	0.02	0.22	295
4	4.9	0.7	5.6	0.33	0.02	0.30	11.88	0.02	0.12	290
5	11.0	1.6	4.8	1.11	0.05	0.20	5.48	0.13	0.15	230
6	9.0	1.2	4.2	0.00	0.06	0.18	11.11	0.02	0.10	222
7	10.1	2.6	4.7	0.69	0.56	0.15	7.95	0.01	0.12	242
8	8.8	1.1	4.3	0.07	0.07	0.12	10.82	0.03	0.10	238
9	15.3	2.2	5.1	0.00	0.16	0.12	8.97	0.03	0.10	308
10	14.1	3.2	4.4	0.02	0.02	0.08	11.42	0.28	0.13	312
11	10.5	1.8	4.1	0.01	0.80	0.08	10.33	0.03	0.09	290
12	12.3	2.4	4.1	0.12	0.07	0.07	10.13	0.05	0.17	260
13	18.1	2.7	4.1	0.00	0.02	0.05	10.02	0.08	0.07	291
14	9.8	0.7	7.5	0.15	0.06	0.09	8.27	0.03	0.13	375
15	19.2	2.0	6.5	0.08	0.01	0.05	9.59	0.03	0.15	362
16	17.7	2.1	7.5	0.13	0.02	0.04	9.86	0.26	0.06	408
17	26.2	2.0	7.1	0.14	0.01	0.03	10.10	0.24	0.06	434
18	12.9	1.3	6.0	0.21	0.04	0.06	9.60	0.25	0.10	351
19	41.0	1.9	5.8	0.12	0.02	0.04	9.56	0.27	0.07	547
20	12.6	1.2	6.3	0.18	0.06	0.03	9.56	0.22	0.08	389
21	9.5	1.1	6.6	0.13	0.03	0.05	10.01	0.21	0.08	384
22	105.9	5.4	6.7	0.04	0.05	0.04	7.47	0.94	0.07	545
23	5.9	0.6	0.7	0.02	0.34	0.23	1.47	0.71	0.24	19
24	6.6	0.6	0.6	0.03	0.26	0.18	1.42	0.16	0.37	22
25	5.4	0.4	2.1	0.00	0.49	0.10	15.38	0.06	0.18	166
26	10.8	0.8	2.0	0.00	0.26	0.07	16.38	0.05	0.12	165
27	17.8	0.8	1.2	0.03	3.40	0.40	9.50	0.06	0.22	95
28	21.2	2.6	6.8	0.01	5.97	0.03	8.31	0.07	0.14	257
29	15.4	2.2	4.9	0.00	0.22	0.04	8.16	0.04	0.09	267
30	5.0	0.3	2.2	0.10	10.96	0.12	8.24	0.06	0.23	155
31	11.0	0.4	4.7	0.40	5.39	0.09	9.15	0.16	0.20	288
32	13.4	0.7	9.5	0.70	0.14	0.03	17.30	1.17	0.37	643

Appendix 2. Vegetation mapping data from 1982-2012 to assess the success of restoration activities (Adapted from Bakker *et al.,* 2015). The vegetation type density per area is shown at four sites: Kappersbult, Gasterense Diep and Oudemolense Diep (Taarlo and Rolderdiep sites) and Deurzer Diep (Deurze).

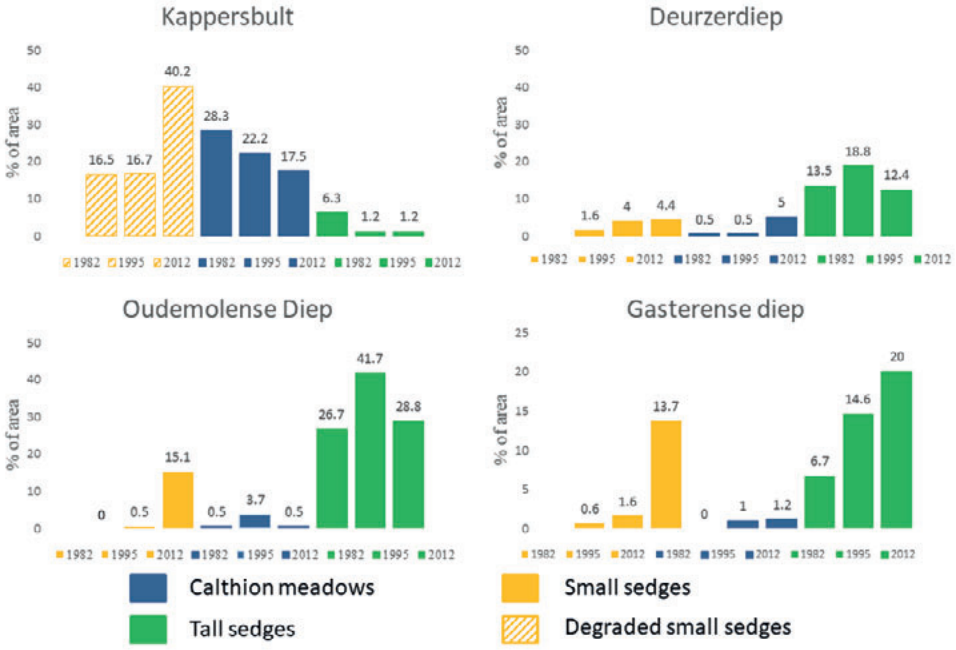

6

Natural isotopes support groundwater control over mire types in Slitere National Park*

Slitere National Park in Latvia is home to rich fens with many endangered and threatened plant species. This study aimed to address how the hydrological systems affect vegetation biodiversity in the mire systems of the park: the base-rich inter-dune mires and extremely base-rich calcareous fens. Groundwater samples from these areas were collected for measurements of ion composition and natural isotopes of C, H and O. Also, we simulated groundwater flow paths from the highest local topographical point (a nearby sandy plateau) to the sea, and calculated the residence times of these groundwater flows. The results show that the inter-dune mires are supplied by a mixture of local and regional groundwater systems. The groundwater supply at one of the inter-dune mires was dominated by local groundwater flow from adjacent dunes, but we also detected a small input of calcareous water. This dominance by local groundwater may have resulted from the presence of drainage ditches and a small stream that drains into the Baltic Sea. In contrast, the extremely base-rich fens were found to be solely dependent on regional groundwater flows, which likely discharge at the plateau foothills due to presence of fault structures. Thus, the mires in Slitere National Park are not as pristine as previously thought. Drainage activities might have affected the original hydrological flow paths. Further research on the extent of these changes is recommended to preserve the endangered species and high biodiversity of these fens. Also, tracing the origin of groundwater flows might require further investigation into the larger landscape beyond the plateau.

* This chapter is submitted as: Elshehawi, S., Spinoza, A.V., Schot, P., Aleksans, O., Pakalne, M., Wolejko, L., Grootjans, A. (in review) Natural isotopes support groundwater origin control over mire types in Slitere National Park, Latvia.

INTRODUCTION

Peatlands are wet landscapes with water tables sustained at or near the surface for extended periods of time (Joosten & Clarke, 2002). When these sustained water tables allow for further accumulation of peat, the resulting wetlands are called mires (Mitsch & Gosselink, 2000a; Joosten & Clarke, 2002). Peat is formed through accumulation of senescing vegetation that does not completely decompose, with organic matter constituting about 30% or more of the total volume (Clymo *et al.,* 1998). Mires, hence, act as important carbon sinks in the carbon global cycle. Furthermore, mires provide refuge to rare and endangered wetland species, e.g. mires in Slitere National Park (Pakalne and Kalnina, 2005).

Slitere National Park is situated in northwestern Latvia. It consists of different wetland types ranging from an active raised bog (Bažu mire) to inter-dune fen complexes and calcareous fens (Figure 1). The park is part of the coastal lowland region of Latvia and stretches along the Baltic Sea coastline (Pakalne and Kalnina, 2005). The mires developed on former Littorina sea lagoons, where sea regression and high groundwater levels allowed for infilling of inter-dune depressions around 4700 years ago (Kalnina *et al.,* 2014). A high proportion of the landscape in Slitere National Park consists of protected habitat types (Natura 2000), representing Europe's most valuable dune forests and mires. This classification indicates that the landscape structure is considered to be untouched, and is thus used as a reference area for conservation and restoration purposes at the international scale (Wolejko *et al*., in review).

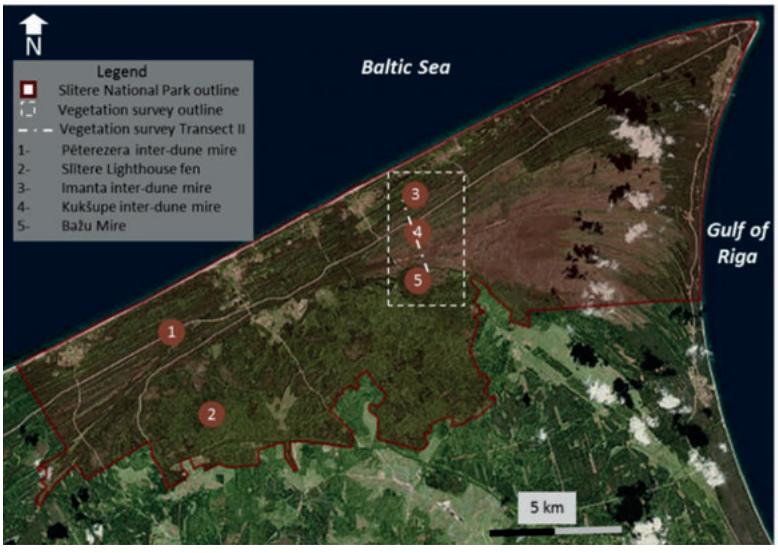

Figure 1. Study area topography and distribution of mires in Slitere National Park. Study sites: 1—Peterezera interdune mire, 2—Spring calcareous fen near Slitere Lighthouse; 3—Imanta interdune mire; 4—Kuksupes interdune mire; 5— Bažu Mire. Map source: GIS_Latvija10.2., LiDAR DEM, LU ĢZZF (Adapted from Wolejko *et al.,* in review).

Hydrology plays an important role in sustaining the function of mires and, therefore, their biodiversity (Gilvear & Bradley, 2009). Wolejko *et al.* (in review) showed that one of the inter-dune mires (Kuksuspes) is dependent on exfiltration of base-rich groundwater flowing from south of the mires to the north. This type of base-rich groundwater flow is important for sustaining high vegetation biodiversity (Grootjans *et al.,* 1993). Furthermore, Wolejko *et al.* (in review) hypothesise that these inter-dune mire systems also depend on exfiltration of base-rich groundwater flowing from other parts of the area, i.e. the bordering plateau.

This paper aims to sketch the groundwater systems in the area that are sustaining the mire landscapes. An ecohydrological approach is used, a quick scan, to analyse the groundwater flows in the area that sustain the natural wet landscapes of this park (Grootjans & Jansen, 2012). This was done using the natural isotopes of C, H and O and macro-ions to verify the water quality types associated with each mire types. This was also coupled with groundwater simulation.

METHODS

Study area

Slitere National Park is bordered by the Baltic Sea and the Gulf of Riga in the north and east respectively, and by agricultural and urban landscapes in the south and west. Furthermore, the area to the south is located on the plateau of the former Littorina coastline, which forms a plateau now (Fig. 1). As this plateau represents the highest point in the local topography, the upper reaches of the groundwater flow are found here. Below the plateau's cliffs, a gentle downward slope continues for a few kilometres landwards forming the middle reaches, and this is where the calcareous fens are currently present. The north parts of the park are home to sand-dune ridges that extend in the east-west direction. Between the ridges, there are inter-dune valleys that have accumulated peat over the years, depending on the level of groundwater supply (Kalnina *et al.,* 2014). Some of these fens have expanded further laterally over the ridges, thus becoming dependent mainly on rainwater, e.g. Bažu mire (Pakalne & Kalnina, 2005; Kalnina *et al.,* 2014).

Precipitation in Slitere National Park averages around 600–700 mm yr^{-1}, with the highest rate occurring during autumn (Remm *et al.,* 2011). Glacial sand deposits form the underlying unconfined Quaternary aquifer (Juodkazis, 1994; Virbulis *et al.,* 2013). This unconfined aquifer is intercalated with a series of inter-spaced clay and sandy moraine sediments, which form aquitards at different depths (Zelčs, *et al.,* 2011, Saks *et al.,* 2012, Virbulis *et al.,* 2013). A regional aquifer is present below the unconfined sands, and it consists of sedimentary sandstone rocks (D2ar# aquifer, See Appendix 1; Virbulis *et al.,* 2013).

Site selection and sampling

Fourteen sites were selected to collect groundwater samples (Figure 2). Four of these sites were established along a south-north transect within a single inter-dune fen, the

Peterezera mire (Pe.ID1 to Pe.ID4). Four other sites were established to the south (Pe.IDS1 and Pe.IDS2) and north (Pe.IDN1 and Pe.IDN2) of the Peterezera mire, with two in each cardinal direction. One site was established in the Kuksupes mire (Ku.ID), which intersects the area studied by Wolejko *et al.* (in review). This site was established in the southern part of mire where we hypothesised that groundwater exfiltration is taking place. Two sites were established in the calcareous fen near the old coast line of the Littorina Sea (Ca.Fen 1 and 2). Three sites were selected along the cliffs that are remnants of the old coast line: a spring mire on the cliff (Cliff.Spring), an open water hole resulting from excavations in a sand quarry on top of the cliff (Cliff.Quarry) and a well that supplies groundwater to a household on the cliff (Cliff.well).

Twelve groundwater piezometers were installed. The piezometers were made of polyvinylchloride (PVC) tubes with a 20-cm screen at the bottom. A Russian hand auger was used to drill the holes to insert the piezometers. Two sites at Peterezera had the screens installed at two depths: one in the mineral soil (Pe.ID2 and Pe.ID3) and one in the peat layer at around 20 cm from the surface (Pe.ID2sh and Pe.ID3sh).
We did not install piezometers at two sites: Cliff.Quarry and Cliff.Well. At these sites, water samples were collected from a drinking water well and an open water hole, respectively. Appendix 1 lists the sampling points, their codes and screen depths.
All the piezometers were flushed three to four days before sampling, which took place during July 2017. The sampling was conducted using a hand pump. Sixteen samples were collected in 100- and 50-ml polyethylene bottles for cation and anion composition analysis, respectively, and in 30-ml dark glass bottles for stable isotopes analysis. Eleven samples were collected in 500-ml dark glass bottles for carbon isotopes. All the bottles were filled to the brim and kept in a refrigerator at 4 °C.

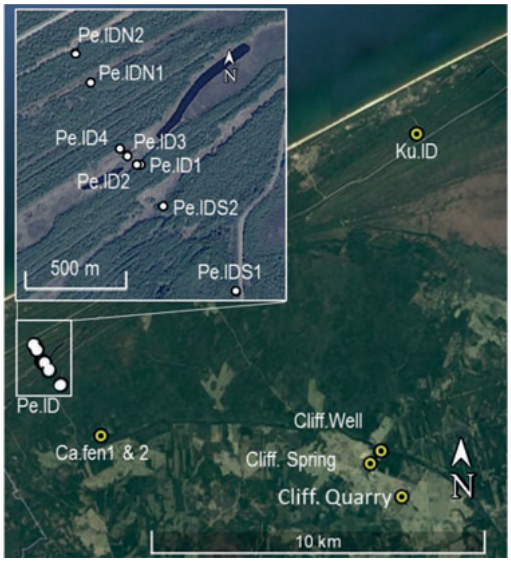

Figure 2. Water sampling sites in Slitere National Park.

Ion composition

Analysis of the ion composition was conducted at the Laboratory of Environmental Ecology at the University of Radboud in Nijmegen, the Netherlands. Sample pH and total alkalinity were measured by titration. Bicarbonate values were derived from the total alkalinity. Ions (Ca, Fe, K, Mg, Mn, Al, P, SO_4, Si, Zn) were measured using an inductive coupled plasma mass spectrometer (ICP-MS). Nutrients (PO_4, NO_3 and NH_4), chloride and sodium contents were measured using an atomic absorption spectroscopy (ASA) auto-analyser (Skalar, Breda, the Netherlands).

Stable isotopes

Measurements of the $\delta^{18}O$ and $\delta^{2}H$ in the water samples were conducted at the Laboratory for Isotope Research (CIO) at the University of Groningen, the Netherlands. The CO_2 gas in the samples was trapped after combustion. The gas was then analysed by Dual Inlet Isotope Ratio Mass Spectrometry (DI-IRMS) following Meijer (2009). The results were calibrated using the Vienna standard mean ocean water reference (V-SMOW), and reported as an isotopic ratio of the reference material (δ) in permil (‰) (Mook, 2006). The global meteoric water line (GMWL) to plot the data was obtained from the international atomic energy agency (IAEA, 2017).

Radiocarbon dating

The carbon isotopes were also analysed at the CIO laboratory. The samples' dissolved inorganic carbon content (DIC) was extracted from the CO_2 gas in the samples and turned into graphite sheets. Radiocarbon (^{14}C) contents were then counted using the atomic mass spectrometer (AMS), while the stable carbon isotope $\delta^{13}C$ was analysed using the DI-IRMS. The ^{14}C results were reported as uncorrected values in percent modern carbon (pMC) with respect to reference material V-PDB (Mook, 2006). Meanwhile, $\delta^{13}C$ results were reported in respect to the V-SMOW reference material in permil (‰).

RESULTS

Ion composition

The samples in the upper (plateau water samples) and middle (Ca.fen1 and 2 and Pe.IDS1) reaches were found to have high calcium and bicarbonate concentrations associated with pH values close to or higher than 7 (Table 1). In the lower reaches, only Ku.ID was found to have high calcium and bicarbonate concentrations associated with a pH higher than 7. Meanwhile, the dune south (Pe.IDS2) of the Peterezera inter-dune mire and the deep sample at its southern edge (Pe.ID2 and Pe.ID3) have intermediate calcium and bicarbonate concentrations and pH values close to 6.5. The rest of the samples in Pe.ID and its surrounding are dominated by silicate ions and generally lower total dissolved salts (TDS). The water collected north of Peterezera (Pe.IDN1 and Pe.IDN2) was more acidic, especially from the northeast dune sample, with pH = 5.64. Notably, iron concentrations higher than 2 mg l^{-1} were observed in the

samples taken from the sand layer underlying or close to peat accumulations, e.g. Pe.ID2 and Pe.ID3, Ca.fen1, Pe.IDN1 and 2, and Pe.IDS2.

The isohypse lines of the chloride concentrations along the Peterezera inter-dune transect show a diluted input of water from the dune at point Pe.ID1, while point Pe.ID2 was found to have an input of groundwater with higher chloride content (Figure 4a). The chloride content was found to be slightly diluted further up in the shallow layer at points Pe.ID2sh and Pe.ID3sh, and northwards at points Pe.ID3 and Pe.ID4. Similar patterns were observed for calcium concentrations, which were found to be higher at point Pe.ID2 by a factor of five than in the shallow samples (Figure 4b).

Table 1. Results of the ion composition (in mg l^{-1}) analysis in 16 groundwater samples from Slitere National Park.

No.	Code	Depth (cm)	pH	Anions (mg l^{-1})				Cations (mg l^{-1})								TDS (mg l^{-1})
				HCO_3	Cl	SO_4	Al	Ca	Fe	K	Mg	Mn	Na	Si	Zn	
1	Pe.IDN2	185	5.64	10	3.3	8.8	1.5	12	4.2	0.9	3.0	0.13	4.9	26	0.2	76
2	Pe.IDN1	120	6.02	12	5.3	5.5	1.5	16	3.0	1.4	3.0	0.07	6.5	35	0.4	91
3	Pe.ID4	85	6.08	11	4.1	4.9	0.8	17	1.4	0.9	3.5	0.23	6.5	19	0.4	71
4	Pe.ID3	200	6.52	71	3.7	1.0	0.1	48	0.0	0.7	7.8	0.02	5.4	26	0.3	164
5	Pe.ID3sh	20	6.18	37	4.4	3.4	0.4	24	0.3	1.9	6.2	0.00	5.8	26	0.2	110
6	Pe.ID2	355	6.82	117	5.8	6.5	1.8	76	5.9	2.2	19	0.05	6.3	21	0.2	263
7	Pe.ID2sh	20	6.14	23	4.9	8.7	0.2	18	0.2	0.8	5.2	0.00	6.0	19	0.2	93
8	Pe.ID1	190	6.47	15	1.2	1.2	0.2	11	1.4	0.4	2.5	0.67	2.4	10	0.1	47
9	Pe.IDS2	130	6.56	68	5.3	4.5	0.3	46	5.6	1.1	11	0.04	7.2	14	0.2	163
10	Pe.IDS1	85	7.25	365	188	8.8	0.1	249	0.1	4.6	29	1.08	113	17	0.2	976
11	Ca.fen1	65	7.49	219	6.7	3.7	0.1	107	4.1	2.0	25	0.01	6.3	14	0.2	389
12	Ca.fen2	200	7.66	196	9.1	15	0.1	100	0.1	3.0	22	0.00	6.5	6.5	0.2	359
13	Ku.ID	205	7.35	215	6.8	3.1	0.3	110	0.6	2.4	10	0.01	7.2	31	0.3	389
14	Cliff.Quarry	0	7.6	154	3.2	51	0.0	77	0.0	2.6	24	0.00	3.8	3.8	0.1	319
15	Cliff.Spring	20	7.73	318	8.7	41	0.1	182	0.0	1.7	34	0.00	4.4	14	0.1	605
16	Cliff.Well	>400	7.82	274	1.5	31	0.0	111	0.0	0.9	61	0.00	3.9	23	0.1	508

Stable isotopes

Regarding the stable isotope content of the groundwater samples, most of the samples were found to have $\delta\,^{18}O$ values between -11 to -10 ‰, and ‰ δ^2H values between -80 to -70 ‰ (Figure 5). More than half of the samples in this range are above the GMWL, while only 4 samples from that range are below this line, including most of the samples collected from the southern part of the Peterezera transect (Pe.ID1 and Pe.ID2). Only the sample collected from below the peat at Pe2 is above the GMWL. A linear regression of the samples along the Peterezera inter-dune transect (Pe.ID1 to Pe.ID4) has a slope of about 5.

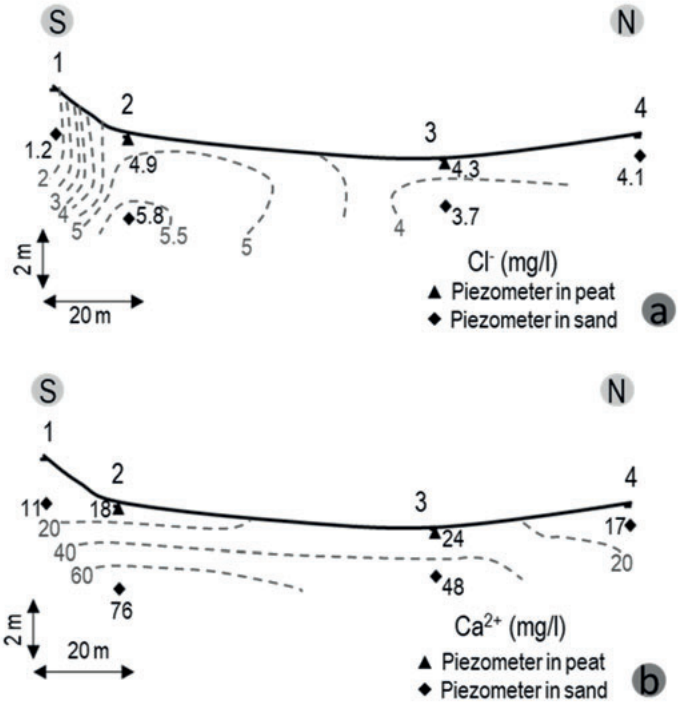

Figure 4. Isohypse of (a) chloride and (b) calcium concentrations in mg l^{-1} along the Peterezera inter-dune transect.

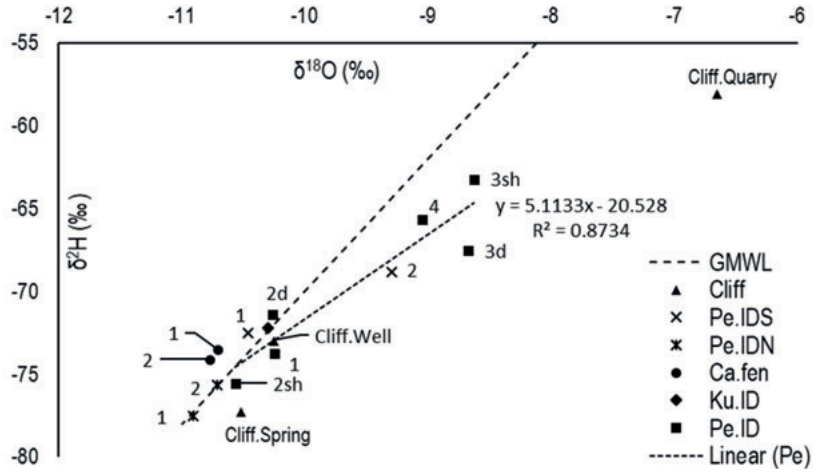

Figure 5. The stable isotope content of $\delta^{18}O$ versus $\delta^{2}H$ (‰) in 16 groundwater samples in relation to the global meteoric water line (GMWL). A trendline was calculated for the samples from the Peterezera inter-dune mire (Pe.ID1 to Pe.ID4).

Radiocarbon dating

The radiocarbon results show that most samples have ^{14}C values above 90 pMC (Figure 6). Different groups were categorised based on the Mook (2006) model for ^{14}C and $\delta^{13}C$ values in groundwater in relation to some geochemical effects. Two samples were found to be below that range, i.e. > 90 pMC: the most northern sample Pe.IDN2, which has a value of about 69 pMC, and the sample collected from the spring in the cliff area of the plateau, Cliff.Spring, which has a value of about 77 pMC. The $\delta^{13}C$ values for those two samples, however, show that the sample from Pe.IDN2 is slightly depleted with respect to $\delta^{13}C$, with values closer to -16 ‰. This sample also has the lowest pH and HCO_3 content of all samples.

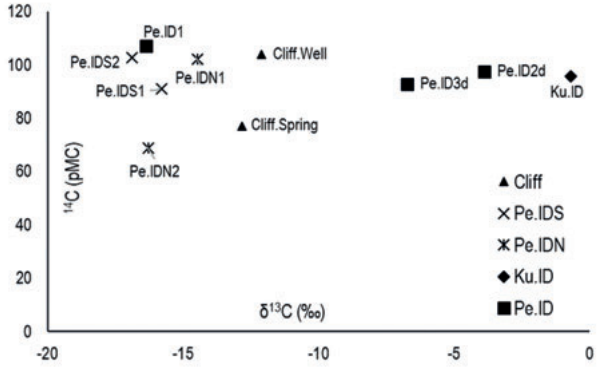

Figure 5. The radiocarbon ^{14}C (pMC) content against the stable carbon isotope $\delta^{13}C$ (‰) content in eleven groundwater samples from Slitere National Park.

DISCUSSION

Analysis of the water quality data indicated the presence of different groundwater systems that feed the mire systems and their vegetation (Figure 6). There are three gradients of groundwater systems (regional, local and their mixture) that have different ranges of TDS and $^{14}C/\delta^{13}C$ values (Toth, 1963). The first groundwater system (regional) was observed in two samples: Cliff.Well and Cliff.Spring samples, with TDS ranges 500–600 mg l^{-1}. They were found to be distinctly more base-rich than the other samples. Also, the $^{14}C/\delta^{13}C$ content of the Cliff.Spring water sample indicates a discharge of groundwater flow that has a residence time longer than 1000 years (Geyh, 2000; Mook, 2006). This is in line with the data from the groundwater flow simulation, which indicates that the regional groundwater flow would have a residence time that is higher than 400 years if the flow path started at the plateau (See Appendix 3). Also, the groundwater particle tracking shows that the flow paths from the regional systems would exfiltrate at the inter-dune mires; however, this depends on the water budget of each system. The water quality data indicate that species-rich fens are like to be fed mostly by the regional groundwater system. The

highest discharge of this regional groundwater flow occurs at the foot of the cliff area, where a vertical flow is likely to originate from the semi-confined sandstone aquifer. This vertical flow could have resulted from a fault line stemming from the Baltic basin subsidence (Virbulis *et al.,* 2013).

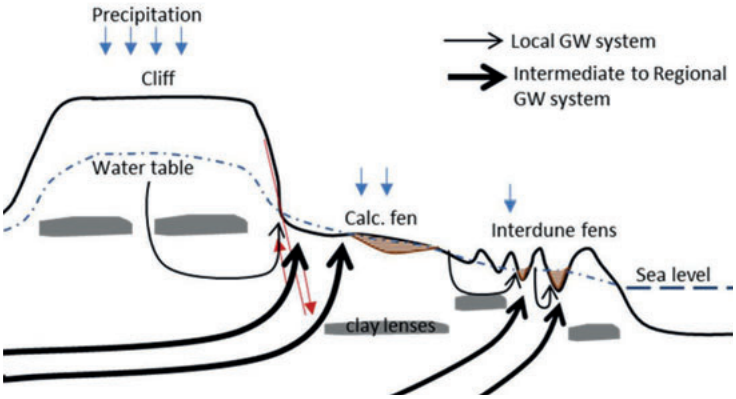

Figure 6. A hypothetical sketch illustrating the origins of the groundwater systems sustaining the biodiversity in Slitere National Park. The regional groundwater enters the study area from external sources and their mixture with local systems create a different vegetation gradient from the extremely (calcareous) rich fens to the rich and poor fens that have higher water input from local dune recharge.

The second TDS range (mixed regional and local), around 350 mg l^{-1}, includes the samples from the middle reaches, Ca.fen1 and 2, Pe.IDS1 and the sample from the Kuksupes inter-dune mire. Also, the water sample from the piezometer screen in the sand at Pe.ID2 has a TDS value close to this range, around 260 mg l^{-1}. This TDS range probably reflects groundwater discharge from the regional system mixing with the local groundwater system recharging from the surrounding dunes. The groundwater simulation model indicates that the presence of clay lenses closer to the mires limits parts of the regional groundwater flow (Virbulis *et al.,* 2013). This mixing of the local and regional groundwater systems leads to the observed lower pH and ion composition. The radiocarbon values for such a mixing process would range between 90–100 pMC and the $\delta^{13}C$ values would be close to 0 ‰ (Figure 7). This mixing process could be the result of groundwater flows similar to that of Cliff.Spring, ^{14}C = 77 pMC, with infiltration water from the local dune, ^{14}C > 100 pMC (Mook, 2006). The mixture of these systems has led to the presence of the extremely rich calcareous fens and the rich inter-dune fen systems (Wolejko *et al.,* in review). It is likely that Kuksupes and Peterezera have similar groundwater flow systems with a discharge of base-rich groundwater flow, which we observed at their southern edges (Wolejko *et al.,* in review). Also, the $\delta^{18}O$ and $\delta^{2}H$ values of the samples taken at the southern edge in Peterezera (Sample Pe.ID2d) and the sample from Kuksupes (Ku.ID) show no interaction with the evaporation processes near the surface of the peat layer. This supports our hypothesis that the regional groundwater discharges at the inter-dune

mires, with a contribution from the local systems, which creates an intermediate mixed system.

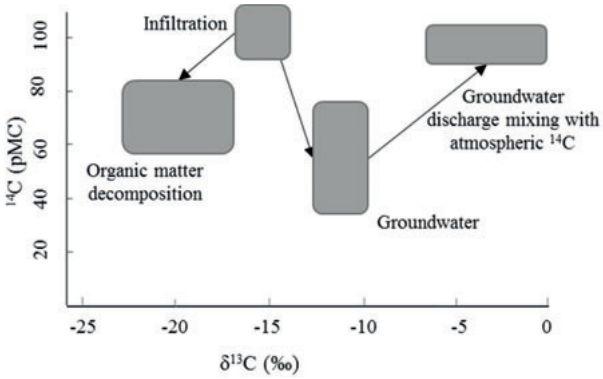

Figure 7. The $^{14}C/\delta^{13}C$ relationships with the possible origins and mixtures of groundwater from infiltration to discharge (adapted from Mook, 2006).

The third range of TDS (locally dominated) was measured in the water samples collected at depths less than 2 m in the Peterezera inter-dune mire. Despite the discharge of the mixed regional and local groundwater systems, the samples from Peterezera mostly have a TDS range around 100 mg l^{-1}. Two inter-dune mire systems, Kuksupes and Peterezera, had a similar input of groundwater flow discharge at one side, which then results in water flowing from one dune to the next following the discharge (Stuyfzand, 1993). Within each valley, the water flows as a through-flow in one valley, influencing the vegetation patterns (Van Loon *et al.,* 2009). Wolejko *et al.,* (in review) indicated the dominant effects of base-rich groundwater on the vegetation in the Kuksupes and Peterezera mires, which were identified as rich fens. In Kuksupes the groundwater was more alkaline (pH ~ 7) and had higher calcium and bicarbonate content. However, the flow within the top 2 meters of the Peterezera mire did not have the same level of water quality as observed in Kuksupes and in the south of Peterezera. Furthermore, the stable isotopes and the ion composition profiles indicate that the increase in chloride values in the shallow layer resulted from through-flow, which is subject to evapotranspiration processes (Gat, 1996; Appelo & Potsma, 2005). This indicates the dominance of the local groundwater system recharging at the adjacent dunes in these mires, despite the discharge of mixed regional and local groundwater systems.

These observed changes in the hydrological systems likely resulted from the presence of former agricultural drainage channels to the north of Peterezera (Wolejko *et al.,* in review). This was strongly indicated in the Pe.IDN2 sample, which is close to these drainage channels and a small river draining to the northeast. This sample showed an increase in acidity, depleted $\delta^{13}C$ values and lower ^{14}C values, which are probably related to the groundwater passing through an upstream mire and becoming exposed to the release of organic matter from the peat soil (Schot *et al.,* 2004; Mook, 2006). Such a process leads to the wetland vegetation becoming mainly dependent on

the shallow, base-poor groundwater supply from the dunes, which takes over from the base-rich seepage flow (Schot *et al*., 2004). Another possibility is that the presence of the interglacial clay layers at some locations limits the access of the regional groundwater to the wetlands, which could also hinder the recovery of previously drained systems, such as Peterezera.

CONCLUSIONS

Although Slitere National Park is a protected area and thought to be in an almost pristine state, this might not be the case for all the systems within it. The mire systems in Slitere National Park are not only fed by groundwater systems that recharge at neighbouring dunes or at the plateau. The groundwater flows originating at the plateau could be considered as mixed intermediate systems. It is possible that a regional groundwater system, with a larger spatial extent, would be recharging further inland. For instance, the inter-dune systems in Slitere National Park depend on groundwater discharge at the southern edge of the dunes, which originate from a mixture of groundwater flows including the regional groundwater systems. While the original groundwater flow is base-rich, some areas seem to have their groundwater flow affected by base-poor flow from adjacent dunes. Furthermore, the groundwater possibly follows cascading systems similar to other inter-dune wetlands in northwest Europe. The change in hydrological regime could also have resulted from activities draining the water table outside the park or the small river system near some of the inter-dune valleys. Further study is needed to determine and understand the role that impermeable clay layers play in controlling the different groundwater supply systems. Also, the impact of remnant drainage ditches on the groundwater flows needs to be assessed and quantified.

ACKNOWLEDGEMENT

We acknowledge Ecological Resotration Advice (ERA) for funding the project. We thank Christ-Janis and Lida Strazdina, Alma Wolejko for helping us with the field work. Also, we thank the researchers at the CIO laboratory Sanne Palstra, Harro Meijer, Hans van der Plicht and the laboratory technicians. Also, we thank Christian Fritz and Jeroen Geurts for allowing the analysis of the water samples for their ion composition at Radboud University in Nijmegen. Lastly, we thank Esther Chang for the language editing.

APPENDIX

Appendix 1. List of the groundwater sampling locations and analysed aspects of groundwater composition the collected water volumes for their respective analysis.

No.	Code	Depth (cm)	Radiocarbon isotopes (500 ml)	Stable isotopes (30 ml)	Ion composition (100 ml for cations and 50 ml for anions)
1	Pe.IDN2	185	1	1	1
2	Pe.IDN1	120	1	1	1
3	Pe.ID4	85	--	1	1
4	Pe.ID3	200	1	1	1
5	Pe.ID3sh	20	--	1	1
6	Pe.ID2	355	1	1	1
7	Pe.ID2sh	20	--	1	1
8	Pe.ID1	190	1	1	1
9	Pe.IDS2	130	1	1	1
10	Pe.IDS1	85	1	1	1
11	Ca.fen1	65	1 (failed in lab)	1	1
12	Ca.fen2	200	--	1	1
13	Ku.ID	205	1	1	1
14	Cliff.Quarry	0	--	1	1
15	Cliff.Spring	20	1	1	1
16	Cliff.Well	>400	1	1	1

Appendix 2. Database of the drilled wells in the study area.

Information on the geological units in the study area were obtained from the database of the Latvian Environment, Geology, and Meteorology Center (LEGMC, accessed in 2018), which contains data from 48 wells in the study area reaching different depths (Figure S1). Wells give indications of soil properties, the presence of groundwater levels, impermeable layers and characteristics of the drilling itself (Figure S2). Furthermore, two wells were drilled at the Peterezera and Kuksupes inter-dune mires to depths of 13 and 20 meters, respectively (blue points 01 and 02 in Fig. S1). Also, additional data were obtained from the LEGMC website, such as horizontal conductivity, effective porosity; others were estimated based on the soil characteristics. Hydrological information were obtained from the Environmental Modeling Center (VMC), like hydraulic conductivity, recharge and evapotranspiration rates. VMC has a larger-scale groundwater model for Latvia and the Baltic states, i.e. LAMO (Virbulis et al., 2013).

Figure S1: Study area with the location of the wells existing in the LEGMC database: (i) red dots indicate wells drilled near the sea, (ii) yellow dots indicate wells drilled on the cliff of the former Littorina coastline, and (iii) blue dots indicate wells drilled at the Kuksupes and Peterezera inter-dune mires.

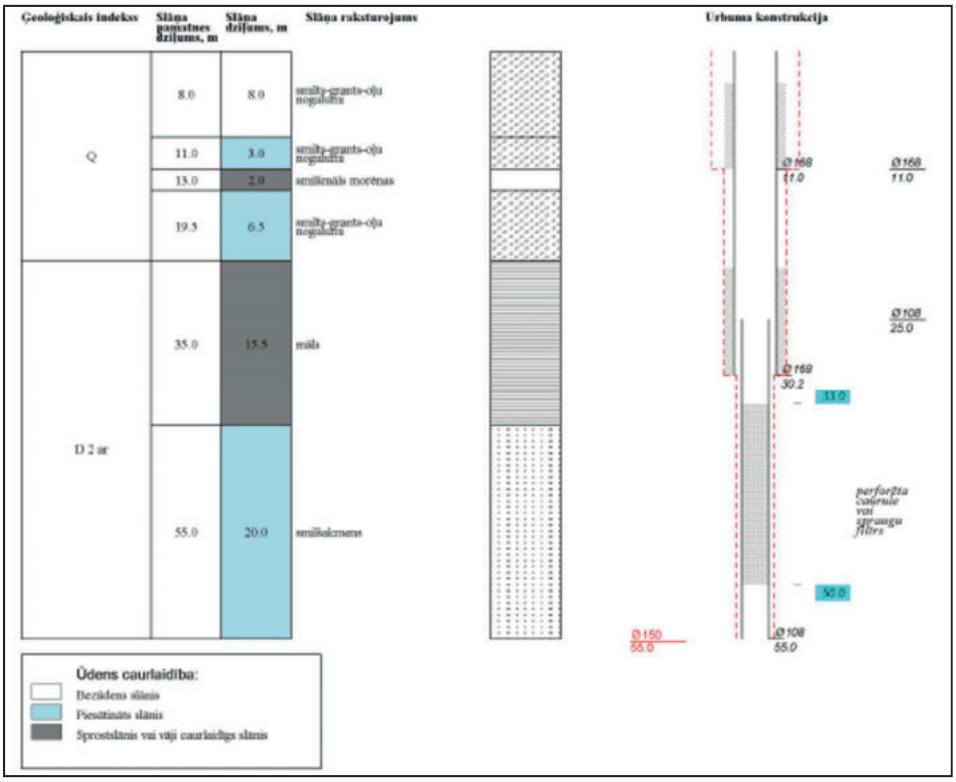

Figure S2: Example of the information obtained from the wells in the LEGMC database.

Appendix 3. Groundwater simulation

A groundwater model was constructed using the software program Processing Modflow for Windows (PMWIN) (Chiang & Kinzelbach, 2001). The model covered a surface area of 25 km by 18 km, which was able to replicate the main topographic characteristics of our study area. The grid design consisted of a matrix of 173 by 181 cells of three types (Figure S3). The first type comprised 40 m by 40 m square cells, representing the area of the inter-dune wetlands (top left corner). The second type of cells (top right and bottom left) were rectangular representing the areas of the plateau and the bog (250 m by 40 m). The remaining cells were of larger square cells (250 m by 250 m), which represented an area of low interest (in the bottom right corner). This model was oriented in the NW-SE direction instead of N-S for the sake of convenience.

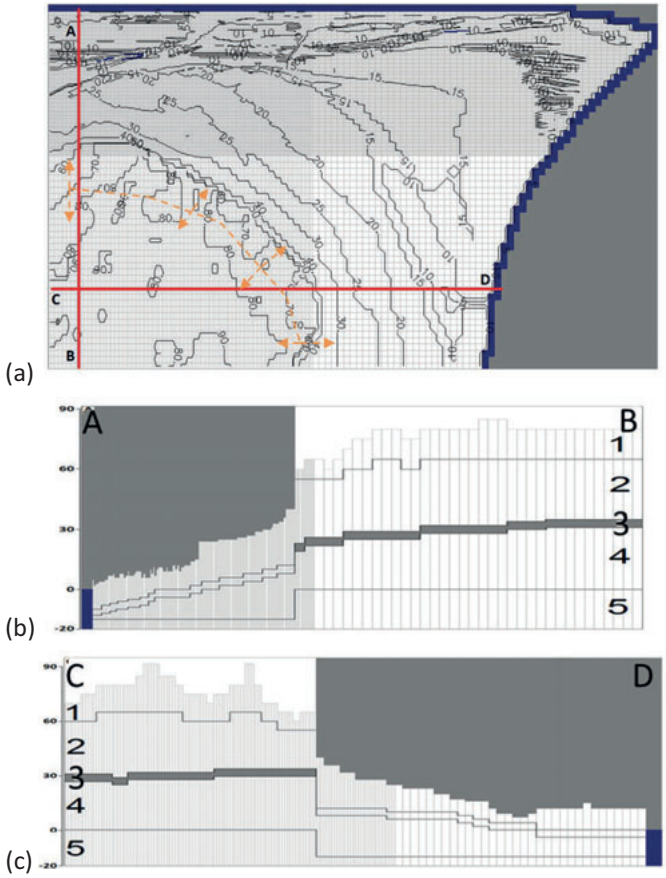

Figure S3. (a) Plan view of the model with contour lines representing the major topographic characteristics of the area. The dashed orange line marks the plateau area. The white and light grey boxes represent active cells; blue boxes represent cells with constant hydraulic heads, i.e. sea level. Finally, dark grey boxes represent inactive cells, where no flow can take place. (b) South [B] to north [A] cross-section showing the main characteristics of the model, and (c) west [C] to east [D] cross-section.

Boundary conditions

The bottom boundary of the model was set as an open boundary at a depth of 20 m below sea level. This depth was defined taking into consideration the available geological data, which shows constant lithologic variation with depth. The lithology corresponded mainly to sandstone. The top boundary condition was defined by a map of vertical fluxes (rainwater infiltration) calculated and provided by the Environmental Modeling Center (VMC) at Riga Technical University. A value for infiltration or evapotranspiration was assigned to each active cell of the model according to the map fluxes. The north and east faces, which are bound by the Baltic Sea and the Gulf of Riga, were defined as closed boundaries. At the coastline, the topography reaches its lowest level; therefore, it was considered as the discharge point for fluxes flowing from inland. The recharge in our study area occurs along the highest topographic levels, which in our model corresponds to the southwest side of the cell matrix. The dashed orange line in Fig. 1 represents the water divide, showing the place where recharge is present, and arrows represent the flow directions. Since flow directions at a certain point, i.e. near the western and southern boundaries, remain unchanged, we decided to leave these boundaries open, i.e. without a fixed head or no flow boundary.

Hydrogeological setting

The hydrogeological data used to create the model was obtained from the following sources: (i) the Latvian registry of mineral resources belonging to the Latvian Environment, Geology, and Meteorology Center (LEGMC), (ii) the VMC at Riga Technical University, and (iii) a literature review. The wells from the LEGMC database were distributed along the two administrative provinces (parishes) of the Dundaga Municipality: the northern Kolka Parish located next to the coastline, where Slitere National park is located, and in the upper areas of Dundaga Parish. This registry contains data from 48 wells in the study area reaching different depths (see App. 2). Figures 3b and c show two cross-sections of the model, where the maximum height was set at 90 meters above sea level and the maximum depth was set at 20 meters below sea level. The model was built using five layers (Table S2). The first layer from top to bottom corresponds to the unsaturated Quaternary sand sediments and it is mainly present on the elevated plateau in the southwest (Fig. S4). The second layer represents saturated Quaternary sand sediments, and the third corresponds to an impermeable layer, depicted as inactive grey cells located between 28 and 34 meters above sea level (Fig. S4). This impermeable layer was observed from well datasets, specifically in higher areas where more boreholes were available. However, in low areas near wetlands where no boreholes had been available, we used the information from two wells drilled during June 2018 and a literature review. The clay glacial deposits were inserted as elongated-shaped lenses, which result from the strong influence of glacial and inter-glacial cycles in the region (Sviridov & Emelyanov 2000, Svendsen et al., 2004, Zelcs et al., 2011, Saks et al., 2012). The fourth and fifth layers represent the sandstone layers, which also serve as the base of the model (Zelcs et al., 2011).

Table S2: Model dimensions and layer parameters.

Study area				Model dimensions	
Length (km)	30			Columns	181
Width (km)	19.8			Rows	173
Depth (m)	120			Layers	5
Model parameters					
Layer	1	2	3	4	5
Lithology	Sand	Sand	Clay	Sandstone	Sandstone
Permeability*	P	P	I	P	P
Horizontal conductivity (Khv) (m/day)	7	4 - 7	-	4	4
Vertical conductivity (Kvv) (m/day)	7	4 - 7	-	4	4
Effective Porosity	0.2	0.1 - 0.2	-	0.1	0.1
Bulk density (Kg/m^3)	2000	2000	2000	2000	2000

* P = permeable, I = impermeable

Analysis of 2-D transects

Figure S4 shows a profile running along the transect from point A to B (Figure S3b), ending at the Peterezera mire. Four particles at different levels were tracked using PMPATH (Chiang & Kinzelbach, 2001). The shallower particles above the impermeable layer (red and orange) infiltrate at the plateau, while the two deeper particles below the impermeable layer (green and pink) are able to reach the southern boundary of the model. The trajectory of the shallow particles is similar to surface delineation, while the deeper particles follow a horizontal trajectory over almost their entire flow path. All four particles show a vertical anomaly, in the shape of a “step” between 10 and 15 meters long, when they reach the cliffs. Further, Figure S5 shows the flow paths of water infiltrating at the plateau and arriving at the calcareous fen. It also shows an input of groundwater flow from the sandstone aquifer, which originates from outside the study area.

Residence time estimation

The recharge areas were not found to be restricted to a specific place. Looking specifically at the inter-dune mire complex, a great part of the recharge was found to occur in the upper plateau and the dunes, while the discharge zones were identified as the ocean and local water bodies. The simulated residence time is between 40 and 45 years for a particle originating from the unconfined aquifer in the plateau to reach the sea, and 25 years to reach the inter-dune mire complex. For a particle located in the same layer in the plateau and discharging in an easterly direction, it takes 100 years to reach the output. For particles located in the sedimentary rock layer following travel paths similar to those shown in Figure S4 (green and pink particles), residence times were found to be 200 years, which is actually the minimum value as the particles originated from outside the study area. Finally, particles coming from the

dunes through infiltration reach the mire system within a period of 1 and 5 years, depending on the distance of the dune from the mire.

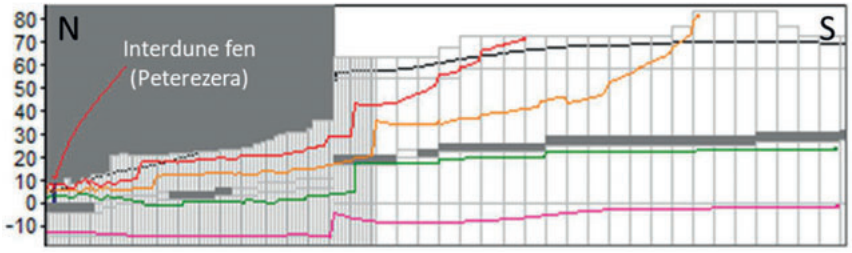

Figure S4. Cross section of the model tracking groundwater particles from the plateau to the inter-dune mire complex (Peterezera Mire): (i) infiltrating at the plateau (red and orange) and (ii) groundwater flow from the sandstone aquifer (green and pink).

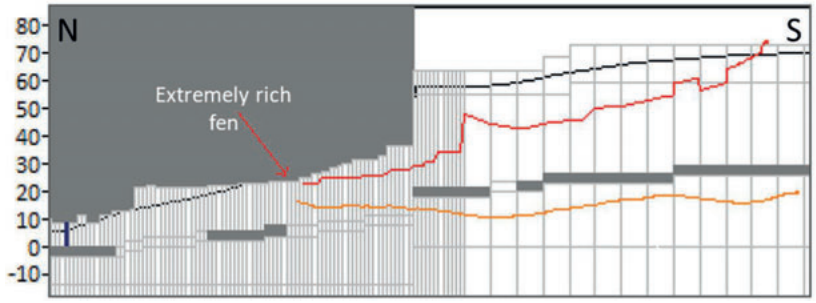

Figure S5. Path lines of two groundwater particles reaching the extremely-rich fens at the foothill of the plateau: (i) infiltrating at the plateau (red) and (ii) from the sandstone aquifer below the clay lenses (orange).

7

Synthesis: natural isotopes in ecohydrological analysis of peatlands

INTRODUCTION

The ecohydrological approach has been developed over the past 40 years by Dutch scientists (see Wassen & Grootjans, 1996). It is an interdisciplinary approach that aims to understand the hydrological processes conditioning an ecosystem (Wassen & Grootjans, 1996). The focus in this thesis is on fen peatland systems, which contain vegetation types that are primarily dependent on groundwater supply (Wheeler & Shaw, 1995; Joosten & Clarke, 2002). The development and restoration of a fen peatland not only depend on the internal hydrological and geochemical processes (Van Wirdum *et al.,* 1992, 1995; Lamers *et al.,* 2015), but also on the larger external system (e.g. Wassen *et al.,* 1990; Van Wirdum 1991; Schot & Molenaar, 1992; Gilvear & Bradley, 2009; Grootjans *et al.,* 2012; Schot & Pieber, 2012). In this study, the past (paleo-) and present conditions of mire systems were analysed in order to predict possible developments in the future. We integrated the use of natural isotopes of C, H and O with different tools, e.g. peat temperature and water level, pressure and chemistry measurements. The isotope approaches we used can be divided into two groups: the commonly-used radiocarbon method of peat dating to assess the paleo-systems and analysing the natural isotopes C, H and O in water to trace groundwater flow systems. The main aim of this thesis is to test the added value of including groundwater isotopic analysis in the ecohydrological approach (see Grootjans & Jansen, 2012).

Different scales of observation boundaries were selected to understand the groundwater flow systems conditioning four peatland systems/complexes. The smallest scale covered a single basin in Matlabas (South Africa), with some attention paid to its attached basin (See Groundwater systems). The other three systems were studied at larger scales than a single basin. Vasi-North (South Africa) was at the centre of the study on the Vasi Peatland Complex, embedded in the wider landscape of the Maputaland Coastal Plain. The groundwater system investigated in Slitere National Park (Latvia) supplied different types of fen peatlands within a topography of high relief, the old coastal cliff of the Littorina Sea. Lastly, the study in the Drentsche Aa Brook Valley (The Netherlands) addressed the hypotheses for the processes affecting restoration success on a regional scale, e.g. origin of the discharging groundwater,

hydrogeological processes in the deep aquifers and groundwater abstraction. Table 1 shows a summary of the study areas' characteristics and the tools used at each of the areas. The duration of the field work using these tools varied from 2 to 3 weeks, with the exception of the water level depth measurements, which needed to be carried out over longer periods to measure variation.

Table 1. Study areas and methods: used measurements (tools) and fieldwork duration. * The duration covers most of the measurements, excluding the water level measurements, which were carried out by other collaborators.

	Measurements							Field Duration (weeks)
	^{14}C / $\delta^{13}C$		$\delta^{18}O$ / $\delta^{2}H$	Ion composition	Peat temperature	Piezometric pressure	Water level	
	Peat	Ground-water						
Matlabas Mire	+	+	+	+	+	+	+	2*
Vasi Peatland Complex	+	+	+	+	+	+	+	3*
Drentsche Aa Brook Valley	-	+	+	+	-	-	-	2
Slitere National Park	-	+	+	+	-	-	-	2

Based on the case studies, this chapter synthesises the main points derived from the studied system. First, the use of isotope analysis of C, H and O in ecohydrological approaches is demonstrated, and their added values and limitations are shown. Further, the ecohydrological systems of the case studies are synthesised over three themes: (i) defining the groundwater flow systems and their resemblance to each other, (ii) the mechanisms of the primary and secondary peat initiation processes associated with these groundwater systems, and (iii) the causes of landscape degradation and existence of local buffers.

C, H AND O NATURAL ISOTOPES

Generally, using the natural isotopes of C, H and O resulted in added value to the approach used by Grootjans & Jansen, (2012). These methods are effective in terms of both cost and time, and they provide a better understanding of the hydrological systems sustaining the functionality of wetlands in a scientifically sound manner. The use of these natural isotopes, however, is optimised when interpreted in the context of other data on groundwater quality, i.e. ion composition. The more frequently used methods of hydrological modelling, estimating the groundwater table and flow directions also help in such ecohydrological approaches to identify the best locations to set up transects or pick areas of interest for groundwater sampling, e.g. peat temperature, piezometric pressure and water level depth. Lastly, radiocarbon dating of the basal peat layer and accumulation rates were used, which shed light on the paleo-conditions that initiated and sustained the systems on the landscape level.

$\delta^{18}O$/ $\delta^{2}H$ stable isotopes

The simple notion in interpreting groundwater quality is that ion composition concentration increases along the flow path, i.e. residence time. However, this picture can be more complicated as geochemical interactions could also affect the ion composition of the groundwater, rendering it difficult to trace groundwater origins. The chloride ion (Cl^-) is rather inert, which means it is not affected by the geochemical processes; rather its concentration only increases with evaporation processes or leaching from marine sediments/rocks. Thus, chloride is favoured by hydrologists to trace groundwater flow and, consequently, origin (Appelo & Postma, 2005). In ecohydrological studies in the Netherlands, chloride ions along with $\delta^{18}O$ and simulation models were used successfully to trace the groundwater flows supplying a wetland (Schot & Van der Waal, 1992). In contrast, calcium ions were shown to be an unreliable tracer, especially near peat accumulations as their concentrations were increased by the release of cations from the peat layer in degraded situations (Schot & Wassen, 1993).

The limitation, however, is that using $\delta^{18}O$ is not sufficient to trace groundwater flow, despite being an inert element like chloride. Both chloride ions and $\delta^{18}O$ can be affected by evaporation processes, which can increase their concentrations and thus lead to misinterpretations of groundwater flow origins. Meanwhile, integrated interpretation using ion tracers, e.g. Cl, Ca and SO_4, combined with data on $\delta^{18}O$/ $\delta^{2}H$ content in water samples allows for more robust identification of water types based on their origin and flow direction. This is because data on $\delta^{18}O$/ $\delta^{2}H$ takes into account the influence of evaporation processes, which also affects the chloride concentration in water samples (Gat 1996; Clark & Aravena 2005; Mook, 2006). Hence, this improves the accuracy of using ion tracers to identify groundwater flow directions that are influenced by evaporation processes both in the groundwater and peat layer. For example, Appelo & Postma (2005) showed that rain water with a chloride concentration of 1 mg/l will increase in its chloride concentration to ca. 4 mg/l after infiltrating the soil, solely due to evaporation processes in the top soil. A further example given in this thesis is the ion tracer profile taken from Peterezera in Slitere National Park (Figure 1). Figure 1a shows the chloride concentration along a transect, which reflects the internal groundwater flow in the peat. There are two possible explanations for the pattern of relatively high chloride concentration in the west (point 2d, Cl = 5.8 mg/l). The first is that this is typical for groundwater that passes through the topsoil and then proceeds as groundwater. When this groundwater discharges into the Peterezera mire, evidence of dilution and evaporation processes can be seen in the upper layers of the peat. The second possibility is that this groundwater originated from a deep source discharging at the west side of the mire, and then mixed with the phreatic (local) flow, which is subject to evaporation. The latter explanation is more likely. The stable isotopes data indicate that sample 2d was not subject to evaporation processes, unlike the other shallower samples (Figure 1b, point 2d is above the global meteoric water line, GMWL). Further, radiocarbon data also support the second explanation. In this case, sample 2d was shown to be an outcome of a mixed groundwater discharge using atmospheric radiocarbon, with

radiocarbon values between 90 to 100 pMC (see next section). Similar ways of interpreting data from Vasi-North and Drentsche Aa (at Kappersbult) also allowed for verification of the relationship between increases in ion concentration and the presence of near-surface evaporation processes from groundwater with longer residence times.

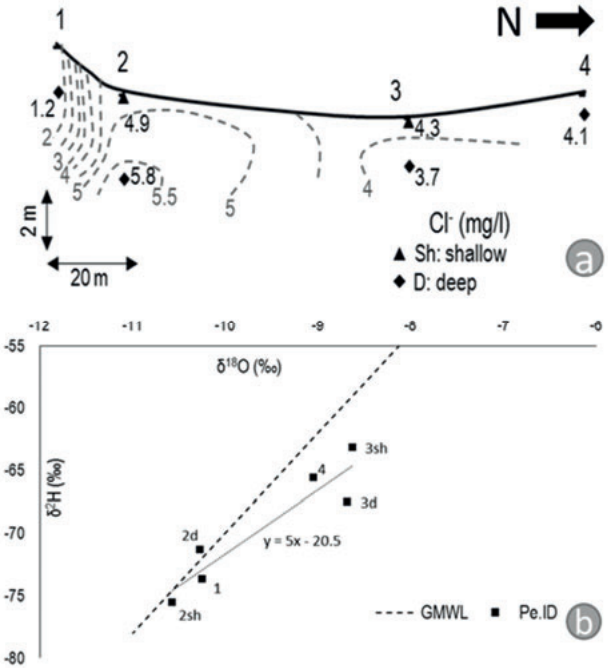

Figure 1. (a) Chloride isohypse in a south-to-north transect in the Peterezera mire in Slitere National Park. (b) The results of the $\delta^{18}O$/ $\delta^{2}H$ of samples taken from the Peterezera mire plotted with the global meteoric water line (GMWL).

Radiocarbon in Groundwater

Schot (1991) suggested that radiocarbon dating of groundwater could be useful in studying the relation of groundwater systems to wet ecosystems. However, the costs and logistic difficulty with sampling sizes remained an issue until recently (Mook, 2006). Also, the interpretation of the radiocarbon dating in terms of accurate residence times or groundwater age remains problematic and requires substantial data on water quality (Geyh, 2000; Mook, 2006). Even though the estimation of accurate residence times is problematic, radiocarbon dating can be used in a qualitative manner, which allows for identifying different groundwater types and possible ranges of residence times, i.e. origin. Simplified representations of the radiocarbon with the natural stable carbon isotope ($\delta^{13}C$) allows for a simplistic classification of groundwater types (Figure 2a) (Mook, 2006; Han *et al*., 2012). In each system, the groundwater supplying the peatland was compared to other areas in the landscape to identify the boundaries of the area of interest.

For instance, the measurement of the radiocarbon content at different locations in Maputaland led to the conclusion that wetlands in Maputaland depend on local, fast-flowing groundwater systems. The dominant radiocarbon values in Maputaland were higher than 100 pMC, while the ones between 90 to 100 pMC had been diluted by organic matter decomposition (Figure 2b). The Muzi swamp system was the only one with an apparently different radiocarbon value, as well as a distinct ion composition. However, high ion composition was also measured in the Vasi Peatland Complex, but radiocarbon dating verified the lack of resemblance between these two systems groundwater supply systems. It also correlated with the different hypotheses on the relation of sea level fluctuation to peatland initiation in Maputaland, which is indicated by the radiocarbon dating of the basal peat samples. Meanwhile, the restoration success at different sites in the Drentsche Aa Brook Valley were related to the origins of groundwater flow. For instance, Kappersbult, which had a low success rate in restoring targeted species, was confirmed to be an infiltration site. In addition, radiocarbon data indicated that the relatively old regional groundwater supplying the meadows near Loon with relatively calcium-rich groundwater in the past has been replaced by calcium-poor groundwater from a local hydrological system (Balloerveld; see Figure 10). Radiocarbon data also indicated that deep saline intrusions have no current effects on the groundwater flow supplying the peatlands. Similarly, the radiocarbon dating of groundwater in Slitere National Park illustrated the difference in the groundwater systems supplying the peatlands. It was able to identify the sites that had suffered a switch in groundwater supply from one originating at the sub-regional level to the base-poor groundwater from the local dune slack system. The smallest system boundary studied was at the Matlabas system, where the groundwater discharging to the system had radiocarbon values between 90 to 100 pMC. Unlike the samples taken from Maputaland, the ground water from the Matlabas mire showed no effects of organic matter decomposition. When compared with the shallow sample with radiocarbon values > 100 pMC, the groundwater from Matlabas clearly indicates that some of the groundwater supply has originated from a deeper source.

GROUNDWATER SYSTEMS

Vasi Peatland Complex

The Vasi Peatland Complex (Chapter 3) is an inter-dune system consisting of two peatlands: Vasi Pan and Vasi-North. Vasi Pan can be further divided into three sub-basins, while Vasi-North is formed from a single basin. The Vasi Peatland Complex has long been divided into these two peatlands following the early investigation of the peatlands in the Maputaland Coastal Plain by Grundling & Blackmore (1998). The study in 2014–2017 (Chapter 3) approached the Vasi Peatland Complex as a single system within a complex setting. The Vasi-North system is a low-lying system with a deeper peat basin of up to 8 meters, while Vasi Pan is located at the upper reach of the system with an extensive peat basin of up to 3 meters (Figure 3). The study of the groundwater system indicated that the Vasi Peatland Complex is likely to behave as a

cascading system. The groundwater discharges at one side of the basin and then flows from one basin to the next one, with through-flow taking place within the basin itself. Stuyfzand (1993) illustrated such a process in dune slacks in the Netherlands, where the groundwater exfiltrates at one side of the dune and infiltrates at the other side (Stuyfzand & Moberts, 1987). The water table data showed the head difference between the basins, with a higher head at Vasi Pan than at Vasi-North. Also, analysis of the water ions showed enrichment from Vasi Pan in the west to Vasi-North in the east. The same enrichment pattern in chloride and sulphates was also evident within Vasi-North itself, which could be attributed to the evaporation processes in the top layer of the peat using $\delta^{18}O/\delta^{2}H$ data.

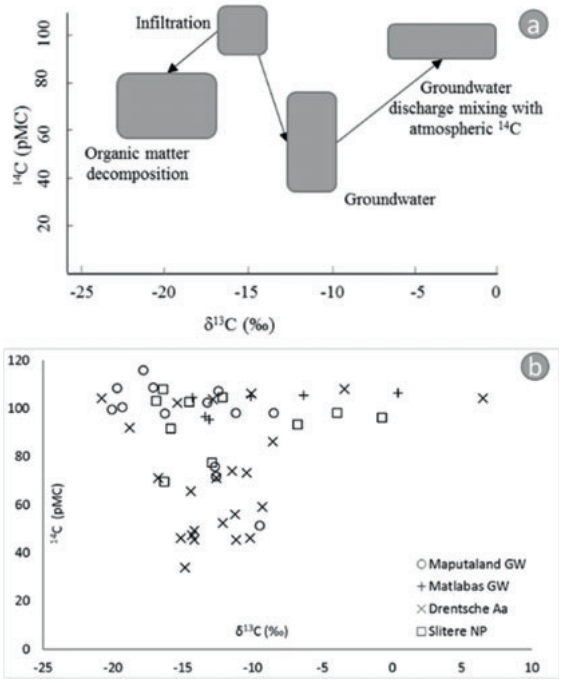

Figure 2. (a) Illustration of the simplistic approach used to interpret radiocarbon dating data in the water samples taken from the peatland study areas (after Mook, 2006). (b) Results of the radiocarbon dating in the water samples from the four case studies.

The complex part of analysing the groundwater system in the Vasi Peatland Complex was to establish its relation to the primary aquifer in the Maputaland Coastal Plane. Landscape-level studies in the Maputaland Coastal Plane hypothesised that areas with water table levels at depths less than 2 meters are likely to be wetland areas (Kelbe *et al.,* 2016). Grundling *et al*. (2013) categorised wetlands using a general elevation divide, with permanent wetlands likely to be located at areas with elevations less than 50 m a.m.s.l. and temporary ones in areas between 50–60 m a.m.s.l (Grundling *et al.,* 2014). As the Vasi-North peat basin extends between 46–54

m a.m.s.l. and the Vasi Pan basins are at elevations between 60–65 m a.m.s.l, further analysis was necessary using groundwater quality from different wetlands in Maputaland.

The follow-up analysis indicated that the groundwater at the Vasi Peatland Complex is different from those found at the other wetland systems in Maputaland. It also indicated that the Vasi Peatland Complex is fed by groundwater of short residence times, which most likely indicates a perched aquifer system, with radiocarbon values close to 100 (pMC). The perched aquifer systems are likely to be iron rich layers (Botha & Porat, 2007). The perched aquifer is strongly affected by peat decomposition and the reversed flow from the peat into the water table, with $\delta^{13}C$ values close to -20 (‰). The isolated nature of the Vasi Peatland Complex from the regional system in Maputaland is evident from the lack of a link with sea level rise, peat initiation in the Vasi Peatland Complex and in Maputaland (see section: Initiation of peat formation).

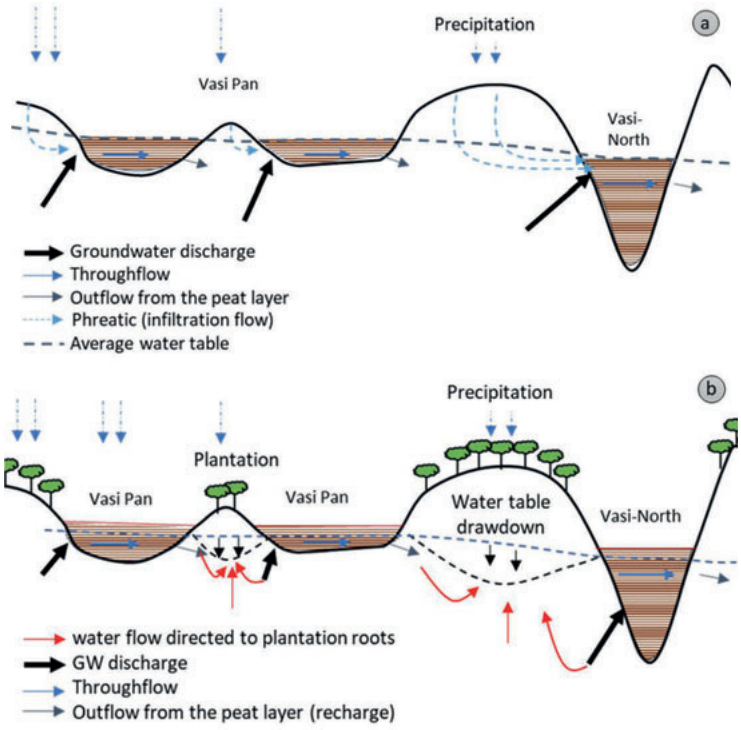

Figure 3. Illustration of the groundwater system in the Vasi Peatland Complex (a) before and (b) after the land-use changes due to setting up of intensive and extensive plantations.

To conclude, while most of the wetlands in the Maputaland Coastal Plain are controlled by a primary regional aquifer (Weitz & Demlie, 2014; Kelbe et al., 2016),

some systems are nested within local features, i.e. perched aquifer systems (Toth, 1963). The local nature of the groundwater feeding the Vasi Peatland Complex makes it quite vulnerable; the perched aquifer has been rapidly affected by increased evapotranspiration caused by plantation activities withdrawing water from the dunes.

Matlabas mire

The smallest studied system is the Matlabas mire (Chapter 4), which is part of the larger protected Marakele National Park. The land use of this area has changed from farming and cattle grazing to an environmental protectorate for animals and plants since 1988 (Bootsma, 2016). The mire is located at an average elevation of about 1800 m a.m.s.l, which makes it one of the highest in South Africa (Grundling & Grobler, 2005). Located in a depression valley, this mire is surrounded by elevated and fractured sandstones. The groundwater system supplying the mire, besides precipitation, can be categorised into three flow types: sheet (surface), phreatic and deep discharge flow (Figure 4a). The sheet and phreatic groundwater flows are affected by the seasonal variation in precipitation rates, which is highest during the summer period from October to April. Seasonal variation is reflected in the $\delta^{18}O/\delta^{2}H$ values, which varied about 1 ‰ between water samples taken in a dry and wet period. The sheet and phreatic flows are ion-poor in comparison to the groundwater discharge, which leads to lower ion content profiles during the wet period. The deep groundwater discharge flow is stable all year long, but it is highest at certain locations in the mire, especially close to the area with the thickest peat accumulation. This area is also characterised by a circular reed zone and ion-rich water, which remains roughly stable over time. The groundwater discharge could be categorised by the radiocarbon values, which were slightly above 90 (pMC), and $\delta^{13}C$ values between -5 to 0 (‰), which indicate sheet and phreatic flow mixing within the discharging flow. These mixed flows then follow a through-flow regime into the peat layer, which redistributes the water solutes (Van Loon *et al.,* 2009; Grundling, 2014b).

Further, dome peat structures are present in the mire, which are zones of ion-rich water. These dome peat structures are also arranged in an alignment similar to that of fault lines (Bootsma 2016). The dome structures likely indicate areas of groundwater discharge. The mire is divided by a fault between the elevated west tributary and lower east tributary (Figure 4b). The west tributary is likely to have similar groundwater flows to the east tributary, but with a limited deep groundwater discharge. There are some channels present in both tributaries, which drain the groundwater flow from the mire to the north. The formation of these channels is not fully understood. They are most likely to be remnants of man-made channels that were used to drain water from the mire during the grazing period when the area was farmed. Also, they could be a connected series of elephant bathing pools; however, this explanation is unlikely to be the case.

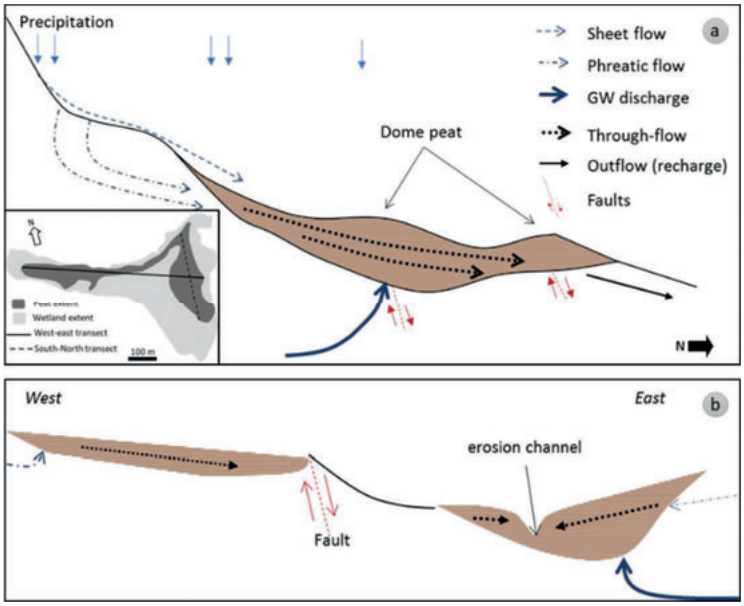

Figure 4. Illustration of the groundwater system in the Matlabas mire along a south-to-north transect (a) and a west-to-east transect (b).

Drentsche Aa Brook Valley

The Drentsche Aa Brook Valley (Chapter 5) is an area where restoration measures have been applied for the last 30 years. The restoration measures were based on studies that established the connection of the wetland vegetation to groundwater flow systems (Everts & De Vries, 1991). The groundwater system in the Drentsche Aa Brook Valley represents a system in which small and intermediate drainage basins are nested in a gently sloping landscape within a regional groundwater system (Toth, 1963). The groundwater flow systems were found to be divided into three flow types: local-, intermediate- and regional-scale groundwater flows (Figure 5). The local groundwater flow supplies areas that are bounded by impervious clay layers close to the surface, e.g. Deurze in the upper/middle reaches. These local groundwater flows are characterised by ion-poor water. The intermediate-scale flows, with radiocarbon values between 60 to 80 pMC, and regional-scale groundwater flows, with radiocarbon values between 40 to 60 pMC, were found to mainly supply sites with groundwater in the middle reaches, e.g. the Taarlo and Rolderdiep sites. The regional groundwater was confirmed to be connected with deeper groundwater flows that are in contact with salt diapir formations, high Cl concentration and lowest radiocarbon value around 33 pMC (Magri & Bregman, 2011). However, such connections were not verified to have an effect on the groundwater supplying the peat deposits nor consequently affect the restoration targets.

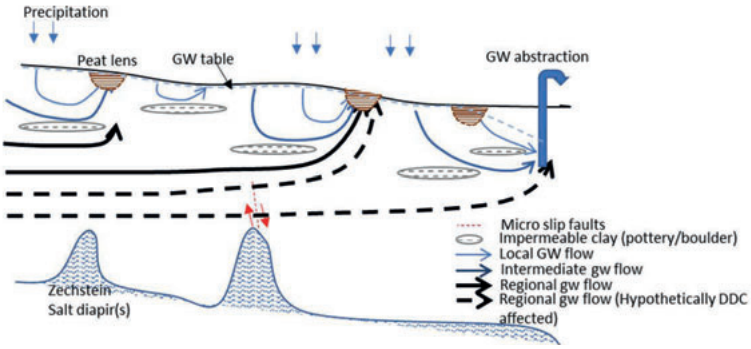

Figure 5. Illustration of the groundwater system in the Drentsche Aa Brook Valley. The peat deposits are supplied by three scales of groundwater systems: local, intermediate and regional. Some of the deep regional groundwater flows are in contact with the Zechstein salt diapirs, which could affect the water quality conditioning the peat deposits at the surface. Groundwater abstraction close to peat deposits was found to cause a drawdown in the groundwater systems supplying the peat deposits, leading to the transformation of these peat deposits into infiltration areas.

Further, some areas were found to have undergone a shift of their groundwater flow regime, from areas supplied by an intermediate/regional source to infiltration areas, e.g. Kappersbult (Figure 6). These alterations in groundwater systems are concentrated in areas closest to groundwater abstraction facilities in De Punt and Assen (Magri & Bregman, 2011). The degree of success in reaching restoration targets was linked to analysis of the groundwater system. An area like Kappersbult showed poor performance in terms of restoration of target species. The transformation of this area into an infiltration area led to the release of adsorbed ions from the cation exchange complex of the peat (Schot & Wassen, 1993; Appelo & Postma, 2005).

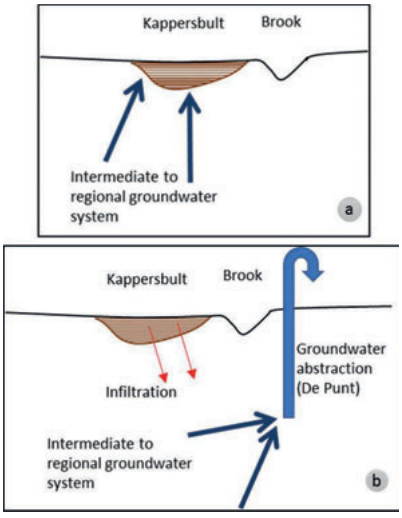

Figure 6. Illustration of the shift in the original groundwater supply to Kappersbult (a) due to the groundwater abstraction facility in De Punt (b).

Slitere National Park

The peatlands in Slitere National Park are located in an area with high relief, similar to that of the Matlabas mire. The cliff on the old coast of the former Littorina Sea creates an entry point for the groundwater systems entering the mires of the park (Figure 7). The groundwater table intersects with the surface at the cliff boundary, with a groundwater discharge from a regional groundwater flow into the wetlands close to the cliff, e.g. cliff springs and the calcareous fen. The regional groundwater is quite alkaline and calcareous, which possibly flows through fault structures that were formed due to the isostatic subsidence of the Baltic basin (Häusler *et al.,* 2017). The inter-dune fens in the lower reaches are also supplied by the regional groundwater system; however, there are also inputs from local groundwater flows, which are more calcareous. The radiocarbon values measured at the dunes indicate that there is a mix of groundwater discharge, with local groundwater in contact with atmospheric CO_2. The local input is likely to indicate that the mires in Slitere National Park are not as pristine as presumed (See Pakalne & Kalnina, 2005). Also, the regional groundwater flow is not limited to the recharge cliff area, as assumed by Woljeko *et al.* (in review). The regional groundwater flow system extends further inland. It remains unclear, however, the extent to which land-use activities, e.g. drainage ditches, infrastructure, have affected the mires in Slitere National Park.

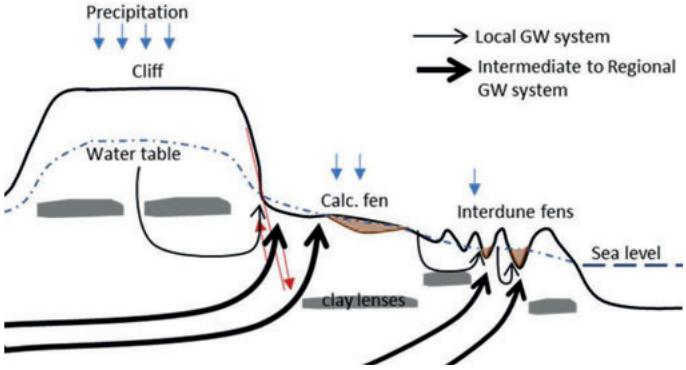

Figure 7. Illustration of the groundwater systems supplying the wetlands in Slitere National Park. The local groundwater systems are supplied by direct recharge in the dunes adjacent to the wetlands. The water recharging at the cliff is considered here as part of the local system, while the regional system originates from areas further away.

INITIATION OF PEAT ACCUMULATION

Primary peatland initiation

The initiation of South African peatlands was correlated to climatic factors on the continent, where the increase in wetness, higher precipitation rate and hence a rise in the recharge of groundwater led to peat accumulation, especially around the Late

Glacial Maximum (LGM) (Chapter 6). Yu *et al.,* (2010) simulated the climatic conditions favouring peat accumulation and found a rise in the initiation of continental peatlands during the LGM (Yu *et a*l., 2010). The initiation of peatlands in the Maputaland Coastal Plain were related to sea rise, especially during the Mid-to-Late Holocene (Chapter 6, Grundling, 2004). Most of the peatland systems in Maputaland are likely to be driven by groundwater systems that developed after reduced drainage, which was caused by the sea level rise in the Indian Ocean. However, the peatland basins in the Vasi Peatland Complex do not seem to be related to fluctuations in sea level (Chapter 2 and 6). Rather, the primary initiation of peat in Vasi-North can be attributed to local hydrogeomorphic conditions, i.e. a perched groundwater table combined with a shift to a wetter climate. The secondary initiation in the Vasi Peatland Complex, Vasi Pan, coincided with a peak in sea level rise around 4000 calBP. However, this may not have been the primary driver. Peat accumulation in Vasi Pan likely resulted from a rise in the perched water table due to the clog caused by the low-lying Vasi-North basin. The high permeability of the sand deposits in the KwaMbonambi formation allows groundwater flows to reach the sea within a short span of time, which is likely to be in the range of few decades at most.

The primary peat initiation in the Matlabas mire was likely to be related to tectonic changes. The fault systems in Matlabas divided the system into a lower eastern part and a higher western one, with the fault throw of around 10 m. The drop in the surface level and the presence of other faults in the eastern part created a possible input of artesian groundwater flow into the centre of the eastern part. The peat accumulation rates during most of the Holocene were very low, only 0.011 mm/yr, and occasionally interrupted by sand deposits from the high energy flow of surface water. This later led to a clog effect because of accumulation of peat, which is less permeable, leading to higher accumulation rates by the Mid-to-Late Holocene (Figure 3b and Figure 9).

The initiation of the peatlands in Slitere National Park also resulted from a primary drop in the land surface due to the subsidence of the Baltic basin and the regression of the former Littorina Sea (Pakalne & Kalnina, 2005; Kalnina *et al.,* 2014). In addition to the drop in the surface, the Littorina Sea regression allowed for peat accumulation, given that this area has an excess of precipitation over evapotranspiration. Similar peat accumulation development has been observed in coastal peatlands in Indonesia (Dommain *et al.,* 2011). Dommain *et al.,* (2011) showed that the coastal peatlands in Indonesia initiated peat accumulation following episodes of sea level regression. Sea level regression allowed for accumulation of groundwater flows in areas abandoned by the sea (Dommain *et al.,* 2011).

Secondary initiation

Dekker *et al.,* (2015) have illustrated that peatland initiation can take place in two phases. The first phase is triggered by a combination of climatic change, i.e. increase of precipitation rates and sea level rise, which decreases the drainage of the groundwater to the sea (Dekker *et al.,* 2015). Secondary processes could initiate the second phase of peat accumulation, which could result from feedback mechanisms

between local geomorphologic factors and decreased drainage due to peat accumulation at low-lying areas (Dekker *et al.,* 2015). We observe this two-phase initiation in Vasi and Matlabas. Within the Vasi complex itself (Figure 8), the lowest lying basin, Vasi-North, developed earlier causing a possible clog that allowed further development in the higher basins in Vasi Pan. In this case the separation of the basins by sand dunes makes it clear that they initiated peat accumulation separately; however, it is important to keep in mind that they are hydrologically connected.

Matlabas consists of two parts: a low-lying eastern part and a higher western one (Figure 4b). The separation between these basins is not visually evident, unlike the basins in the Vasi Peatland Complex. If we separate the two sides, then we can think of the system as having been initiated in two phases. The peat accumulation in the centre of the eastern part, which started at the end of the Late Pleistocene, lowered the drainage from the higher parts in the landscape (Figure 9a). This was likely due to the lower permeability of the highly decomposed peat. This led to the initiation of the secondary phase during the Mid Holocene, when the peat started to accumulate in the higher areas south of the east side, and also in the west side (Figure 9b). Lastly, the lowest-lying areas in the north of the east side initiated peat accumulation during the Late Holocene (Figure 9c). In terms of degradation, the soil profiles in the mire show that the west tributary, on average, had higher decomposed peat profiles in comparison to the east tributary (Bootsma, 2016). This indicates the higher vulnerability of the west tributary compared with the east tributary.

DEGRADED LANDSCAPES AND LOCAL BUFFERS

Most of the areas studied in this thesis are completely or partly managed landscapes; however, the Vasi Peatland Complex is an exception. The Drentsche Aa Brook Valley and Slitere National Park have conservation and restoration plans put in place to conserve and restore some of the eco-services, e.g. biodiversity, prevent CO_2 release. The Matlabas mire is also conserved but no intervention has taken place, and the mire system is still under assessment. The Vasi Peatland Complex remains unprotected, and it is unclear whether any interventions will take place in the future. However, in 1998, a small part of the plantations was removed from the basin of Vasi-North but not from the surroundings (Grundling & Blackmore, 1998). Later, a fire burned Vasi-North in 2017, which led to a total loss of vegetation cover, similar to the loss of vegetation cover in Vasi Pan basins.

Hydrological research (also Kelbe *et al.,* 2016) verified that the plantations are a direct cause of the degradation found in the Vasi Peatland Complex. As the Vasi Peatland Complex has shown a sustained growth in peat accumulation during the past 9000 years under a changing climate, it is unlikely that recent climate change could be the main driver of degradation in this area. However, it could be an amplifying factor in the future, but this remains unclear. As such, restoration measures should be implemented immediately.

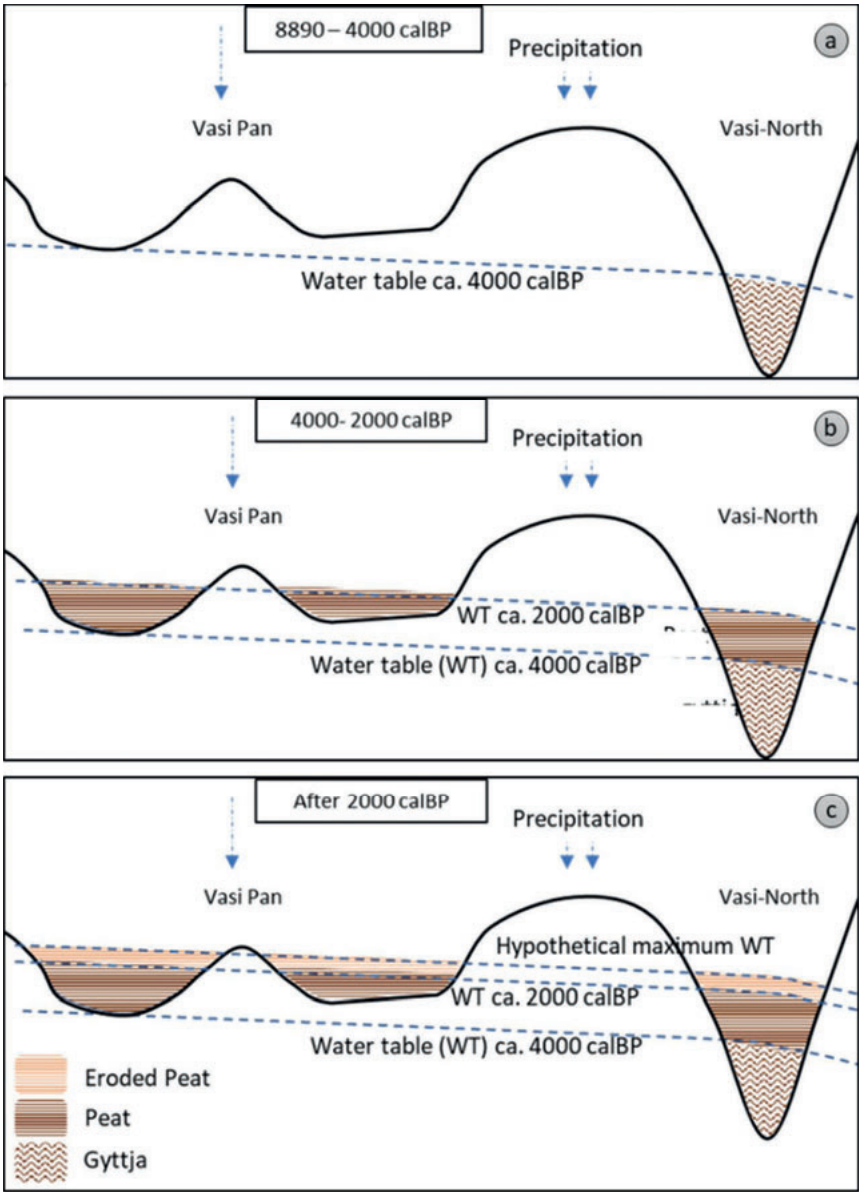

Figure 8. Illustration of peat initiation in the Vasi Peatland Complex with hypothetical water table levels over time. (a) The initiation of gyttja deposition in Vasi-North around 9000 calBP allowed for (b) initiation of peat accumulation ca 4000 calBP in Vasi-North and Vasi Pan. (c) The peat accumulated after ca 2000 calBP, which possibly represents the maximum water table height, was lost through erosion due to degradation.

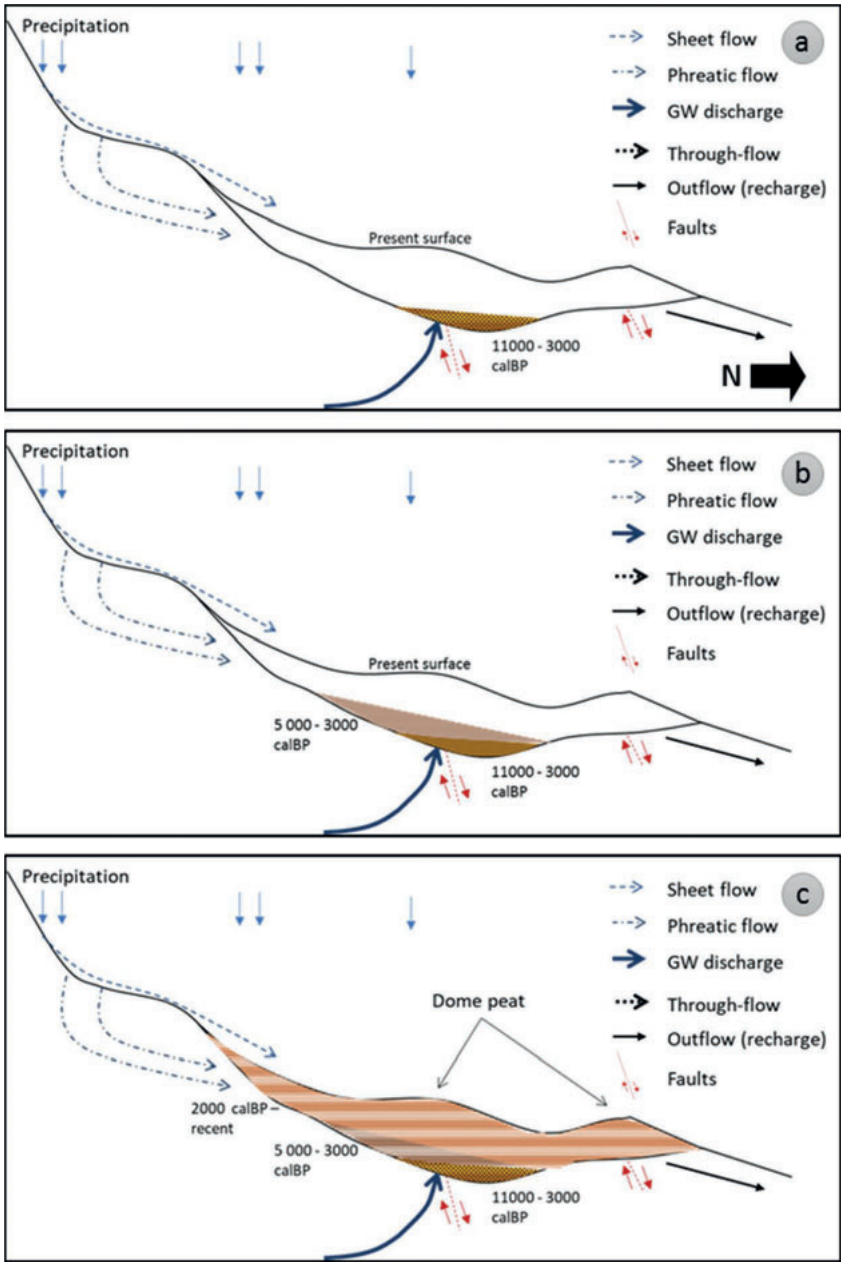

Figure 9. Peat development in the east side of the Matlabas mire. (a) Early, slow accumulation in the central part of the basin took place between 11 000 to 3000 calBP, (b) the peat accumulation expansion to the south started around 5000 calBP and lastly, (c) peat accumulation was initiated in the northern part around 2000 calBP.

These degraded systems have suffered similar patterns of change in groundwater systems, with local systems recharging from a nearby elevated area replacing the lost deeper systems. The water chemistry of the local groundwater systems is often different from the sub-regional/regional groundwater flow, and often base-poor. For instance, the Peterezera mire, which is an inter-dune mire in Slitere National Park, is fed by a base-rich groundwater flow at its southern side of a dune. Yet, this flow is mixed with base-poor groundwater from the dunes (Figure 1), which dominates the quality of the through-flow in the upper parts of the peat layer and consequently affects the vegetation patterns (Van Loon *et al.,* 2009). This leads to acidic conditions, especially in the dune slacks closer to a draining river north of Peterezera, which might explain the undesired loss in target red list species observed by Woljeko *et al.,* (in review). In the Vasi Peatland Complex, recharge by dunes might be the major supplier to Vasi-North, which is the lowest basin in the complex. This is likely to have acted as a buffer, keeping the basin in a better state than its counterparts in Vasi Pan. Similar observations were made in Loon system (Figure 10), which is part of the Drentsche Aa Brook Valley. In Loon, there is a relic water pocket from the original groundwater flow system still present in the peat layer, while the exfiltrating groundwater is pre-dominantly local groundwater flow from a nearby dune area. However, this was not a major problem in Loon as the targeted vegetation species were not affected as much. In fact, this local groundwater might be acting as buffer preventing further peat decomposition like at the other sites, e.g. Kappersbult (Figure 6). The difference in these situations is likely to be related to the deficit in precipitation to evapotranspiration rates in Maputaland versus the other areas, which are located in the temperate zones.

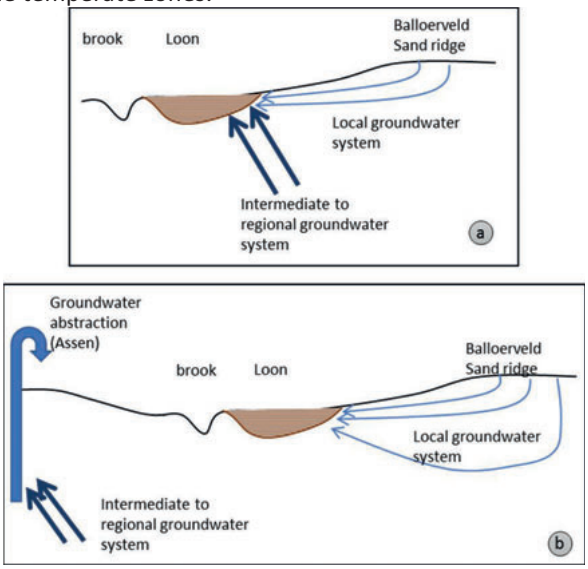

Figure 10. Illustration of the change in the groundwater supply from (a) an original supply from intermediate- to regional-level groundwater systems to (b) one dominated by groundwater infiltrating at Loon from a sand dune (Balloerveld), due to the groundwater abstraction facility in Assen.

SUMMARY: IMPLICATIONS FOR MANAGEMENT

A- The use of natural isotopes provides an opportunity to improve the ecohydrological approach. These isotopes provide the opportunity to address different level of groundwater systems, i.e. local and regional systems, and verify their classification.

B- The Vasi Peatland Complex
This system depends on a local groundwater system, which makes it very vulnerable to changes in land use. Research has shown that peat accumulation in the Vasi Peatland Complex has been continuous for the past 9000 years. This strongly indicates that the recent degradation of this system is directly related to land-use change; this situation requires immediate intervention with restoration measures. Further, most of the peatlands in the Maputaland Coastal Plain are conditioned by a primary groundwater system. Using natural isotopes provided an opportunity to classify the primary groundwater table identified by hydrological modeling into groundwater systems, i.e. local and regional systems.

C- The Matlabas mire
The Matlabas mire already has some interventions in place to close the erosion channels, which are draining the mire. However, some further features need to be considered. For instance, the effect of the road surrounding the mire on the input of sheet flow needs to be investigated to verify whether or not the road affects mire's condition. Also, less likely hypotheses regarding the effects of elephants on mire surface features should be addressed.

D- Drentsche Aa Brook Valley
The restoration success of the Drentsche Aa depends upon the maintenance and restoration of the original hydrological flow systems. While restoration has been successful in most of the restored areas, some others are strongly affected by groundwater abstraction for drinking water. Also, a continuous monitoring of the groundwater in deep groundwater wells are required to ensure the separation of the deep brackish groundwater from the fresh systems supplying the peatlands.

E- Slitere National Park
The groundwater systems sustaining the wetlands in the park are much larger than the areal extent of the park. Therefore, a successful management plan for the wetlands in Slitere National Park needs to consider a larger observation area than its internal and nearby external features.

Summary

This thesis focuses on improvements of ecohydrological analyses of European and South African peatlands in relation to the surrounding landscape. The natural isotopes of the elements C, H and O in groundwater are used to obtain a better insight in the origin of groundwater flows. In four case studies a relatively simple, time-effective but integrated approach was used to make an ecohydrological assessment of peatland ecosystems and how they are affected by land use. In three case studies groundwater systems are analysed in a regional setting, involving sub-catchments (Chapters 3, 5 and 6). The fourth case study focusses on only one catchment level (Chapter 4). The actual field work necessary to assess the natural isotope contents of groundwater was conducted within a time frame of 7 to 15 fieldwork days.

In South Africa radiocarbon dating of peat was used to study the spatial and temporal conditions for initial peat formation and subsequent peat accumulation rates (Chapter 2). These results indicate that different mechanisms determine the starting- and subsequent development conditions of peatland systems in South Africa. Peat initiation and accumulation rates appear to be dependent on sea level fluctuations, climatic transitions, and hydrogeomorphic conditions. The peaks in the coastal peatlands initiation and development are consistent with sea level fluctuation data. Peaks in sea level rise cause a reduction in groundwater drainage, resulting in a higher water table. On a local scale hydrogeomorphic conditions are controlling peat accumulation rates. The initiation of inland peatlands is consistent with the transition to more moist conditions following the Late Glacial Maximum (LGM), which was roughly 25,000 years ago.

An ecohydrological approach using contents of natural isotopes in the groundwater was applied in the Vasi peatland complex situated in the Maputaland Coastal Plain in the north eastern coast of South Africa (KwaZulu Natal; Chapter 3). The peatland complex consists of several sub-basins. Results of radiocarbon dating of the peat showed that peat accumulation in the Vasi Peatland Complex has been continuous for the past 9000 years. The dates also show that the geomorphology, together with the hydrological conditions, controlled the start of peat formation in the sub-basins. Differences in topography were a controlling factor as well; the lower sub-basins were closer to the groundwater table, enabling peat accumulation at earlier stages. Furthermore, the radiocarbon isotopes in groundwater indicated that the Vasi peatland complex is most likely dependent on water supply from its local hydrological system, i.e. a perched groundwater aquifer. Consequently, it means that the system is less dependent of the primary (regional) aquifer of Maputaland, which makes it very vulnerable to changes in land use. This strongly indicates that the recent peat fires that repeatedly occurred are directly related to the start of pine and blue gum

plantations in the 1960's. This situation requires immediate intervention with restoration measures. Further, radiocarbon dating of groundwater showed that most of the peatlands in the Maputaland Coastal Plain are determined by groundwater systems of different size. The analysis of natural isotopes in the groundwater provides a method to distinguish the presence of (sub)groundwater flows/systems, and that not only a primary groundwater aquifer is sustaining the peatlands in Maputaland, but local hydrological systems can be decisive for peat growth as well.

Matlabas in Marakele National Park in South Africa is another area where we applied the improved ecohydrological approach to assess the hydrological functioning of the peatland (Chapter 4). Matlabas is one of the few inland mountainous peatlands in South Africa and is located within the headwaters of the Limpopo River. This mire consists of various spring mire complexes with small elevated peat domes. The occurrence of decaying peat domes and desiccated wetland areas, which is clearly expressed in the vegetation composition, with terrestrial vegetation. Concerns about this situation initiated an ecohydrological study to shed more light on the past peat development and hydrological conditions that had conserved the mire until now. The data indicate that the Matlabas mire developed in the lowest central-east side of the valley by paludification at the onset of the Holocene. Peat coring showed clear indications of the presence of high energy water flows that had led to repetitive erosion in earlier development stages before stabilizing. Under more stable conditions during the Mid Holocene (around 5000 to 3000 years ago), the development of peat was extended laterally due to allogenic and autogenic factors. The autogenic processes took place due to infilling with peat, that stabilized the water fluctuation on the peat and stimulated lateral expansion to the elevated areas of the mire. Meanwhile, peat accumulation rates increased due to a shift to wetter climatic conditions, which is an allogenic factor. During the Mid Holocene, peat accumulation rates in the mire increased from about 0.1 to 1.5 mm per year, which was much higher than observed in other areas in South Africa. The water quality and isotopic data in the groundwater indicated three water flows determining the mire: sheet flow, phreatic groundwater flow and deep groundwater flow. The recent occurrence of decaying peat domes and desiccated wetland areas were related to redirection of some of the groundwater flows, especially the sheet and phreatic groundwater flows. This was a result of interception of water by an access road that was built, and by channels probably dug by farmers before the mire was protected within the National Park. Recently restoration measures have been taken to stop the channel erosion at several sites. Further research on the water budget of the mire remains necessary. For instance, the effect of the road surrounding the mire and its influence on sheet flow needs to be investigated to verify whether or not the road affects the condition of the mire.

Chapter 5 discusses a regional landscape approach to understand groundwater flow origins in the Drentsche Aa brook valley in the Netherlands. Various groundwater flows influence the vegetation biodiversity. Restoration activities have been carried out in the entire brook valley during the last 40 years to improve ecological conditions for species-rich meadows and heathlands, and also to reduce carbon emissions from the desiccated peat soils and to preserve cultural values. The

ecological characteristics in the valley were largely dependent on the occurrence of a large variety in water types, i.e. rain-, surface- and subsurface groundwater flows. Further research has indicated that the groundwater origins are also affected by brine groundwater flows, which are in contact with deep salt diapirs. Whether or not this salt groundwater could reach the surface in the brook valley was largely unknown. In the present thesis, we used the natural isotopes of carbon, hydrogen and oxygen as well as macro-ions to test hypotheses on the influence of the various groundwater systems on vegetation composition. The study verified that the subsurface geological features determine the interaction of fresh groundwater systems (local, intermediate and regional). The regional systems are indeed in contact with deep salt formations (Zechstein Formation), which could lead to upwelling of undesired brackish water under unsustainable groundwater abstraction. The study also indicated that the restoration success is consistent with areas, where drinking water abstraction have been stopped. Hence, a regular monitoring of the groundwater in deep groundwater wells is required to ensure the separation of the deep brackish groundwater from the fresh water systems feeding the peatlands.

In chapter 6 we studied a series of almost pristine mires in Slitere National Park in Latvia. This National Park harbours very different mire types: bogs, inter-dune mires and extremely rich calcareous fens. These wetlands were presumed to be almost unaffected by anthropogenic impacts. However, small changes in vegetation development were observed, particularly in the inter-dune mires, during a preliminary ecohydrological study in 2009. It was assumed that these changes were caused by limited, small local hydrological interventions. However, little is known about the hydrological conditions of the National Park as a whole, especially with respect to the origin of the groundwater flows influencing the mires. We performed a study using water chemistry, i.e. ionic composition, natural isotopes in groundwater. We also used a hydrological model to calculate residence times of various groundwater flows. The data indicate that there are several groundwater systems conditioning the vegetation composition and occurrence or rare and protected species. The larger (regional) groundwater system appeared reach some mires via geological faults. This very calcareous groundwater sustains extremely rich fen ecosystems. There are other systems in place like local groundwater flow from adjacent dunes. Negative effects originate from both past and present interventions with the hydrology. This study concludes that the groundwater systems determining the biodiversity of the wetlands in the park are much larger than the areal extent of the park. Therefore, a successful management plan for the wetlands in Slitere National Park needs to consider a larger area than the present borders of the park and its nearby surroundings.

Samenvatting

Dit proefschrift doet verschillende suggesties om ecohydrologische analyses van veengebieden in relatie met het omliggende landschap te verbeteren door natuurlijke isotopen van de elementen C, H en O in grondwater te analyseren om een beter inzicht te verkrijgen naar de oorsprong van grondwater stromingen. In een viertal studies in Nederland, Zuid Afrika en Letland wordt een relatief eenvoudige, effectieve maar geïntegreerde benadering toegepast om een ecohydrologische beoordeling van veenecosystemen te verkrijgen, inclusief hoe ze worden beïnvloed door landgebruik. In drie studies worden grondwater systemen geanalyseerd in regio's met verschillende lokale voedingsgebieden (Hoofdstukken 3, 5 en 6). De vierde studie betreft een systeem met maar één voedingsgebied (Hoofdstuk 4). Het veldwerk om grondwatermonsters te verzamelen voor de analyse van natuurlijke isotopen was beperkt en varieerde per studie tussen 7 tot 15 werkdagen.

In Zuid Afrika zijn tevens koolstof-14 dateringen van veen verricht om de ruimtelijke en historische condities voor de beginfase van veengroei en de daaropvolgende groeisnelheid van het veen te bestuderen (Hoofdstuk 2). De resultaten laten zien dat verschillende mechanismen de beginfase en daaropvolgende accumulatiesnelheid van het veen bepalen. Beide blijken af te hangen van fluctuaties in het zeespiegel niveau, klimaatveranderingen en hydrogeomorfische condities. In kustgebieden van Zuid Afrika komt het begin van de veenontwikkeling, en ook de daaropvolgende groeisnelheid van het veen, overeen met gepubliceerde gegevens over veranderingen in zeespiegelrijzing. Een hoger zeeniveau veroorzaakt een afname in de afvoer van grondwater, resulterend in een hogere waterstand. Op lokale schaal, bepalen hydrogeomorfische condities de groeisnelheid van het veen. De start van veengroei in het binnenland komt overeen met de overgang naar meer vochtige omstandigheden volgend op het Laat Glaciale Maximum (LGM), ongeveer 25.000 jaar geleden.

Voor het veengebied Vasi-wetlands genoemd, gesitueerd in de kustvlakte van Maputaland in het noordoosten van Zuid Afrika (KwaZulu Natal), is een ecohydrologische studie verricht gebruik makend van de natuurlijke isotopen in het grondwater (Hoofdstuk 3). Het veencomplex bestaat uit verschillende bekkens. Koolstof-14 dateringen van het veen laten zien dat de groeisnelheid van het veen in Vasi constant is geweest gedurende de afgelopen 9000 jaar. De dateringen laten ook zien dat de geomorfologie, in combinatie met hydrologische omstandigheden, de beginfase van de veengroei in de bekkens heeft bepaald. Verschillen in topografie waren eveneens een bepalende factor; de diepere bekkens zijn lager gelegen en natter, wat een eerdere veengroei mogelijk maakte. De koolstof-14 concentraties in het grondwater laten eveneens zien dat het Vasi veencomplex zeer waarschijnlijk afhankelijk is van water afkomstig uit een lokale grondwatersysteem. Dit betekent dat het de Vasi-wetlands minder afhankelijk zijn van het belangrijkste regionale

aquifer van Maputaland. Het betekent ook dat de Vasi venen erg kwetsbaar zijn voor veranderingen in landgebruik. Er zijn sterke aanwijzingen gevonden dat de nu regelmatig optredende branden in het veen rechtstreeks zijn gerelateerd aan de aanleg van dennen- en eucalyptus plantages in de jaren 1960. Deze situatie vereist onmiddellijke interventie met herstel maatregelen. De koolstof-14 dateringen van grondwater laten ook zien dat de meeste veengebieden in de kustvlakte van Maputaland worden bepaald door grondwater systemen van verschillende grootte. De analyse van isotopen in het grondwater maakt het mogelijk om de verschillende grondwater stromen binnen regionale hydrologische systemen te onderscheiden. Hieruit komt naar voren dat de conditie van venen in Maputaland niet alleen door de primaire grondwater aquifer wordt bepaald, maar dat ook de lokale hydrologische factoren mede de groei van het veen bepalen.

Matlabas in het Marakele National Park in Zuid Afrika is een ander gebied waar we een verbeterde ecohydrologische aanpak hebben toegepast om de huidige en vroeger condities van het veen in kaart te brengen (Hoofdstuk 4). Matlabas is een van de weinige veengebieden in het bergachtige binnenland en is gelegen in het stroomgebied van de Limpopo River.

Het nog grotendeels levende veen omvat een serie kwelvenen geflankeerd door een reeks van kleine veenkoepels, waarvan sommige in verval zijn door verdroging. Deze verdroging komt nu met name tot uiting in de vegetatiesamenstelling en de bezorgdheid hierover was aanleiding om nader onderzoek te doen naar oorspronkelijke veenontwikkeling en de hydrologische condities die het veen conserveren. De gegevens laten zien dat het Matlabas veen zijn ontwikkeling begon in het diepste gedeelte van de vallei tijdens het begin van het Holoceen. De geboorde veenkernen laten ook zien dat in het verleden erosie heeft plaats gevonden, met name tijdens de vroege ontwikkelingsfasen van het veen. Gedurende de meer stabiele fasen tijdens het midden van het Holoceen (ca. 5000-3000 jaar geleden) strekte het veen zich in de breedte uit, onder invloed van zowel allogene als autogene factoren. De autogene processen vonden plaats door opvulling met veen, waardoor de afvoer van het water van het levend veen afnam wat leidde tot een veenuitbreiding in de breedte in de hoge gebieden. Tegelijkertijd begon versnelde de veengroei in de lagere gedeelten van de vallei vanwege een natter klimaat, een allogene factor. Gedurende het midden Holoceen nam de groeisnelheid van het veen toe van ongeveer 0.1 mm/jaar tot 1.5 mm/jaar, wat veel hoger is dan wat tot nu toe gerapporteerd is uit andere gebieden in Zuid Afrika. Zowel de watersamenstelling als de isotopen concentraties van het grondwater duiden op drie soorten waterstroming: oppervlakkig afstroming, ondiep grondwater stroming, en stroming van diep grondwater. In meer recente tijden wijzen verdroging van veenkoepels en erosie in het veenpakket op veranderingen in grondwaterstroming, met name wat betref de stroming over het oppervlak en wat betreft ondiepe grondwaterstroming. Deze veranderingen werden mogelijk veroorzaakt door een blokkering van de wateraanvoer door de aanleg van een weg en heel waarschijnlijk ook door het graven van sloten door boeren in de periode voordat het gebied een wettelijke bescherming kreeg. Recent zijn herstelmaatregelen genomen om de erosie op diverse plaatsen te

stoppen. Wel is er meer onderzoek nodig naar het de waterbalans van het veen. Zo is nog onduidelijk in hoeverre de weg rondom het veen van invloed is op de oppervlakkig aanvoer van water naar het veen.

Hoofdstuk 5 beschrijft een regionale studie die is uitgevoerd om een beter inzicht te verkrijgen in de complexe grondwaterstroming in de vallei van de Drentsche Aa in Nederland. Diverse grondwater stromingen beïnvloeden de biodiversiteit van de vegetatie. Gedurende de laatste 40 jaar hebben herstelactiviteiten plaatsgevonden om de soortrijke moerassen en heidegebieden te herstellen, en ook om de koolstof emissies uit de verdrogend veenpakketten te verminderen en culturele waarden te behouden. De ecologische variatie in het beekdal werd in belangrijke mate bepaald door variatie in water typen als gevolg van toestroming van regenwater, oppervlaktewater en grondwater. Verder onderzoek laat zien dat de oorsprong van het grondwater eveneens worden beïnvloed door stroming van grondwater uit zeer diepe lagen van waarin zeer zout water wordt aangevoerd. Dit grondwater heeft in contact gestaan met diepe zoutpijlers. Of dit zoute grondwater type ook inderdaad in het beekdal de oppervlakte bereikt was onbekend. In het voorliggende proefschrift gebruiken we de natuurlijke isotopen van koolstof, waterstof en zuurstof alsmede analyses van macro-ionen in het grondwater om hypotheses betreffende de invloed van diverse grondwaterstromingen op de samenstelling van de vegetatie te testen. Deze studie bevestigt dat de geologische structuur onder de oppervlakte de interacties bepalen van de verschillende grondwater systemen, zowel lokaal als regionaal. De regionale systemen blijken inderdaad in contact te staan met diepe zoutformaties (de Zechstein Formatie), welke ongewenste opwelling van brak water kunnen veroorzaken. De studie laat ook zien dat in bepaalde gebieden het succes van herstelmaatregelen consistent is met stoppen van grondwaterwinning. Het regelmatig "monitoren" van grondwater in diepe putten is nodig om de scheiding van diep brak grondwater en zoetwatersystemen welke de veengebieden voeden te waarborgen.

Hoofdstuk 6 beschrijft een studie naar vrijwel ongerepte veengebieden in het Slitere National Park in Letland. In dit park komen erg verschillende types veenmoeras voor: hoogveen, kalkarm- tot zeer kalkrijk laagveen. Van deze moerasgebieden werd verondersteld dat ze niet of nauwelijks worden beïnvloed door antropogene ingrepen. Tijdens een voorlopig ecohydrologisch onderzoek in 2009 zijn echter geringe veranderingen waargenomen in de ontwikkeling van de vegetatie, in het bijzonder in veensystemen die tussen duinruggen liggen. Er werd aangenomen dat deze veranderingen worden veroorzaakt door beperkte lokale hydrologische interventies. Er is weinig bekend over de hydrologische condities in het National Park als geheel, in het bijzonder betreffende de oorsprong van de grondwater stromingen die de venen beïnvloeden. Wij hebben een studie verricht naar de chemische samenstelling van het grondwater, alsmede de concentraties van natuurlijke isotopen in het grondwater geanalyseerd. Daarnaast werd met behulp van een hydrologisch model verblijftijden van grondwater berekend. De gegevens laten zien dat er verschillende grondwater systemen bestaan welke de samenstelling van de vegetatie en het voorkomen van zeldzame en beschermde soorten bepalen. Het regionale grondwater lijkt sommige venen te kunnen bereiken via geologische breuken. Dit zeer kalkrijke grondwater is

van belang om kalkminnende laagveen vegetaties te conserveren. Er is ook sprake van invloed van lokale hydrologische systemen in de omliggende duinen. Negatieve effecten zijn veroorzaakt door hydrologische interventies, zowel recente als ingrepen uit een verder verleden. Onze studie laat zien dat de biodiversiteit in de wetlands in het park niet alleen door lokale hydrologische systemen wordt bepaald, maar zeer waarschijnlijk ook door grondwater uit een veel groter intrekgebied. Een succesvol beheersplan voor de wetlands in het Slitere National Park moet daarom een groter gebied beschouwen dan het park zelf en zijn directe omgeving.

References

Aerts, A.T., van der Plicht, J., & Meijer, H.M.J. (2001) Automatic sample combustion (AMS) and CO_2 collection. *Radiocarbon*, 43(2), 293–298.

Anderson, R., Foster, D., & Motzkin, G. (2003) Integrating lateral expansion into models of peatland development in temperate New England. *Journal of Ecology*, 91(1), 68-76.

Appelo, C.A.J. & Postma, D. (2005) *Geochemistry, Groundwater and Pollution* (2nd edition). A.A. Balkema Publishers, Amsterdam, the Netherlands.

Baker, A., Routh, J., Blaauw, M., & Roychoudhury, A.N. (2014) Geochemical records of palaeoenvironmental controls on peat forming processes in the Mfabeni peatland, Kwazulu Natal, South Africa since the Late Pleistocene. *Palaeogeography, Palaeoclimatology, Palaeoecology*, 395, 95–106.

Bakker, J.P., Dekker, M., & De Vries, Y. (1980) The effect of different management practices on a grassland community and the resulting fate of seedlings. *Acta Botanica Neerlandica* 29, 469–482.

Bakker, J.P., Everts, H., Grootjans, A.P., De Vries N.P.J., & De Vries Y. (2015) Het grote experiment – Vijftig jaar natuurbeheer. In: Spek, T., Elerie H., Bakker, J.P., & Noordhoff, I. (eds.), *Landschapsbiografie van de Drentsche Aa* (pp. 418-461). Koninklijke Van Gorcum BV, Assen.

Bate, G., Kelbe, B.E., & Taylor, R. (2016) *Mgobezeleni, the linkages between hydrological and ecological drivers*. Report to the Water Research Commission (WRC REPORT NO. K5/2259/1/1**)**, Pretoria, 225 pp.

Bell, M., & Walker, M.J.C. (1992) *Late Quaternary environmental change: Physical and human perspectives*. Longman Group UK Ltd. Essex, England.

Blaauw, M., & Christen, J.A. (2005) Radiocarbon peat chronologies and environmental change. *Journal of the Royal Statistical Society. Series C: Applied Statistics,* 54(4), 805–816.

Blaauw, M., & Christen, J.A. (2011) Flexible paleoclimate age-depth models using an autoregressive gamma process. *Bayesian Analysis*, 6, 457–474.

Blaser, P.C., Coetsiers, M., Aeschbach-Hertig, W., Kipfer, R., Van Camp, M., Loosli, H.H., & Walraevens, K. (2010) A new groundwater radiocarbon correction approach accounting for palaeoclimate conditions during recharge and hydrochemical evolution: The Ledo-Paniselian Aquifer, Belgium. *Applied Geochemistry* 25, 437–455.

Bonn, A.T., Allott, T., Evans, M., Hans, J., & Stoneman, R. (2016) *Peatland Restoration and Ecosystem Services: Science, Policy and Practice*. Cambridge University Press. British Ecology Society, England.

Bootsma, A. (2016) *Mechanisms of erosion prevention and stabilization in a Marakele peatland; implications for conservation management*. University of South Africa, College of Agriculture and Environmental Sciences, South Africa, 99 pp. MSc. Thesis.

Bos, C.B., & Fredeen, K.J. (1989) *Concepts instrumentation and techniques in Inductively Coupled Plasma Atomic Emission Spectroscopy*. Perkin-Elmer Cooperation, Norwalk.

Botha, G.A., Bristow, C.S., Porat, N., Dullerj, G., Clarkei, B.M., Armitagej, S.J. & Schoemani, P. (2003) Evidence for dune reactivation from GPR profiles on the Maputaland Coastal Plain, South Africa. In: Bristow, C.S. & Jol, H.M. (eds.), *Ground Penetrating Radar in Sediments*. (Special Publication, pp. 29–46). London: Geological Society of London.

Botha, G., & Porat, N. (2007) Soil chronosequence development in dunes on the southeast African coastal plain, Maputaland, South Africa. *Quaternary International*, 111–132.

Botha, G., Haldorsen, S., & Porat., N. (2013) Geological history. In: Perissinotto, R., Stretch, D.D., Taylor, R.H. (eds) *Ecology and Conservation of Estuarine Ecosystems: Lake St Lucia as a Global Model.* Cambridge University Press, Cambridge, UK.

Brady, N., & Weil, R. (1998) *Nature and properties of soils* (12th edition). Upper Saddle River, N.J.: Prentice Hall.

Bregman. E.P.H., Maas, G., Makaske, B., & Meyles, E, (2015) Vormgegeven door ijs, water en wind. In: Spek, T., Elerie, H., Bakker, J.P., & Noordhoff, I. (eds): *Landschapsbiografie van de Drentsche Aa*, pp. 18-53. Van Gorcum, Assen.

Bronk Ramsey, C. (2008) Deposition models for chronological records. *Quaternary Science Reviews*, 27(1-2), 42–60.

Bronk Ramsey, C. (2009). Bayesian analysis of radiocarbon dates. *Radiocarbon,* 51(1), 337-360.

Brown, L.R., Du Preez, P.J., Bezuidenhout, H., Bredenkamp, G.J., Mostert, T.H.C. & Collins, N.B., (2013) Guidelines for phytosociological classifications and descriptions of vegetation in southern Africa.

Koedoe 55 (1), a1103, 1-10.
Bruton, M.N., & Cooper, K.H. (1980) *Studies on the Ecology of Maputaland.* Grahamstown: Rhodes University.
Charman, D. (2002) *Peatlands and Environmental Change*. John Wiley and Sons Ltd, Chichester, 301 pp.
Chase, B., & Meadows, M. (2007) Late Quaternary dynamics of southern Africa's winter rainfall zone. *Earth-Science Reviews*, 84(3-4), 103-138.
Clark, I., & Aravena, R. (2005) Environmental Isotopes in Ground Water Resource and Contaminant Hydrogeology. National Ground Water Agency, US.
Clymo, R.S., Turunen, J., & Tolonen, K. (1998) Carbon accumulation in peatland. *Oikos,* 81(2), 368–388.
Dahl, M., Nilsson, B., Langhoff, J.H., & Refsgaard, J.C. (2007) Review of classification systems and new multi-scale typology of groundwater-surface water interaction. *Journal of Hydrology* 344, 1–16.
De Gans, W. (2007) Quaternary. In: Wong, T.E., Batjes, D.A.J., & De Jager, J. (eds.), *Geology of the Netherlands,* pp. 173–195. Royal Netherlands Academy of Arts and Sciences.
De Mars, H., & Garritsen, A.C. (1997) Interrelationship between water quality and groundwater flow dynamics in a small wetland system along a sandy hill ridge. *Hydrological Processes* 11, 335–351.
De Mars, H., Wassen, M.J., & OldeVenterink, H.O. (1997) Flooding and groundwater dynamics in fens in eastern Poland. *Journal of Vegetation Science* 8, 319–328.
De Vleeschouwer, F., Chambers, F.M., & Swindles, G.T. (2010) Coring and sub-sampling of peatlands for palaeoenvironmental research. *Mires and Peat,* 7(11), 1–10.
De Vries, J.J. (2007) Groundwater. In: Wong, T.E., Batjes, D.A.J., & De Jager, J. (eds.), *Geology of The Netherlands,* pp. 295–315. Royal Netherlands Academy of Arts and Sciences.
Dekker, S.C., De Boer, H.J., Dermody, B.J., Wagner-Cremer, F., Wassen, M.J., & Eppinga, M.B. (2015) Holocene peatland initiation in the Greater Everglades. *Journal of Geophysical Research G: Biogeosciences*, 120(2), 254–269.
Diersch, H., & Kolditz, O. (1998) Coupled groundwater flow and transport: 2. Thermohaline and 3D convection systems. *Advances in Water Resources* 1708, 401–425.
DINOLOKET (2014) Retrieved October 15, 2014, from https://www.dinoloket.nl/
Dise, N.B. (2009) Biogeochemical Dynamics III: The critical dynamics of Carbon in wetlands. In: Maltby, E., & Barker, T. (eds.): *The Wetlands Handbook*, pp. 249–256. Wiley-Blackwell Publishing, Chichester.
Dommain, R., Couwenberg, J., & Joosten, H. (2011) Development and carbon sequestration of tropical peat domes in south-east Asia: Links to post-glacial sea-level changes and Holocene climate variability. *Quaternary Science Reviews,* 30(7–8), 999–1010.
Engelen, G.B., Kal, B.F. M., Buyse, J.J., & Van Pruissen, F.G.M. (1992) The hydrology of the Loosdrecht lakes area. *Hydrobiologia*, 233(1-3), 21-38.
Eppinga, M.B., Rietkerk, M., Wassen, MJ., & De Ruiter, P. C. (2009) Linking habitat modification to catastrophic shifts and vegetation patterns in bogs. *Plant Ecology*, 200(1), pp. 53-68.
Everts, F.H., & de Vries, N.P.J. (1991) De vegetatieontwikkeling van beekdalsystemen. Proefschrift Rijksuniversiteit Groningen/ Historische uitgeverij Groningen. PhD Thesis.
Faurescu, I., Varlam, C., Faurescu, D., Vagner, I., Cosma, C., & Costinel, D. (2015) Underground water dating and age corrections using radiocarbon. *Journal of Radioanalytical and Nuclear Chemistry,* 306(1), 263–269.
Finch, J.M., & Hill, T.R. (2008) A late Quaternary pollen sequence from Mfabeni Peatland, South Africa: Reconstructing forest history in Maputaland. *Quaternary Research*, 70(3), 442–450.
Gabriel, M., Gałka, M., Pretorius, M.L., & Zeitz, J. (2017a) The development pathways of two peatlands in South Africa over the last 6200 years: implications for peat formation and palaeoclimatic research. *The Holocene,* 27 (10), 1499-1515.
Gabriel, M., Toader, C., Faul, F., Roßkopf, N., van Husyssteen, W.C., Grundling, P.L. & Zeitz, J. (2017b) Peatland substrates in northern KwaZulu-Natal - Their forming environments, their properties and an approach towards their classification. *South African Journal of Plant and Soil,* 53(2), 149-160.
Gasse, F. (2000) Hydrological changes in the African tropics since the Last Glacial Maximum. *Quaternary Science Reviews*, 19, 189–211.
Gat, J.R. (1996) Oxygen and hydrogen isotopes in the hydrologic cycle. *Earth Planet Sciences*, 24, 225–262.
Geyh, M. (2000) An overview of 14C analysis in the study of groundwater. *Radiocarbon* 42, 99–114.
Gibson, J.J., Edwards, T.W.D., Birks, S.J., St Amour, N.A., Buhay, W.M., McEachern, P., & Peters, D.L. (2005) Progress in isotope tracer hydrology in Canada. *Hydrological Processes*, 19(1), 303–327.
Gillson, L., & Duffin, K., (2007) Thresholds of potential concern as benchmarks in the management of

African savannahs. *Philosophical Transactions of the Royal Society B: Biological Sciences*, 362 (1478), 309-319.

Gilvear, D.J., & Bradley, C. (2009) Hydrological Dynamics II: Groundwater and Hydrological Connectivity. In: Maltby, E., & Barker, T. (eds.): *The Wetlands Handbook*, pp. 169–193. Wiley-Blackwell Publishing, Chichester.

Graham, E. (1991) Northern Peatlands: Role in the Carbon Cycle and Probable Responses to Climatic Warming. *Ecological Applications*, 1(2), 182–195.

Grootjans, A.P., Van Diggelen, R., Everts, F.H., Schipper, P.C., Streefkerk, J., De Vries, N.P.J., & Wierda, A. (1993). Linking ecological patterns to hydrological conditions on various spatial scales: a case study of small stream valleys. In: Vos, C.C., & Opdam, P. (eds.), *Landscape Ecology of a Stressed Environment*, pp. 60–78. Chapman and Hall, London.

Grootjans, A.P., Adema, E.B., Bleuten, W., Joosten, H., Madaras, M., & Janakova, M. (2006) Hydrological landscape settings of base-rich fen mires and fen meadows: an overview. *Applied Vegetation Science*, 9, 175–184.

Grootjans, A.P., & Van Diggelen, R. (2009) Hydrological Dynamics III: Hydro-ecology. In: Maltby, E., & Barker, T. (eds.), *The Wetlands Handbook*, pp. 194–212. Wiley-Blackwell Publishing, Chichester.

Grootjans, A.P., & Jansen, A. (2012) An eco-hydrological approach to wetland restoration. In: Grootjans, A.P., Stanova, V.S., & Jansen, A. (eds.), *Calcareous Mires of Slovakia*, pp. 21–28. KNNV Publishing, Zeist.

Grootjans, A.P., Van Diggelen, R., Joosten, H., & Smolders, A.J.P. (2012) Restoration of Mires. In: Van Andel, J., & Aronson, J. (eds.), *Restoration Ecology: The New Frontier*, 203–213. Blackwell Science Ltd.

Grundling A., Van Den Berg, E.C., & Price, J.S. (2013a) Assessing the distribution of wetlands over wet and dry periods and land-use change on Maputaland Coastal Plain, north-eastern KwaZulu-Natal, South Africa. *South African Journal of Geomatics*, 2 (2), 120-139.

Grundling, A.T. (2014) Remote sensing and biophysical monitoring of vegetation, terrain attributes and hydrology to map, characterise and classify wetlands of the Maputaland Coastal Plain, KwaZulu-Natal, South Africa. University of Waterloo. PhD Thesis.

Grundling, P.L., & Blackmore, A. (1998) *Peat fire in the Vasi Pan Peatland: Manzenwenya Plantation*. Report no.: 1998-0208, Council of Geoscience, Pretoria.

Grundling, P.L., Mazus, H. & Baartman, L., (1998) *Peat Resources in Northern KwaZulu-Natal Wetlands: Maputaland*. Department of Environmental Affairs and Tourism Report no. A25/13/2/7. Grundling, P.L., Baartman, L., Mazus, H. & Blackmore, A. (2000) *Peat resources of KwaZulu-Natal Wetlands: Southern Maputaland and the North and South Coast*. Council for Geoscience report 2000-0132. Pretoria: Department of Environmental Affairs and Tourism.

Grundling, P.L. (2004) The Role of Sea-Level Rise in the Formation of Peatlands in Maputaland. Ministerio Dos Recursos Minerais E Energia. Direccao Geral de Geologia; *Boletim Geologico,* 43, 58–67.

Grundling, P.L., & Grobler, R. (2005) Peatlands and mires of South Africa. *Stapfia*, 85, 379-396.

Grundling, P.L., Grootjans, A.P., Price, J.S., & Ellery, W.N. (2013b) Development and persistence of an African mire: How the oldest South African fen has survived in a marginal climate. *Catena*, 110, 176-183.

Grundling, P.L. (2014). Genesis and hydrological function of an African mire: understanding the role of peatlands in providing ecosystem services in semi-arid climates. University of Waterloo. PhD Thesis.

Grundling, P.L., Clulow, A.D., Price, J.S., & Everson, C.S. (2015) Quantifying the water balance of Mfabeni Mire (iSimangaliso Wetland Park, South Africa) to understand its importance, functioning and vulnerability. *Mires and Peat*, 16, 1–18.

Grundling P.L., Grundling A.T., & Pretorius L. (2017) *South African peatlands: Ecohydrological characteristics and socio-economic value*. Water Research Commission Report Research Report No. 2346/1/17. Pretoria, South Africa.

Han, L.F., Plummer, L.N., & Aggarwal, P. (2012) A graphical method to evaluate predominant geochemical processes occurring in groundwater systems for radiocarbon dating. Chemical Geology 318-319, 88–112.

Häusler, K., Moros, M., Wacker, L., Hammerschmidt, L., Dellwig, O., Leipe, T., Kotilainen, A., & Arz, H.W. (2017) Mid- to late Holocene environmental separation of the northern and central Baltic Sea basins in response to differential land uplift. *Boreas,* 46(1), 111–128.

Heathwaite, A.L., Gottlich, K., Burmeister, E.G., Kaule, G. & Grospietsch, T. (1993) Mires: Definitions and Form. In: Heathwaite, A.L. & Gottlich, K. (eds.), *Mires: Process, Exploitation and Conservation* (3rd ed.),

pp. 1–64. John Wiley & sons.
Hill, M.O. (1979) *TWINSPAN – A FORTRAN program for arranging multivariate data in an ordered two-way table by classification of individuals and attributes*. Cornell University Ithaca, N.Y.
Hogg, A.G., Hua, Q., Blackwell, P.G., Niu, M., Buck, C.E., Guilderson, T.P., & Zimmerman, S.R.H. (2013) SHCAL13 Southern Hemisphere Calibration, 0-50,000 Years CAL BP. *Radiocarbon*, 55(2), 1–15.
Hua, Q., Barbetti, M., & Rakowski, A.Z. (2013) Atmospheric radiocarbon for the period 1950-2010. *Radiocarbon*, 55(4), 2059-2072.
Irving, S.J.E., & Meadows, M.E. (1997) Radiocarbon Chronology and Organic Matter Accumulation at Vankervelsvlei, Near Knysna, South Africa. *South African Geographical Journal*, 79(2), 101–105.
IAEA/WMO, (2017) *Global Network of Isotopes in Precipitation. The GNIP Database*. Accessible at: http://www.iaea.org/water
Isokangas, E., Rossi, P.M., Ronkanen, A.K., Marttila, H., Rozanski, K. & Kløve, B. (2017) Quantifying spatial groundwater dependence in peatlands through a distributed isotope mass balance approach. W*ater Resources Research,* 53, 2524-2541.
Joosten, H., & Clarke, D. (2002). Wise Use of Mires and Peatlands- Background and Principles including A Framework for Decision-Making. *Journal of Chemical Information and Modeling,* 53. Saarijarvi, Finland: International Mire Conservation Group and International Peat Society.
Joosten, H., & Tanneberger, F. (2016) *The European Mire Book*. Stuttgart: Schweizerbart'sche Verlagsbuchhandlung.
Joosten, H., Tanneberger, F., & Moen, A. (2017) *Mires and Peatlands of Europe: Status, Distribution and Conservation*. Stuttgart: Schweizerbart Science.
Juodkazis, V. (1994) Groundwater quality and its monitoring in the Baltic states. *GeoJournal,* 33(1), 63-70, Baltic Peoples, Baltic Culture and Europe (May 1994).
Kalnina, L., Stivrins, N., Kuske, E., Ozola, I., Pujate, A., Zeimule, S., & Ratniece, V. (2014) Peat stratigraphy and changes in peat formation during the Holocene in Latvia. *Quaternary International*, 383(2015), 1–10.
Kassambara, A. (2017) Practical Guide to Principal Component Methods in R. Retrieved from: www.Sthda.com.
Kelbe, B., Grundling, A.T. & Price, J. (2016) Modelling water table depth in a primary aquifer to identify potential wetland hydrogeomorphic settings on the northern Maputaland Coastal Plain, KwaZulu-Natal, South Africa. *Hydrogeology Journal,* 24(1), 249-265.
Klimkowska, A., Kotowski, W., Van Diggelen, R., Grootjans, A.P., Dzierża, P., & Brzezińska, K. (2010) Vegetation re-development after fen meadow restoration by topsoil removal and hay transfer. *Restoration Ecology,* 18(6), 924–933.
Loosli, H., & Aeschbach-Hertig, W. (2001) Isotopic methods and their hydrogeochemical context in the investigation of palaeowaters. *Geological Society* 189, 193–212.
Lowe, J.J. & Walker, M.J.C. (1984) *Reconstructing Quaternary environments*. Longman Scientific & Technical, Harlow.
Madaras, M., Grootjans, A.P., Šefferová Stanová, V., Janáková, M., Laštůvka, Z. & Jansen, A. (2012) Fen meadows of abroad; in urgent need of protection. In: Grootjans, A.P., Jansen, A.M.J. & Stanova, V. (eds.) 2012. *Calcareous mires of Slovakia,* pp. 77-96. KNNV Publishing, Zeist.
Magri, F., & Bregman, E.P.H. (2011). Regional-scale numerical model of coupled fluid flow and mass transport along a deep geological profile in the Drenthe area, The Netherlands. Final Report of the Demo Pilot Project. Geowissenschaften Institut für Geologische Wissenschaften, Berlin.
Maltby, E. & Barker, T. (eds.). (2009) The Wetlands Handbook. Blackwell Publishing.
Mars, H., Wassen, M., & Venterink, H. (1997). Flooding and groundwater dynamics in fens in eastern poland. *Journal of Vegetation Science*, 8(3), 319-328.
Marneweck, G.C., Grundling, P.L., and Müller, J.L. (2001) *Defining and Classification of Peat Wetland Eco-Regions in South Africa*, Wetland Consulting Services (Pty) Ltd. Report to the Institute for Soil, Climate and Water (ISCW), Agricultural Research Council for the Directorate for Land and Resources Management (DLRM), Department of Agriculture, Pretoria.
Mayer, A., Sültenfuß, J., Travi, Y., Rebeix, R., Purtschert, R., Claude, C., & Conchetto, E. (2014). A multi-tracer study of groundwater origin and transit-time in the aquifers of the Venice region (Italy). *Applied Geochemistry* 50, 177–198. http://doi.org/10.1016/j.apgeochem.2013.10.009
McCarthy, T. S., Ellery, W. N., Backwell, L., Marren, P., Klerk, B. De, Tooth, S., & Woodborne, S. (2010) The character, origin and palaeoenvironmental significance of the Wonderkrater spring mound, South

Africa. *Journal of African Earth Sciences*, 58(1), 115–126.
Meadows, M.E. (1988) Late Quaternary peat accumulation in southern Africa. *Catena*, 15, 459–472.
Meadows, M.E. (2001) The role of Quaternary environmental change in the evolution of landscapes: case studies from southern Africa. *Catena,* 42, 39–57.
Meijer, H.A.J. (2009) Stable isotope quality assurance using the "calibrated IRMS" strategy. *Isotopes in Environmental and Health Studies*, 45(2), 150–63.
Mendizabal, I., & Stuyfzand, P. (2009) Guidelines for interpreting hydrochemical patterns in data from public supply well fields and their value for natural background groundwater quality determination. *Journal of Hydrology* 379(1-2), 151-163.
Mendizabal, I., Stuyfzand, P. & Wiersma, A. (2011) Hydrochemical system analysis of public supply well fields, to reveal water-quality patterns and define groundwater bodies: The Netherlands. *Hydrogeology Journal* 19, 83-100.
Mitsch, W. J., & Gosselink, J. G. (2000a) *Wetlands* (3rd ed.). John Willey & sons, Newyork.
Mitsch, W. J., & Gosselink, J. G. (2000b) The value of wetlands: Importance of scale and landscape setting. *Ecological Economics*, 35(1), 25–33.
Mook, W., & van der Plicht, J. (1999) Reporting 14C Activities and Concentrations. *Radiocarbon,* 43(3), 227-239.
Mook, W. (2006) *Introduction to Isotope Hydrology: Stable and Radioactive Isotopes of Hydrogen, Oxygen and Carbon* (International contributions to hydrogeology, 25). London: Taylor & Francis.
Morris, P., Belyea, L., & Baird, A. (2011) Ecohydrological feedbacks in peatland development: A theoretical modelling study. *Journal of Ecology*, 99(5), 1190-1201.
Mucina, L., & Rutherford, M.C. (2006) *The Vegetation of South Africa, Lesotho and Swaziland*. *Strelitzia* 19. South African National Biodiversity Institute, Pretoria.
Naucke, W., Heathwaite, A.L., Eggelsmann, R., & Schuch, M. (1993) Mire chemistry. In: Heathwaite, A.L., & Gottlich, K. (eds.), *Mires: Process, Exploitation and Conservation* (Third edition). John Wiley & sons.
Norström, E., Scott, L., Partridge, T.C., Risberg, J., & Holmgren, K. (2009) Reconstruction of environmental and climate changes at Braamhoek wetland, eastern escarpment South Africa, during the last 16, 000 years with emphasis on the Pleistocene – Holocene transition. *Palaeogeography, Palaeoclimatology, Palaeoecology,* 271(3-4), 240–258.
Neumann, F.H., Scott, L., Bousman, C.B., and van As, L. (2010) A Holocene sequence of vegetation change at Lake Eteza, coastal KwaZulu-Natal, South Africa, *Review of Palaeobotany and Palynology,* 162, 39– 53.
O'Leary, M. (1981) Carbon isotope fractionation in plants. *Phytochemistry*, 20(4), 553-567.
O'Leary, M. (1988) Carbon isotopes in photosynthesis: Fractionation techniques may reveal new aspects of carbon dynamics in plants. *Biosciences*. 38(5), 328-336.
Page, S.E., Wűst, R.A.J., Weiss, D., Rieley, J.O., Shotyk, W., & Limin, S.H. (2004) A record of Late Pleistocene and Holocene carbon accumulation and climate change from an equatorial peat bog (Kalimantan, Indonesia): implications for past, present and future carbon dynamics. *Journal of Quaternary Science*, 19(7), 625–635.
Pakalne, M., & Kalnina, L. (2005) Mire ecosystems in Latvia. In: Steiner G.M. (ed.), *Moore - von Sibirien bis Feuerland*, Stapfia, 85, pp. 147–174.
Peet, R.K., & Roberts, D.W. (2013) Classification of natural and semi-natural vegetation, in: Van der Maarel, E., Franklin, J. (eds.), *Vegetation Ecology,* pp. 28-70. Wiley-Blackwell.
Piotrowska, N., Blaauw, M., Mauquoy, D., & Chambers, F.M. (2011) Constructing deposition chronologies for peat deposits using radiocarbon dating. *Mires and Peat*, 7(10), 1–14.
Porat, N., & Botha, G. (2008) The luminescence chronology of dune development on the Maputaland coastal plain, southeast Africa. *Quaternary Science Reviews*, 27(9-10), 1024–1046.
Province of Drenthe (1995) *Research on the dynamic behaviour of groundwater systems*. Report (in Dutch). Province of Drenthe, Assen.
Ramsay, P.J. (1995) 9000 years of sea-level change along the Southern African Coastline. *Quaternary International,* 31, 71–75.
Ramsay, P.J., & Cooper, J.A.G. (2002) Late Quaternary sea-level change in South Africa. *Quaternary Research*, 57(1), 82–90.
Reimer, P.J., Bard, E., Bayliss, A., Beck, J.W., Blackwell, P.G., Bronk R.C., Buck, C.E., Cheng, H., Edwards, R.L., Friedrich, M., Grootes, P.M., Guilderson, T.P., Haflidason, H., Hajdas, I., Hatte, C., Heaton, T.J., Hoffmann, D.L., Hogg, A.G., Hughen, K.A., Kaiser, K.F., Kromer, B., Manning, S.W., Niu, M., Reimer,

R.W., Richards, D.A., Scott, E.M., Southon, J.R., Staff, R.A., Turney, C.S.M., & van der Plicht, J. (2013) IntCal13 and Marine13 radiocarbon age calibration curves 0–50,000 years cal BP. *Radiocarbon, 55(4), 1869-1887.*

Remm, K., Jaagus, J., Briede, A., Rimkus, E., & Kelviste, T. (2011) Interpolative mapping of mean precipitation in the Baltic countries by using landscape characteristics. *Estonian Journal of Earth Sciences*, 60(3), 172.

Richardson, C.J., & Vaithiyanathan, P. (2009) Biogeochemical dynamics II: Cycling and storage of Phosphorus in wetlands. In: Maltby, E., & Barker, T. (eds.), *The Wetlands Handbook*, pp. 228–248. Blackwell Publishing, Chichester.

Roleček, J., Tichý, L., Zelený, D., & Chytrý, M. (2009) Modified TWINSPAN 986 classification in which the hierarchy respects cluster heterogeneity. *Journal of Vegetation Science,* 20, 596–602

Saks, T., Kalvans, A., & Zelcs, V. (2012) OSL dating of Middle Weichselian age shallow basin sediments in Western Latvia, Eastern Baltic. *Quaternary Science Reviews*, 44, 60-68.

SANPARKS (2008) Marakele National Park, Park Management Plan. South African National Parks, Pretoria.

Schot, P.P., & Molenaar, A. (1992) Regional changes in groundwater flow patterns and effects on groundwater composition. *Journal of Hydrology*, 130(1-4), 151–170.

Schot, P.P., & Van der Wal, J. (1992) Human impact on regional groundwater composition through intervention in natural flow patterns and changes in land use. *Journal of Hydrology*, 134(1-4), 297–313.

Schot, P.P., & Wassen, M.J. (1993) Calcium concentrations in wetland groundwater in relation to water sources and soil conditions in the recharge area. *Journal of Hydrology*, 141, 197–217.

Schot, P.P., Dekker, S.C., & Poot, A. (2004) The dynamic form of rainwater lenses in drained fens. *Journal of Hydrology*, 293, 74–84.

Schot, P.P., & Pieber, S.M. (2012) Spatial and temporal variations in shallow wetland groundwater quality. *Journal of Hydrology*, 422–423, 43–52.

Scott, L., & Vogel, J. (2000) Evidence for environmental conditions during the last 20 000 years in southern Africa from ^{13}C in fossil hyrax dung. *Global and Planetary Change*, 26(1), 207-215.

Scott, L., Holmgren, K., Talma, A.S., Woodborne, S., & Vogel, J.C. (2003) Age interpretation of the Wonderkrater spring sediments and vegetation change in the Savanna Biome, Limpopo province, South Africa. *South African Journal of Science*. 99(9-10), 484-488.

Smit, F.W.H., Magri, F., Bregman, E.P.H. (2018) Coupling earth surface processes and geological structures to explain environmental features as observed onshore Northern Netherlands. SEG conference 2018 paper (accepted).

SACS (1980) *Stratigraphy of South Africa. Part 1* (Comp. L.E. Kent). Lithostratigraphy of the Republic of South Africa, South West Africa/ Namibië and the Republics of Bophuthatwana, Transkei, and Venda. Pretoria: Government Printer. Handbook for Geological Survey in South Africa 8, South African commission for stratigraphy.

Stuyfzand, P.J. & Moberts, F.M.L. (1987) De bijzondere hydrologie van kwelplassen in duinen met kunstmatige infiltratie. *H_2O*, 20, 52-55.

Stuyfzand, P.J. (1993) Hydrochemistry and hydrology of the coastal dune area of the Western Netherlands. Free University of Amsterdam. PhD Thesis.

Tamers, M.A. (1975) The validity of radiocarbon dates on groundwater. *Geophysical Survey* 2, 217–239.

Thamm, A. G., Grundling, P.L., & Mazus, H. (1996) Holocene and recent peat growth rates on the Zululand coastal plain. *Journal of African Earth Sciences*, 23(1), 119–124.

Toth, J. (1963) A Theoretical Analysis of Groundwater Flow in Small Drainage Basins. *Journal of Geophysical Research*, 68(16), 4795–4812.

Trambauer, P., Maskey, S., Werner, M., Pappenberger, F., Van Beek, L.P.H., & Uhlenbrook, S. (2014) Identification and simulation of space-time variability of past hydrological drought events in the Limpopo River basin, southern Africa. *Hydrology and Earth System Sciences*, 18(8), 2925–2942.

Truc, L., Chevalier, M., Favier, C., Cheddadi, R., Meadows, M.E., Scott, L., & Chase, B.M. (2013) Quantification of climate change for the last 20, 000 years from Wonderkrater, South Africa: Implications for the long-term dynamics of the Intertropical Convergence Zone. *Palaeogeography, Palaeoclimatology, Palaeoecology*, 386, 575–587.

Van Andel, J., & Grootjans, A.P. (2006) Concepts in restoration ecology. In: Van Andel, J., & Aronson, J. (eds.), *Restoration Ecology: The New Frontier*, pp. 316-28. Blackwell Science Ltd.

Van der Plicht, J., Wijma, S., Aerts, A., Pertuisot, M., & Meijer, H.A. (2000) Status report: The Groningen AMS facility. *Nuclear Instruments and Methods in Physics Research Section B: Beam Interactions with*

Materials and Atoms, 172(1-4), 58–65.
Van Diggelen R., Grootjans, A.P., & Burkunk, R. (1994) Assessing restoration perspectives of disturbed brook valleys: the Gorecht area, The Netherlands. *Restoration Ecology* 2, 87-96.
Van Diggelen, R., Beukema, H., & Noorman, K.J. (1995) *Ranunculus hederaceus* L. as indicator of land use changes in the Netherlands. *Acta Botanica Neerlandica* 44, 161–175.
Van Diggelen, R. (2006) Landscape: Spatial interactions. In Van Andel, J., & Aronson, J. (eds.), *Restoration Ecology: The New Frontier*, pp. 31–45. Blackwell Science Ltd.
Van Loon, A.H., Schot, P.P., Griffioen, J., Bierkens, M.F.P., Batelaan, O., & Wassen, M.J. (2009) Throughflow as a determining factor for habitat contiguity in a near-natural fen. *Journal of Hydrology,* 379, 30–40.
Van Staden, P.J. (2002) *An ecological study of the plant communities of Marakele National Park.* University of Pretoria, Pretoria. MSc. Thesis.
Van Wirdum, G. (1991) *Vegetation and hydrology of floating rich fens.* University of Amsterdam. PhD Thesis.
Van Wyk, E., & Vermeulen, D. (2011) Characteristics of local groundwater recharge cycles in South African semi-arid hard rock terrains – rainwater input. *Water SA,* 37(2), 147–154.
Virbulis, J., Bethers, U., Saks, T., Sennikovs, J., Timuhins A. (2013) Hydrogeological model of the Baltic Artesian Basin. *Hydrogeology Journal,* 21(4) pp. 845-862.
Vogel, J.C. (1970) Carbon-14 dating of groundwater. In: *Isotope Hydrology, Proceedings of a symposium,* pp. 225–236. Vienna: International Atomic Energy Association.
Von Post, L. (1922) Sveriges Geologiska Undersöknings torvinven- tering och några av dess hittills vunna resultat. *Svenska moss- kulturföreningens tidskrift*, 37, 1–27.
Wassen, M.J., Barendregt, A., Palczynski A., De Smidt, J.T., & De Mars, H. (1990) The relationship between fen vegetation gradients; groundwater flow and flooding in an undrained valley mire at Biebrza, Poland. *Journal of Ecology* 78, 1106–1122.
Wassen, M., & Grootjans, A.P. (1996) Ecohydrology: an interdisciplinary approach for wetland management and restoration. *Vegetatio,* 126, 1-4.
Weitz, J., & Demlie, M. (2014) Conceptual modelling of groundwater–surface water interactions in the Lake Sibayi Catchment, Eastern South Africa. *Journal of African Earth Sciences*, 99, 613-624.
Westhoff, V. & Van der Maarel, E. (1978) The Braun-Blanquet approach. In: Whittaker, R.H. (ed), *Classification of Plant Communities,* pp. 289 - 374. Junk, The Hague.
Wheeler, B.D., & Shaw, S.C. (1995) Plants as Hydrologists? An assessment of the value of plants as indicators of water conditions in fens. In: Hughes M.R., & Heathwaite A.L. (eds.), *Hydrology and Hydrochemistry of British Wetlands*, pp. 63–82. West Sussex: John Wiley.
Wolejko, L., Grootjans A.P., Pakalne, M., Strazdiņa L., Aleksāns O., & Grabowska E. The biocenotic values of Slitere National Park, Latvia, with special reference to interdune mires. *Mires and Peat. (in review)*
Yu, Z., Loisel, J., Brosseau, D.P., Beilman, D.W., & Hunt, S.J. (2010) Global peatland dynamics since the Last Glacial Maximum. *Geophysical Research Letters*, 37(13), 1–5.
Zelčs, V., Markots, A., Nartišs, M., & Saks, T. (2011) Pleistocene Glaciations in Latvia. In: Ehlers, J., Gibbard, P.L. (eds.), *Quaternary Glaciations – Extent and Chronology,* pp. 225–243. Developments in Quaternary Sciences, 2. Elsevier, Amsterdam.